

International Ni-Cu Symposium

August 6-8th 2024

Lakehead University,
Thunder Bay, Canada

International Ni-Cu Symposium

Thunder Bay 2024

International Ni-Cu Symposium

August 6-8th 2024

Lakehead University, Thunder Bay, Canada

Meeting Chair - Pete Hollings

Organising committee - Matt Brzozowski, Robert Cundari, David Good, Peter Hinz, Al MacTavish, Jim Miller, Dean Rossel, Mark Smyk

Reference to material in this volume should follow the example below:

Authors, 2024, Abstract title, 2024 International Ni-Cu Symposium Abstracts Volume, Thunder Bay, August 6-8th 2024, p. xx-xx.

Thank you to our sponsors

CLEAN AIR METALS INC

CEDC TOURISM DEVELOPMENT FUND

GENERATION PGM

Actlabs

BIG ROCK EXPLORATION

TALON METALS CORP

AGAT Laboratories

AGC GeoConsulting

SOCIETY for GEOLOGY APPLIED to MINERAL DEPOSITS

Teck

Centre of Excellence for Sustainable Mining & Exploration

EXPLORE GEOSOLUTIONS

See you next time!

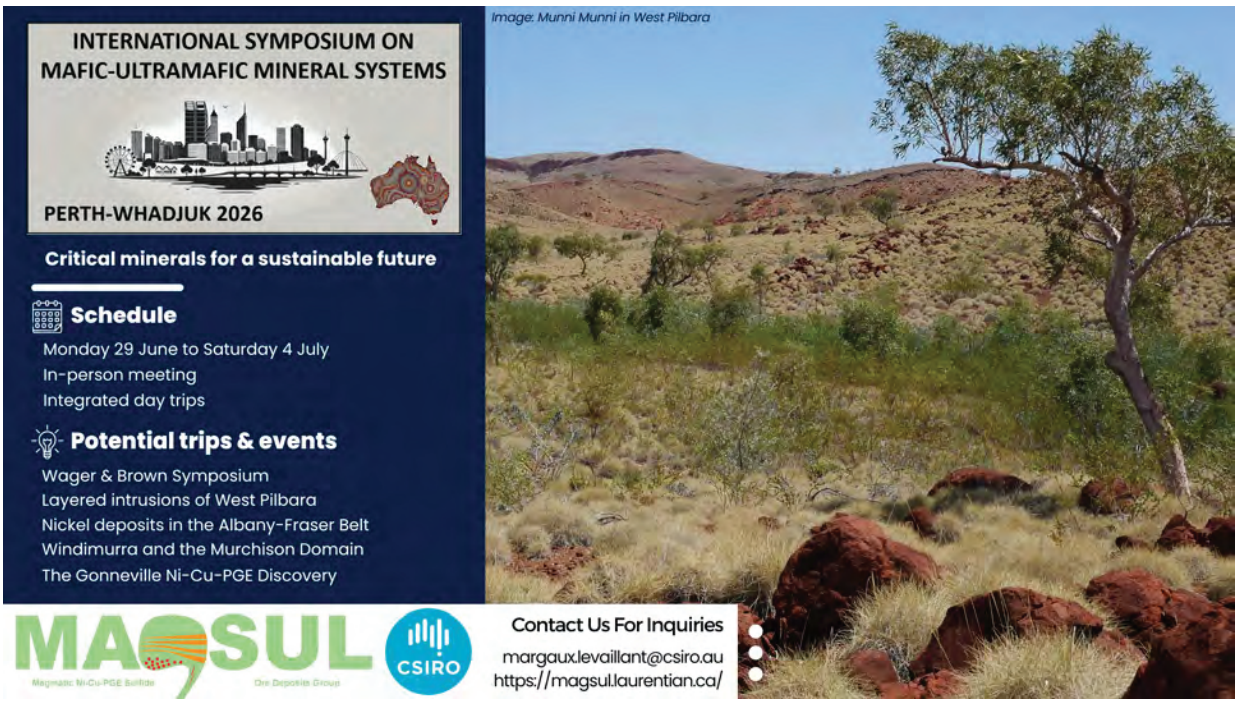


Table of Contents

One parental magma for them all: Unveiling the crystallization of the Raptor Zone, Tamarack Intrusive Deposit, Minnesota 1
Augustin, C.T.[1], Mungall, J.[1]* *1*

A Paradigm Shift: The Evolution of Nickel-bearing Ultramafic Emplacement Models 3
Aubut A. *3*

The LDI Intrusive Suite: Geology, tectonic setting, magmatic evolution, and possible controls of sulphide mineralization 5
Bain, W.B.[1,2], Tolley, J. [1], Djon, L.M.[3], Hamilton, M.A.[4], and Hollings, P.[1] *5*

Mineral geochemistry and textural relations of Ni sulfides and Co arsenides ores from the atypical Avebury nickel deposit, western Tasmania, Australia 7
Barillas-Diaz, J.L.[1], Cooke D.R.[1], Zhang, L.[1], Wei Hong[1], Cajal, Y.[1], Denholm, J.[2] and Chisnall, T.[2] *7*

Whole Rock Geochemistry and Down Hole Vectoring as an Exploration Strategy in the Coldwell Complex 8
Boucher, C.[1], Pitts, MJ. [1], Good, D.J.[2], and Laxer, M.[2] *8*

What does magmatic sulfide liquid hide? 9
Cherdantseva, M.V. [1], Anenburg M.[2], Mavrogenes J.E.[2] and Fiorentini M.L.[1] *9*

Characterization of Sulfides in Gorgona Island Komatiites: Insights into Cretaceous Mantle Plume Melting and Magmatic Processes 11
Camilo Conde[1], Mateo Espinel[1], Ana Elena Concha[2] *11*

Magmatic and hydrothermal evolution of the PGE-Cu-Ni Current Lake deposit 12
Corredor Bravo, A. P.[1], Hollings, P.[1], Brzozowski, M.[1], and Heggie, G.[2] *12*

Sulfide percolation and drainback process in magmatic conduit system in the Huangshan-Jingerquan mineralization belt 14
Deng, Y.-F.[1], Xie-Yan Song[2] and Feng Yuan[1] *14*

Weathering of non-ore grade rock from Duluth Complex deposits: Outcomes from comprehensive pre-mining geochemical characterization 16
Diedrich, T.R.[1] and Theriault S.[2] *16*

Application of FactSage to Model the Compositional Variability of the Ni-Cu-PGE Mineralization at the Main Zone of the Tamarack Intrusive Complex 18
El Ghawi, A.K.[1] and Mungall, J.E.[1] *18*

Petrophysics Applied to Magmatic Sulfide Deposits: The Physical Properties - Mineralogy Link 20
Enkin, R.J.[1] *20*

Regional changes in plume-generated stress linked to MCR (Keweenawan LIP) chonolith emplacement 23
Ernst, R.E.[1], El Bilali, H.[1], Buchan, K.L.[2] and Jowitt, S.M.[3] *23*

A proposed cryptic common thread among Ni-Cu-PGE-(Au-Te) systems spanning the boundary between Laurasia and Gondwana 25
Fiorentini, M.[1], Holwell, D.[2], Blanks, D.[3], Cherdantseva, M.[1], Denyszyn, S.[4], Ince, M.[1], Vymazalova, A.[3], and Piña Garcia, R.[5]* *25*

How exploration geologists can and should use "soft NSRs" to represent assays of Ni-Cu-PGE mineralization 27
Goldie, R.J. *27*

Characterizing the Early (Plume) and Main (Rifting) Stages in the evolution of the Midcontinent Rift 28
Good, D.J. *28*

Lithospheric structure controls for large magmatic Ni-Cu discoveries 30
Hayward, N.[1,2] *30*

Deep orogenic magmatic Ni and Cu sulfide systems in the Curaçá Valley, Brazil 32
Holwell, D.A.[1], Thompson, J.[2] , Blanks, D.E.[1], Oliver, E.[1], Porto, P.[3], Oliviera, E.[3]., Tomazoni, F.[4], Lima, A.[4], D'Altro R.,[4]., Graia, P.[4] and Sant'Ana, T.[4]. *32*

Spatial distribution, lithological associations, and geochemical signatures of Ring of Fire Intrusive Suite within the McFaulds Lake Greenstone Belt in the Superior Province: Implications for the Ni-Cu-PGE, Cr, and Fe-Ti-V Metal Endowment of the Region 33
Houlé, M.G.[1,2], Sappin, A.-A.[1,] Lesher, C.M.[2], Metsaranta, R.T.[3], Rayner, N.[4], and McNicoll, V.[4] *33*

Spatial distribution of mafic and ultramafic units in the Canadian north: Implications for critical minerals (Ni, Cu, Co, PGE) potential 35
Houlé, M.G.[1,2], Bédard, M.-P.[1], Lesher, C.M.[2], and Sappin, A.-A.[1] *35*

Copper and komatiitic magmatism – source of copper in the Sakatti Cu-Ni-PGE deposit in northern Finland 37
Höytiä, H.[1,2], Peltonen P.[1], Halkoaho, T.[3], Makkonen, H.V.[3,5] and Virtanen, V.J.[1,5] *37*

The Koperberg Suite of the Okiep Copper District - an overlooked target for magmatic nickel sulphides in a convergent margin system 39
Hunt J.P.[1], van Schalkwyk L.[1], Smart E.[1] and Benhura C.[1] *39*

A multi-methodological approach: Combining textural observations and geochronology to study the J-M Reef Package and its Hanging Wall, Stillwater Complex, Montana 41
Jenkins, M.C.[1], Corson, S.[2], Geraghty[2], E., Kamo S.L.[3], Lowers, H.[4], and Mungall, J.E.[5]* *41*

Nickel-copper-platinum group elements potential of mafic and ultramafic intrusions in northwestern Ontario 44
Jonsson, J.[1], Malegus, P.[1], Churchley, S.[1], Price, R.[1] *44*

Petrogenesis of the mineralized horizons in the Offset and Creek zones, Lac des Iles Complex, N. Ontario 46
Jonsson, J.[1], Hollings, P.[1], Brzozowski, M.[1], Bain, W.[1], Djon, L.[2] *46*

Quantum full tensor magnetic gradiometry to better define conduit type Ni-Cu-PGE targets 48
Kaski, K.[1], Smith, J.[1], Tschirhart, Victoria[1], Heggie, G., Enkin, R.[1] *48*

Exploration-Based Classification Scheme for Magmatic Ni-Cu-(PGE) Systems 50
Lesher C.M.[1] and Houlé M.G.[2,1] *50*

Thermodynamic constraints on the generation of cubanite-rich magmatic sulfides 52
Maghdour-Mashhour, R.[1], Mungall, J.[1] *52*

Constraining the Sunday Lake mineralization: A Ni-Cu-PGE deposit 54
Mexia, K.[1], Hollings, P.[1] *54*

Primitive arc magmatism and the development of magmatic Ni-Cu-PGE mineralization in Alaskan-type ultramafic-mafic intrusions 56
Milidragovic, D.[1,2], Nixon, G.T.[3], Spence, D.W.[2], Nott, J.A.[2], Goan, I.R.[2], Scoates, J.S.[2] *56*

Stratigraphy of the Grasset Ultramafic Complex and its Ni-Cu-(PGE) mineralization, Abitibi Greenstone Belt, Superior Province, Canada. 58
Milier, K.[1], Houlé M.G.[2] and Saumur B.M.[1] *58*

Geochemistry of Camp Lake Block Lac des Iles Palladium Mine, N. Ontario, Canada 60
Njipmo Ngoko, B.[1], Hollings, P.[1], Djon, L.[2] and Hamilton, M.[3] *60*

Hf-Nd-Pb isotopic evidence for variable impact devolatilization in the Sudbury Igneous Complex and its relevance for Ni-Cu-(PGE) sulfide ore formation 62
Peters, D.[1], Lesher C.M.[1] and Pattison E.[1] *62*

Deformation in mafic protoliths: Impacts from late faults on Ni-Cu-PGE mineralization at Lac des Iles Mine, Canada 64
Peterzon, J.[1], Phillips, N.[1], Hollings, P.[2], and Djon, M.L.[2] *64*

Formation of euhedral silicate megacrysts within magmatic massive sulfides 66
Raisch, D.[1], Staude S.[1], Fernandez, V.[2] and Markl G.[1] *66*

Applying Magnetic Vector Inversion (MVI) on Aeromagnetic Data in the Thunder Bay Region of the Mid-Continent Rift 68
Riahi, S.[1], Mungall J.E.[1], Ernst, R.E[1] *68*

Potential links between the Midcontinent Rift (MCR) related Baraga-Marquette dyke swarm and early MCR related magmatic Ni-Cu sulfide deposits in Michigan, USA. 70
Rossell, D.M.[1], Strandlie, J.[2]* *70*

Texture and composition of Fe-Ti oxides of the Neoarchean Big Mac mafic intrusion and its implication for Fe-Ti-V-(P) mineralization in the McFaulds Lake greenstone belt, Superior Province, Canada 72
Sappin, A.-A.[1], Houlé, M.G.[1,2], Metsaranta, R.T.[3], and Lesher, C.M.[2]* *72*

Complexly zoned pyroxenes at Kevitsa record magma mixing and survive alteration 74
Schoneveld, L.[1], Luolavirta, K.[2,3], Barnes, SJ[1], Hu, S.[1], Verrall, M.[1] and Le Vaillant, M.[1] *74*

New indicator mineral signatures for nickel sulfide exploration 76
Schoneveld, L.E.[1], Williams M.[1], Salama, W.[1], Spaggiari, C. V.[1], Barnes, S. J.[1], Le Vaillant, M. 1, Siegel, C.[1], Hu, S.[1], Birchall, R.[1], Baumgartner, R.[1], Shelton, T.[1], Verrall, M.[1], and Walmsley, J.[1] . *76*

Apatite as an indicator for volatile involvement in the genesis of the Marathon Cu-PGE deposit, northwestern Ontario 78
Shahabi Far, M.[1], Good, D.[2] and Samson, I[3] *78*

Geochemical and Petrologic Investigation of the Eagle's Nest Intrusion, McFaulds Lake Greenstone Belt, Ontario, Canada 81
Sheshnev, V.[1], Hollings, P.[1], Phillips N.J.[1], Weston, R.J.[2], Deller, M.[2] and Campbell, D.[2] *81*

Reconstitution of the Merensky Reef footwall during chamber replenishment 83
Smith, W.D.[1,2], Henry, H.[3], Maier, W.D.[4], Muir, D.D.[4], Heinonen, J.S.[5,6], Andersen, J.Ø[7] *83*

Future research areas to aid in exploration for Ni sulfides 85
Sproule, R.A.[1] *85*

Exploring the footwall: Sulfide Mineralization in the footwall Granite of the Maturi Deposit, Minnesota. 86
Steiner, R. A.[1] *86*

The Anatomy of a Cu-Ni-Co-PGE Mineralized Mafic Magmatic System: The South Kawishiwi Intrusion of the Duluth Complex, Northeastern Minnesota 90
Sweet, G.S.[1] and Peterson, D.M.[2] *90*

Multi-thermochronological records of cooling, denudation and preservation of ancient ultrabasic magmatic ore deposits: An example from the Neoproterozoic Jinchuan giant magmatic Cu-Ni sulfide deposit 94
Ni Tao[1,2], Jiangang Jiao[1], Jun Duan[1], Haiqing Yan[1], Ruohong Jiao[3], Hanjie Wen[1]* *94*

Compositional variability in olivine: New data on the occurrences of Ni and Co as guides to mineral prospectivity 95
Thakurta, J.[1], Wagner, Z.[1], Nagurney, A.[2], and Schaef, H.T.[2] *95*

The effects of diagenetic and metamorphic processes on the sulphur liberation from the Virginia Formation black shale during magmatic assimilation by the Duluth Complex, Minnesota, USA 97
Virtanen V.J.[1,2], Heinonen J.S.[2,3], Märki L.[4], Galvez M.E.[5] and Molnár F.[6] *97*

Mantle-to-crust scale chemical fractionation and sulphide saturation of the Paleoproterozoic komatiites of the Central Lapland Greenstone Belt, Finland – implications for geochemical exploration 99
Virtanen V.J.1,[2], Höytiä H.M.A.[2], Iacono-Marziano G.[1], Yang S.[3], Moilanen M.[3] and Törmänen T.[4] *99*

Ni-Cu-PGE prospectivity of the Mackenzie Large Igneous Province 102
Williamson, M.-C.[1], Rainbird, R.H.[1], O'Driscoll, B.[2] and Scoates, J.S.[3] *102*

Siluro-Devonian Mafic-Ultramafic Intrusions in New Brunswick, Northern Appalachians, and their Associated Nickel-Copper-Cobalt Sulphide Deposits: A preliminary review 103
Yousefi, F.[1], Lentz D.R.[1], Walker J.A.[2] ,Thorne K.G.[3], and Karbalaeiramezanali A.[3] *103*

Geochemistry of Archean komatiitic greenstone terranes of the Wyoming Province: implications for geodynamic setting and mineralization 105
Zieman, L.J.[1], Poletti, J.E.[1], and Jenkins, M.C.[1]* *105*

One parental magma for them all: Unveiling the crystallization of the Raptor Zone, Tamarack Intrusive Deposit, Minnesota

Augustin, C.T.[1]*, Mungall, J.[1]

[1]Mineral Deposits Laboratory, Earth Sciences Department, Carleton University, Ottawa.
*claudiaaugustin@cmail.carleton.ca

The Tamarack Intrusive Complex (TIC) is one of the mafic complexes intruded in the context of the Midcontinent Rift (MCR) system in the Midwestern United States. The Tamarack Intrusive Complex is located ca. 80 km west of Duluth, Minnesota, and it is intruded within the Paleoproterozoic (~1.85 Ga) slates and greywackes of the Thomson Formation of the Animikie Group [1,2]. It was emplaced in the Early Stage of the MCR, with a baddeleyite U-Pb age of 1105.6 ± 1.2 Ma [1] and zircon Concordia age of 1103.81±0.92 [3]. The TIC is characterized by an aeromagnetic anomaly with a broader, rounded region at the south leading into a narrower, elongated extension towards the north, extending approximately 13 km northwest-southeast and varying from hundreds of m to ca. 4 km in width [1]. Its morphology contains distinct shaped intrusive bodies, such as the ovoid-shaped Bowl Intrusion in the south and a dike-like area in the north, which includes the Raptor zone [1,2; figure 1].

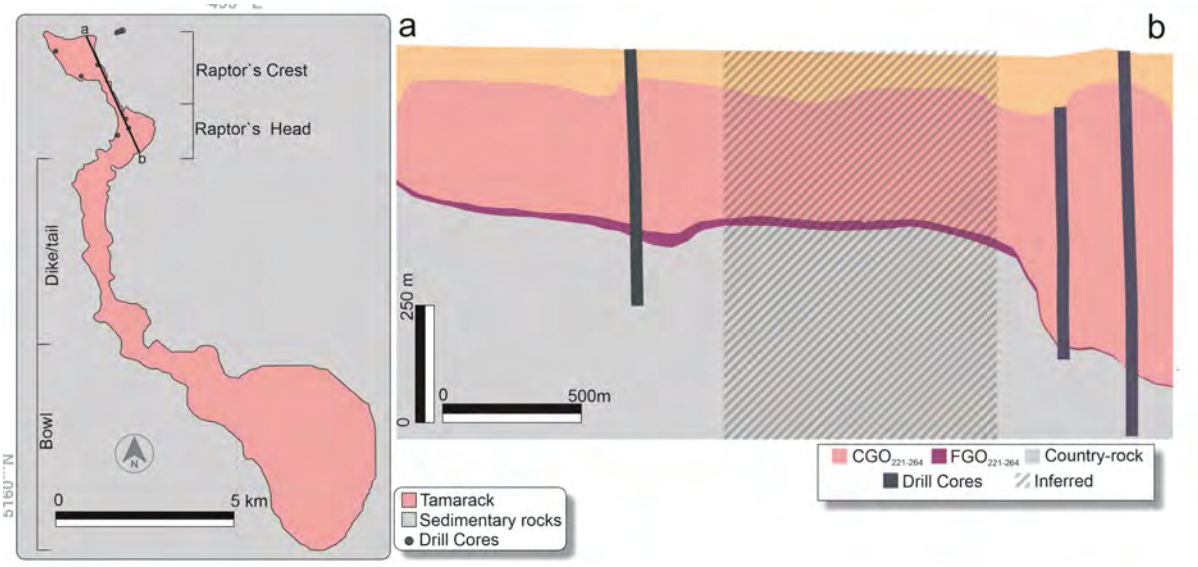


Figure 1 Schematic local geological map and cross-section of the Raptor zone.

The rocks of the Raptor zone usually show a consistent vertical sequence, except when in proximity to lateral contacts, where drill cores show a more complex variation in texture and mineralogy. Usually, the sequence consists of a basal portion of fine-grained olivine cumulate rock; therefore, this unit will be called Basal Raptor Zone Unit (BRZ), keeping the name consistent with what has been used for previous TIC studies. The most abundant primary minerals in the BRZ unit are olivine, clino- and ortho-pyroxene, and plagioclase (figure 2a). The olivine size ranges from 170 µm to 3.3 mm, but most grains are <0.5 mm. The coarser grains of olivine are more prevalent in the upper section and gradually diminish downwards. Commonly, the coarser olivine grains display plane-oriented dendritic exsolution of chromium-spinel and clinopyroxene along a consistent orientation. Above this unit is a thick, coarse-grained olivine cumulate called CGO_{Raptor} unit (figure 2b). The mineral proportions of the CGO_{Raptor} are variable along the stratigraphy; the intercumulus/cumulus ratios phases increase to the center, i.e., the cumulus phase decreases towards the upper and lower contacts. These two rock units are characterized by similar primary mineralogy and classified as feldspathic lherzolite, with the most notable difference being a variation in olivine grain size and a slight increase in earlier chromium-spinel. The subtle grain-size distinction makes it difficult to identify their gradual contact visually. The upper portion of CGO_{Raptor} shows intercalation of olivine cumulates with

pockets/domains of a varitextured gabbro. The gabbro that is intercalated with CGO and the contact with it is mostly diffused, marked only by the disappearance of olivine cumulate.

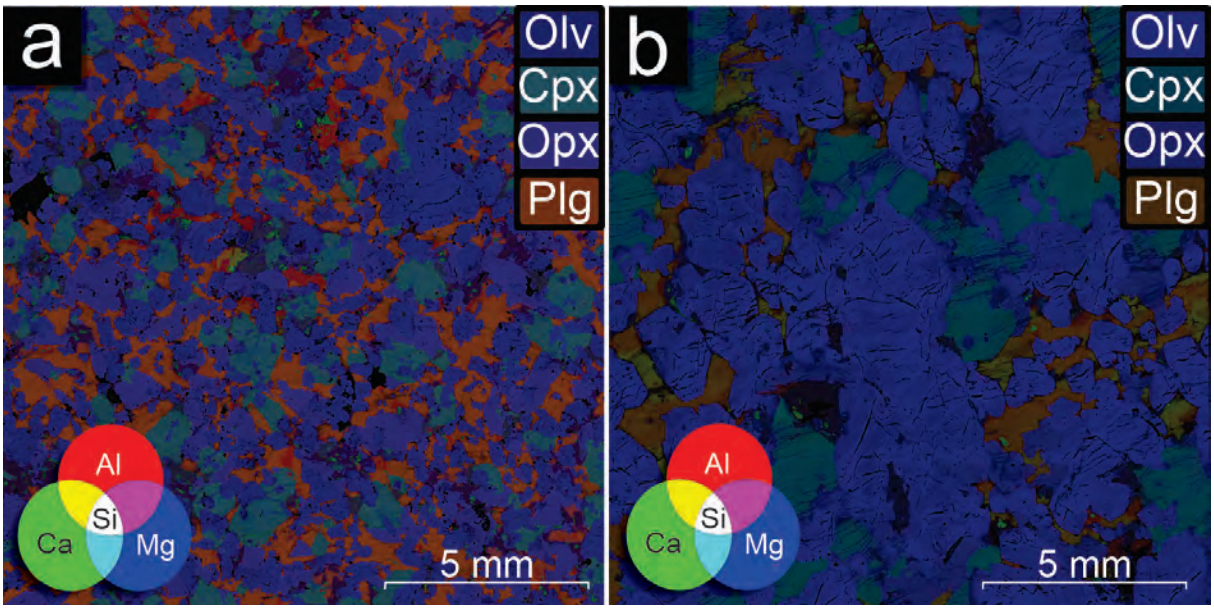


Figure 2: EDS phase maps showing textural differences between the BRZ (a) and CGO(b), with minor large olivines in a finer matrix in the BRZ compared with the more uniform CGO.

To address the composition and evolution of the melt parental to the CGO_{Raptor} rocks of the TIC, we have modeled crystallization using the alphaMELTS thermodynamic software [4-5]. The starting composition used was derived from the chilled margin of the Raptor zone. The cooling of the liquid under isobaric conditions and fO_2 at the fayalite–magnetite–quartz (FMQ) solid oxygen buffer produced a similar sequence of crystallization, modal proportions of solids to the observed bulk-rock and mineral compositions of all major constituents of the rocks of the Raptor Zone. This method successfully mirrored the crystallization order, the relative amounts of solid phases, and the chemical composition of the primary cumulus minerals. Our results show a crystallization sequence beginning with olivine (Fo_{87}), followed by clinopyroxene, chromium-rich spinel, orthopyroxene, and plagioclase. Specifically, at 1170 °C, the simultaneous formation of olivine and clinopyroxene, adjusted in proportion, reflects the varied compositions within the unit. Moreover, the liquid remaining at this temperature aligns with the mineralogy and composition observed in the gabbro unit. Using the same composition and parameters but slightly increasing the f_{O2} levels to NNO, the model predicts that spinel forms earlier, leading to similar BRZ composition and mineralogy. This change explains the prevalent spinel and the observed exsolution textures between cr-spinel and clinopyroxene in the coarse-grained olivine—features typically linked to variations in cooling rates and oxygen fugacity.

Our thermodynamic analysis shows that the three main rock types in the Raptor Zone can originate from a single magma source, with only minor adjustments needed to explain their variations. The categorization into BRZ and CGO units appears to be based on slight differences in oxidation states and crystal sizes rather than suggesting they are from two separate magmatic intrusions. The findings suggest these units might represent different stages of the same magmatic event.

References:

[1] Goldner B (2011) Min University Thesis
[2] Taranovic V et al. Lithos 212-215 (6-31)
[3] Bleeker W et al. (2020) Geol Survey of Canada, Open File 8722, p. 7–35
[4] Asimow P D (1998) Am. Mineral. 83 (1127-1132)
[5] Smith P M and Asimow P D (2005) Geochem. Geophys. Geosyst. 6(1-8)

A Paradigm Shift: The Evolution of Nickel-bearing Ultramafic Emplacement Models

Aubut A.

M Sibley Basin Group Ltd., PO Box 304, Nipigon, Ontario.
sibley.basin.group@gmail.com

An important class of nickel deposit are those hosted by stratabound dunite-peridotite bodies. This class includes the Kambalda district of Australia, Pechenga in the Kola Peninsula of western Russia, Kabanga in south-central Africa, the Shaw Dome area of northern Ontario, Raglan in northern Quebec and Thompson in northern Manitoba. All have been, or currently are attributed to the intrusion of ultramafic sills [e.g. 2,8,9]. Key evidence in support of this model is that the ultramafic bodies typically exhibit at least some differentiation and are sub-concordant to the host sediments. This tendency to default to an intrusion model now includes the Tamarack deposit in Minnesota [11] even though another model, one that incorporates extrusion, may be just as valid.

Despite the prevalence of the intrusion model there are many nickel deposits hosted by ultramafic bodies that display clear evidence of being the product of extrusive flows, often exhibiting the same key features used to invoke an intrusive origin [e.g. 1,3,4,7].

Major komatiite hosted nickel deposits share some common features: 1) the nickel mineralisation is hosted by ultramafic rocks; 2) the sulphides are at the stratigraphic base of the host ultramafics; 3) the ultramafic rocks are hosted by, or in contact with, sulphidic and carbonaceous argillaceous rocks; 4) the ultramafic bodies are stratabound and generally conformable to the host lithology; and 5) they are hosted within extensional basins usually with a significant sedimentary component with Kambalda being the one exception.

As Maier et al. [3] point out, the reason magmatic feeder systems rather than large intrusions are important hosts to economic nickel deposits is because of flow dynamics. Rice and Moore [11] have studied flow dynamics and concluded that open-channel flows were turbulent, and that this turbulence was required to expose the sulphides present to enough magma to generate the tenors observed. This turbulence explains how sedimentary sulphides can be integrated and assimilated by ultramafic magma and result in significant nickel tenors, nickel in 100% sulphide [4,5].

Turbulent flow is difficult, if not impossible, to explain by a simple intrusive mechanism. In addition, to get the size of deposit observed there needs to be significant volumes of ultramafic magma. The one environment that does allow turbulent flow to take place, and have the volumes required, is with high volume surface flows with gravity settling of the magmatic and assimilated sedimentary sulphides, along with significant magma mixing to get the observed partitioning of the silicate nickel into the sulphides.

But there is a density “problem” in that ultramafic magmas are typically denser than the host rocks, especially when they are sedimentary. This paradox is typically glossed over or totally ignored. For example, see Hubbert et al. [5]. Ultramafic magma is not buoyant as the contrast is negative. So, how were these high-density liquids able to ascend through the crust? When rocks melt, they become about 10% less dense. In the case of ultramafic rocks, they have an average density of about 3.1 grams per cubic centimetre (g/cc) depending on the proportion of olivine present which has a density of 3.27–4.27 g/cc. Hubbert et al. [5] assumed a value of 2.8 g/cc. The average crust has a density of 2.7 g/cc or less and thus buoyancy could not have taken place. To move upward from the mantle through the crust there must have been a mechanism other than buoyancy.

An alternative mechanism proposed in the literature is “overpressure” defined by Walwer et al. [12] as “the difference between the pressure inside the magma and the local pressure acting orthogonal to the magma body wall.” Melting of the mantle creates magma plumes that move upward due to buoyancy to the Mantle-Crust boundary where the magma collects and then moves laterally thus creating extensional forces in the overlying crust. This accumulating magma would be constrained by the overlying lithostatic load and in doing so would build up overpressure. Eventually the crust would thin enough such that vertical fractures would form allowing the trapped magma to escape, not through buoyancy but due to the built-up overpressure exceeding the lithostatic load. At surface the hot, dense ultramafic magma would then flow over, and into, deep water sediments where the magma would mechanically and thermally erode and assimilate sulphide rich sediments.

This mechanism would explain the correlation with rift basins, as well as how a dense magma can penetrate a less dense substrate and produce the type of volumes required to attain high R values, while also generating the turbulent flow needed to assure incorporation, and assimilation of sulphide with resultant nickel partitioning required to get the high tenors typical of most sulphide deposits found associated with extensional basins. An extrusive model is more compatible with these commonalities and issues. It explains why the host ultramafic bodies are stratabound. It provides a better mechanism for incorporating sedimentary sulphide. It provides more opportunity for high R values creating high tenors. And it presents a tectonic environment, rifted basins, that can be easily targeted.

Currently nickel is an under explored commodity primarily because, using the intrusion model, limited opportunities are available. The flow model on the other hand is more robust as it does a better job of explaining things like the high volumes of magma needed and the fluid dynamics required to ensure thorough mixing of the denser sulphides with the magma to attain the tenors present in these deposits. In addition, being tied to a specific tectonic event, rifting, it is not fixed in time or place as much as the intrusive model is. While intrusive environments do exist where these conditions are met, they are always in primary magma conduits.

References:

[1] Arndt NT (1975) Unpub Ph.D. Thesis, U of T.
[2] Bleeker W (1990) Unpub PhD Thesis, UNB.
[3] Hill RET et al. (1995) Lithos 34: 159-188.
[4] Hubbert HE and Sparks RSJ (1985) J of Petro 26-3: 694-725.
[5] Hubbert HE et al. (1984) Nature 309:19-22.
[6] Maier WD et al. (2001) Cana Mine 39:547-556.
[7] Marston RJ et al. (1981) Econ Geol 76:1330-1363.
[8] Melezhik VA et al. (1994) Tran Inst Min Meta B 103:B129-B145.
[9] Naldrett AJ (1981) Econ Geol 75th Anni Volu :628-685.
[10] Rice A and Moore JM (2001) Cana Mine 39:491-503.
[11] Taranovic V et al. (2018) Econ Geol 113-5:1161-1179.
[12] Walwer D et al. (2021) Phys of the Earth and Plan Inte 312,

The LDI Intrusive Suite: Geology, tectonic setting, magmatic evolution, and possible controls of sulphide mineralization

Bain, W.B.[1,2], Tolley, J. [1], Djon, L.M.[3,] Hamilton, M.A.[4], and Hollings, P.[1]

[1] Department of Geology, Lakehead University, Thunder Bay, ON P7B 5E1, Canada
[2] British Columbian Geological Survey, Victoria, BC V8T 4J1, Canada
[3] Impala Canada, Thunder Bay, ON P7B 6T9, Canada
[4]Department of Earth Sciences, University of Toronto, Toronto, ON M5S 3B1, Canada

---

The Archean Lac des Iles (LDI) complex hosts a world-class platinum group element (PGE) deposit. This mafic-ultramafic intrusive complex is situated near the suture between the Wabigoon and Quetico subprovices and is spatially associated with a suite of satellite intrusions: the Tib Lake, Legris Lake, Wakinoo Lake, Demars Lake, Dog River, and Buck Lake intrusions- known collectively as the LDI intrusive suite (Fig 1 a). Textural, petrographic and geochemical similarities between the LDI Mine Block intrusion and the LDI intrusive suite suggest a genetic association and potentially a comparable degree of PGE mineralization. Here, we present an overview of the geology of the LDI intrusive suite and provide new U-Pb age dates, Sm-Nd isotopes, and parental melt modelling.

Zircon U-Pb ages for the Buck Lake (2698.1 $\pm$ 1.6 Ma), Wakinoo Lake (2696.6 $\pm$ 0.8 Ma), Demars Lake (2694.1 $\pm$ 1.5 Ma), Legris Lake (2690.6 $\pm$ 0.8 Ma), Dog River (2689.9 $\pm$ 0.7 Ma), and Tib Lake (2685.9 $\pm$ 1.6 Ma) intrusions show a spatial trend of younging to the north and demonstrate a temporal association with the Lac des Iles Mine Block intrusion (2689.0±1.0 Ma; [1]; Fig 1 b). Whole rock εNd_T values from the Wakinoo Lake, Tib Lake, Legris Lake, and Lac des Iles intrusions overlap and similarly display a trend of increasingly negative values with decreasing age (Fig 1 c). These patterns likely reflect the initial assimilation of Wabigoon tonalite country rock early in the magmatic evolution of the LDI intrusive suite and progressively more assimilation of Quetico metasedimentary rocks in later stages.

Model parental magma compositions for the LDI intrusive suite produce similar trace element profiles with highly fractionated REE content, moderately negative Ta-Nb and Zr-Hf anomalies, and strong enrichment in the large ion lithophile elements. This pattern is consistent with an arc setting and might indicate a common source reservoir of parental melt. The observed Sm-Nd isotopic signature of the LDI intrusive suite supports this interpretation and suggests that host rock assimilation was a main control of the magmatic differentiation of individual intrusions. However, magma mixing may also have occurred during the formation of the Tib Lake and North LDI intrusions, as indicated by the more primitive compositions of individual cyclic units [2].

Magmatic sulphides from the Legris Lake intrusion have $\delta^{34}S$ values that overlap the mantle range but trend toward the composition of Wabigoon tonalite [3]. This suggests that external S addition drove sulphide saturation during its formation. However, a comparison of whole rock S/Se and Cu/Pd ratios of mineralized lithologies suggests sulphide melt retention during emplacement was a key control on the scale of sulphide mineralization in the Legris Lake intrusion and other intrusions of the LDI intrusive suite.

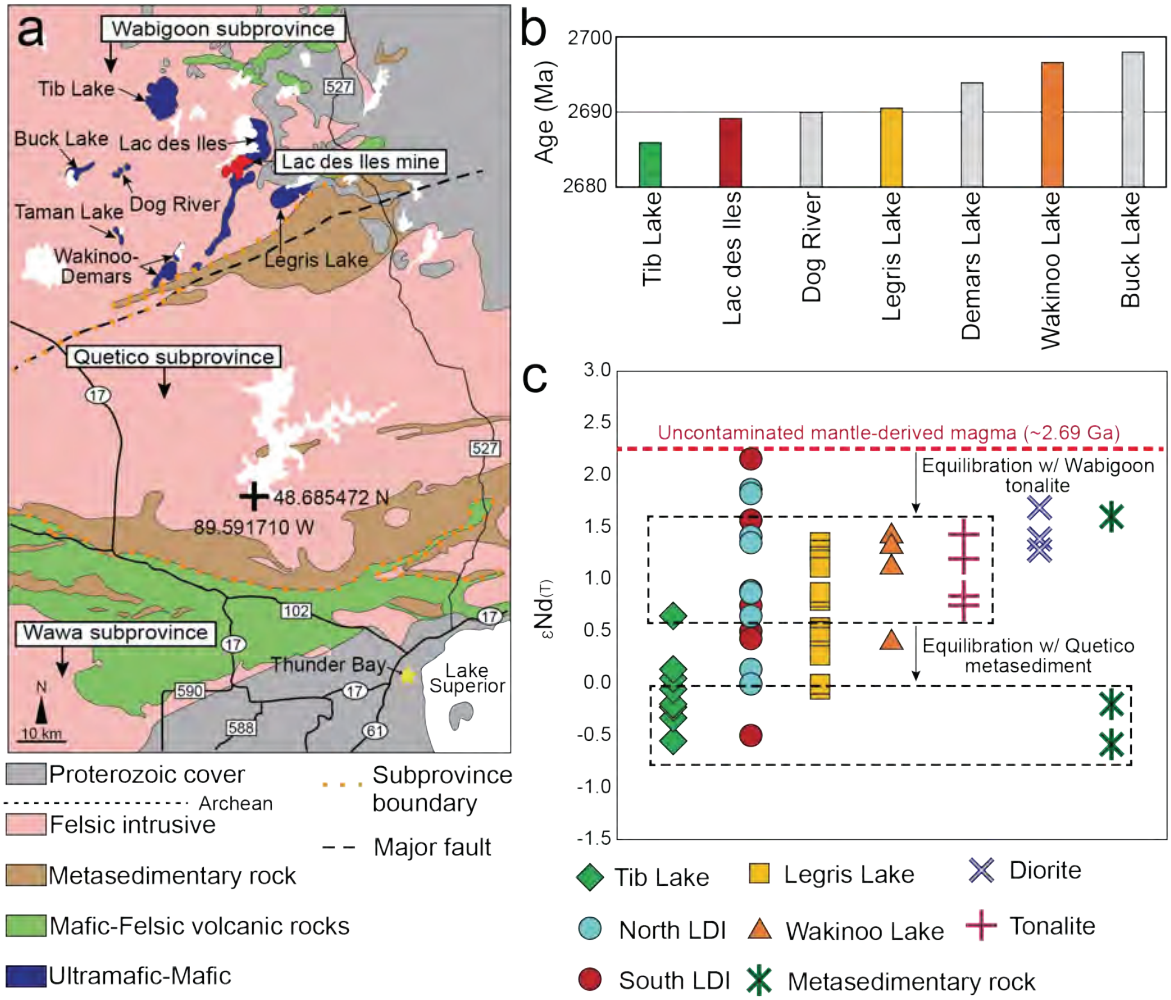


Fig 1. **a.** Regional geologic map showing locations of Thunder Bay, the Lac des Iles mine (in red), and the Lac des Iles intrusive suite (in blue). **b.** U-Pb ages for individual intrusions in the Lac des Iles intrusive suite. **c.** Whole-rock εNd_T values for the LDI intrusive suite and host rock lithologies. North LDI, South LDI and Shelby Lake diorite data from Brügmann et al. [4]

References:

[1] Stone D (2010) Ontario Geological Survey, Open File Report 5422:1–130
[2] Djon LM et al. (2017) Can Min 55:349-374
[3] Bain WM et al. (2023) Min Deps doi:10.1007/s00126-023-01183-x
[4] Brügmann MJ et al. (1997) Precambrian Res 81:223-239

Mineral geochemistry and textural relations of Ni sulfides and Co arsenides ores from the atypical Avebury nickel deposit, western Tasmania, Australia

Barillas-Diaz, J.L.[1], Cooke D.R.[1], Zhang, L.[1], Wei Hong[1], Cajal, Y.[1], Denholm, J.[2] and Chisnall, T.[2]

[1]Centre for Ore Deposit and Earth Sciences (CODES), University of Tasmania, Private Bag 79, Hobart, TAS 7001, Australia, joseluis.barillasdiaz@utas.edu.au
[2]Avebury Nickel Mine, Trial Harbour Road Zeehan TAS 7469, Australia

---

The unusual Avebury metasomatic nickel sulfide deposit in western Tasmania was discovered in 1998 and is the best-known case of an economic hydrothermal-remobilized Ni deposit [1]. The nickel sulfide ores are hosted in the Middle Cambrian serpentinized peridotites of the allochthonous mafic-ultramafic ophiolite complex, while cobalt arsenides within the Neoproterozoic Crimson Creek volcanoclastic sequence. The Avebury Ni deposit lies in the halo of the strongly fractionated, reduced Devonian Sn-mineralized ~360 Ma Heemskirk granite [2]. Apatite U-Pb ages from 374 ± 14 Ma to 347 ± 15 Ma from mineralized serpentinite and Crimson Creek skarn imply that hydrothermal remobilization of Ni-Co occurred at Avebury due to hydrothermal fluids derived from Devonian Heemskirk granite. The compositional and mineralogical transformations associated with chemical reactions triggered by the response of hydrothermal fluids from the granite resulted in a magnesian-skarn including brucite + diopside + hedenbergite + augite and tremolite-actinolite in the ultramafic rocks and pyroxene + garnet + axinite-(Mg) ± ludwigite and tourmaline in the volcanoclastic rocks of Crimson Creek.

The dominant nickel sulfide mineral at Avebury is pentlandite, which is associated with pyrrhotite and minor chalcopyrite. Pentlandite is hosted in olivine + clinopyroxene cumulates, which have been serpentinized in most cases where pentlandite occurs mainly as relatively coarse-grained sulfide blebs with pyrrhotite. Pentlandite also occurs in relatively fine-grained shattered disseminations within actinolite. The coarse-grain pentlandite is fractured and encapsulated by magnetite, and Ni-arsenides have partly replaced pentlandite grains. Pentlandite has altered slightly along grain edges to violarite and pyrite. Chalcopyrite may occur as exsolution intergrowths in millerite and pentlandite. The high-resolution XRF scanning analysis from core rock and whole rock assay from mineralized serpentinite samples show positive Ni/Ti and Ni/Cr ratios and discriminated between two nickel mineralization zones. The Ni vs MgO diagram shows that nickel mineralization is hosted primarily in MgO-rich and pyroxene-rich serpentinites. In contrast, the low-MgO and Cr-rich serpentinite negatively correlate with Ni. However, the serpentinite FeO-rich positively correlates with pentlandite rich in cobalt. Although some serpentinite horizons have strong metasomatism, all the serpentinized ultramafics have >16% magnetite and are depleted in Al_2O_3, TiO_2, Sr, Y and Zr. The whole rock assay results indicate a negative correlation of Cu and Zn with Ni. Mineral characterization using an automated energy dispersive X-ray spectroscopy mineral mapping (AMICS) shows nickel sulfides and cobalt arsenides do not coexist in the same mineral assemblage. Cobaltite, alloclasite and minor glaucodot are the two main arsenides of cobalt restricted to the magnesian-skarn of prehnite + augite and hedenbergite in Crimson Creek. The laser ablation analyses (LA-ICPMS) in pentlandite minerals from the Avebury deposit do not show strong correlations with other elements. However, a small group of pentlandite shows incipient correlations between Au, Ag and Co. Analysis in pentlandite and pyrrhotite shows some crystals with Pt values between 2.5 to 4.0 ppb. Cobaltite shows a slight trend in which the cobalt content decreases as the Ni content increases. On the other hand, the pyrite crystals show a strong correlation between Au, Co, Cu and Ni. The correlation between nickel and cobalt in pentlandite is modest in the Avebury deposit compared to Trial Harbour pentlandite, which shows strong correlations between these two elements. The paragenesis relationships, mineral textures, and compositional trends exhibited by Ni-Co ores at the Avebury deposit provide evidence of a multi-stage depositional history.

References:

[1] Keays R and Jowitt S (2013) Ore Geology Reviews 52: 4–17

[2] Hong W eta al. (2017) Gondwana Research 46: 124–140

Whole Rock Geochemistry and Down Hole Vectoring as an Exploration Strategy in the Coldwell Complex

Boucher, C.[1], Pitts, MJ. [1], Good, D.J.[2], and Laxer, M.[2]

[1] Generation Mining, Marathon, ON, Canada. cboucher@genpgm.com
[2] Department of Earth Sciences, Western University, London, ON N6A 5B7, Canada

---

The Eastern Gabbro-Basalt Suite of the Coldwell Complex has been widely explored for decades by various operators, resulting in the discovery of numerous exploration Prospects and Deposits. Although numerous economic and academic studies have been completed on the flagship Marathon Deposit, Sally deposit, and Boyer and Four Dams occurrences, little work has been done to advance understanding of relationships between trace-element geochemistry and mineralization at the Complex-sized scale. For instance, earlier work has described stratigraphic and trace-element relationships between metabasalt and the mineralized Two Duck Lake intrusions, and between mineralized and unmineralized phases of the host gabbro. In this presentation we examine these relationships at a larger scale and test for their usefulness as an exploration vector tool in the Coldwell Complex.

A second objective of this presentation is to examine the 3D spatial relationships between Cu/Pd and Cu/S and the associated mineralization style, footwall topography and faulting at the Marathon deposit. This study takes advantage of the dynamic conduit model that it is used to explain many features of Cu-PGE mineralization in the Marathon Series rocks. For instance, the spatial distribution of mineralization relative to topographic lineaments is explained by magma transport along early fault zones that were reactivated late in the history of the complex to create the lineaments. This study also takes advantage of significant changes or inflection points in the trends for Cu/Pd, Cu/S, Pd/Au, and Cu/Ni values between the three dominant mineralization styles in the Two Duck Lake gabbro: Footwall Zone, Main Zone, and W-Horizon. Large deflections in the downhole trends of these ratios, particularly Cu/Pd, act as a proxy for identification of individual pulses of magma (or stacking of intrusions). Although contacts between pulses are difficult to recognize in thick packages of gabbro, they can be identified by sharp changes in Cu, Pd and S content or, more importantly, by inflection points in metal ratio proxy trends (Cu/Pd or Cu/S). Here we present results of our study for these factors at the deposit scale and propose key features that might be useful for recognizing settings in the conduit model from down hole assay data.

The implementation of geochemistry and downhole vectoring will continue to advance and provide insight into refined geological modelling. Future work on in-depth classification of units will include Layered Series rocks and proximity to major structures, differentiation of TDL Gabbro based on mineralogy and texture, origin of the two varieties of oxide-melatroctolite pods and relationship to underlying conduits and identifying key indicators to aid in lithological classification based on basic assay package.

What does magmatic sulfide liquid hide?

Cherdantseva, M.V. [1], Anenburg M.[2], Mavrogenes J.E.[2] and Fiorentini M.L.[1]

[1] Centre for Exploration Targeting, School of Earth Sciences, University of Western Australia, Australia, maria.cherdantseva@uwa.edu.au
[2] Research School of Earth Sciences, Australian National University, Canberra, Australia

---

In natural examples, magmatic sulfides hosted in mafic-ultamafic intrusions, regardless of textural variability (massive, globular, net-textured, disseminated), are almost ubiquitously found in spatial association with alkali-, lithophile- and volatile-rich minerals, such as phlogopite, ilmenite, chlorite, amphibole, calcite, etc. These minerals display diverse textures, either surrounding sulfide margins or found inside sulfides as euhedral crystals as well as irregular, rounded or vermicular inclusions. The presence of the listed minerals in association with sulfides has been previously attributed to secondary processes, late circulation of fluids or highly differentiated melts [1, 2, 3]. However, existing models fail to provide a satisfactory explanation on why these alkali-, lithophile- and volatile-rich minerals so often occur in direct contact with sulfides or as inclusions in them.

Here, we argue that the common spatial association of alkali-, lithophile- and volatile-rich minerals with magmatic sulfides could be explained by the partial dissolution of lithophile and volatile elements in sulfide liquid at high temperature and pressure and their subsequent release upon cooling of the system. Indeed, several experimental studies show that at high temperatures and additional various conditions (e.g., oxygen fugacity, melt composition), regular magmatic sulfide liquid has the capacity to dissolve a wide range of lithophile elements (such as Al, Mg, Mn, Ti, Ca, K, etc. [4, 5, 6]), halogens (Cl, Br, F, I [6, 7]) and water [8]. However, there has never been a clear connection made between formation of alkali-, lithophile- and volatile-rich minerals in close spatial association with sulfides and the potential chalcophile behaviour of some lithophile elements and halogens dissolved in sulfide liquids under some specific conditions. We put forward the idea that a genetic link between these elements and sulfide liquid could not only explain the formation of volatile-rich halos around sulfides but also elucidate the cryptic link between magmatic and hydrothermal mineralising processes as explained below.

Our new experiments were conducted to investigate the potential of magmatic sulfide liquids to dissolve K, Na and chloride in magmatic conditions (1200-850 °C, 5 kbar, ΔFMQ = –1.5). All experiments were run using piston cylinder apparatus at the National Australian University. The experiments were run in 3.5 mm Pt capsules lined with graphite to prevent sulfides from coming into contact with the metal capsule. The Pt capsule was welded and enclosed within 5/8-inch MgO-Pyrex-NaCl assembly (Fig. A1a). Temperature measurement was carried out with a B-type Pt-Rh thermocouple.

We investigated the fate of these elements as the system crystallizes, both in isolation and in equilibrium with silicate melts. The experiments where sulfide liquid was mixed with K, Na and Cl without presence of silicate melt had layered set-up to monitor the melting and mixing process between sulfide phases, alkalis and Cl. Three runs with the same set up and and starting composition were heated up to 1100 °C (at 5 kbar) and then cooled down and quenched at different temperatures (1100 °C, 850 °C and 300 °C). The result of the experiments show that at high temperature the initial layering is not retained and sulfide liquid homogenizes, dissolving ~3 wt% of K, 0.3 wt% of Na and 0.03 wt% of Cl. During quenching, sulfide liquid forms elongated skeletal crystals of mss and interstital residual mixed sulfide matrix. Medium temperature experiment consisted of rounded grains of Ni-rich monosulfide solid solution (mss) in a Cu-rich fine-grained matrix interpreted as quenched liquid. The mss contains negligible concentrations of alkali elements and Cl (< 0.03 wt% of Na, <0.03 wt% K and < 0.003 wt% Cl), whereas the Cu-rich sulfide matrix contains 2.7 wt% of K, 0.6 wt% of Na, and 0.6 wt% of Cl. Slowly cooled to 300 °C experiment contain

alkali- and Cl-free pyrrhotite, pentlandite, chalcopyrite and alkali-rich sulfides such as murunskite ($K_2(Cu,Fe)_4S_4$) and djerfisherite ($K_6(Fe,Cu,Ni)_{25}S_{26}Cl$).

The second experiments were designed to examine the behavior of sulfides in equilibrium with silicate melt. The high temperature experiment was quenched after heating to 1250 °C (at 5 kbar), resulting in the formation of sulfide globules comprising elongate skeletal crystals of alkali-free mss intergrown with sulfide matrix of mixed Fe-Ni-Cu composition containing up to 2 wt% Na and 1.3 wt% K, along with 0.1 wt% chloride. Another experiment was slowly cooled from 1250 °C to 300 °C (at 5 kbar) and crystallized to an alkali-rich silicate matrix composed of chromian spinel, nepheline, apatite, Na–K–Ca-carbonate, clinopyroxene and sulfide globules. The sulfide blebs differentiated to pyrrhotite, pentlandite, chalcopyrite and bornite with K, Na or Cl concentrations below detection limit.

Results of our experiment show that sulfide liquid can dissolve a substantial amount of alkalis and Cl at high pressures and temperature at geologically relevant redox conditions. Incorporation of these elements into the melt network of magmatic sulfide liquid can affect its physical properties. Thus, the presence of alkalis and Cl dissolved in sulfides could play a crucial role in reducing the melting point of mantle sulfides, akin to the effect of other fluxes on silicate assemblages [9]. Consequently, the presence of alkalis, Cl and water may enhance sulfide melting in localized mantle domains, where molten metal-rich sulfides can be extracted and incorporated into ascending magmas without the requirement of anomalously high heat triggers, widening the spectrum of geodynamic scenarios where fertile melts can be generated on a global scale [10].

Our slowly cooled experiments indicate that alkalis and Cl become immiscible with sulfide liquid during cooling and crystallization. Indeed, magmatic sulfides have never been documented to contain any impurities of lithophile elements or halogens. The only known K and Cl-rich sulfides, such as djerfisherite and murunskite, are very rare and form only in extremely alkali-rich conditions [11]. As a result of immiscibility, it is proposed that sulfide liquid “sweats out” the alkalis and chloride during magma crystallization. This process erases any direct evidence of the former presence of alkalis and Cl in the sulfide itself. Instead, it leaves behind a subtle association of alkali silicates surrounding them, including phlogopite, amphibole, scapolite, and Cl-apatite. However, this process of direct exsolution of Cl, K, Na and water [8] contributes into the metal butget of overlying hydrothermal systems. Magmatic hydrothermal fluids enriched in chloride and alkalis may be important carriers of Cu, Au, and PGEs [e.g., 12] which tend to form aqueous chloride complexes. The exsolution of chalcophile metals, alkalis, and Cl as well as their partitioning into magmatic-hydrothermal fluids supports previous models that link mineralized deep magmatic systems to overlying hydrothermal systems [13].

In summary, alkalis and chlorine play a pivotal role in enhancing metal extraction from the mantle by reducing the melting point of sulfides and lowering their density. During crystallization, these elements exsolve from sulfide liquids into adjacent silicates and late fluid phases, thus increasing the mineralizing potential of magmatic-derived hydrothermal fluids.

References:

[1] Kanitpanyacharoen W and Boudreau AE (2013) Miner Depos 48(2):193–210
[2] Yuan Q et al. (2023) Lithos 438-439:107014
[3] Ballhaus C and Stumpfl E (1986) Contrib Mineral Petrol 94(2):193-204
[4] Kiseeva E and Wood B (2015) Earth Planet Sci Lett 424:290-294
[5] Wood B and Kiseeva E (2015) Am Mineral 100:2371-2379
[6] Steenstra E et al. (2020) Geochim Cosmochim Ac 273:275-290
[7] Mungal J and Brenan J (2003) Can Min 41(1):207-220
[8] Wykes J and Mavrogenes J (2005) Econ Geol 100:157-164
[9] Sakamaki T (2017) Chem Geol 475:135-139
[10] Holwell DA et al. (2019) Nat Commun 10(1):1–10
[11] Osadchii VO et al. (2018) Contrib to Mineral Petrol 173 (5):1–9
[12] Sullivan N et al. (2022) Geochim Cosmochim Ac 316:230-252
[13] Heinrich C and Connolly J (2022) Geol 50(10):1101-1105

Characterization of Sulfides in Gorgona Island Komatiites: Insights into Cretaceous Mantle Plume Melting and Magmatic Processes

Camilo Conde[1], Mateo Espinel[1], Ana Elena Concha[2]

[1]University of Geneva, [2] Universidad Nacional de Colombia

---

The demand for copper, aluminum, nickel, zinc, and lead is ever increasing. Advances in new models and technology are helping the exploration industry to discover new resources of these important minerals and meet the requirements of the global population. This theme will include all aspects of exploration of these metals, from genesis and mineral processing to the circular economy.

Komatiites from Gorgona Island, Colombia, are unique as the only Phanerozoic spinifex-textured ultramafic lavas and the only Cretaceous-age occurrences globally reported (dated at approximately 90 million years old (Kerr et al., 1997)). These rocks have been central to discussions about high temperature melting in mantle plumes, with recent studies developing into the melting event's details, source materials, and melting depths. This study is the first focus on sulfides within Gorgona komatiites, showing the presence of interstitial sulfides, typically larger than 20 microns. Through detailed petrography, SEM imaging, and QUEMSCAN analysis, the research aims to identify and characterize these sulfides, identifying their composition and relating them with magmatic processes. Key sulfides identified include chalcopyrite, pyrite, pentlandite and pyrrhotite positioning Gorgona as a significant new site for magmatic sulfides studies.

For the sulfide characterization, the electron microprobe analyzer (EPMA), provide precise compositional data crucial for understanding the magmatic evolution. This is particularly important as it helps determine the timing of sulfur saturation, which in turn reveals whether nickel or copper with PGE becomes more prevalent. Understanding these processes is vital for developing nickel-copper-PGE models and gaining insights into mantle-core conditions, underscoring the geological significance of the Gorgona komatiites.

Magmatic and hydrothermal evolution of the PGE-Cu-Ni Current Lake deposit

Corredor Bravo, A. P.[1], Hollings, P.[1], Brzozowski, M.[1], and Heggie, G.[2]

[1]Department of Geology, Lakehead University, 955 Oliver Road, Thunder Bay, ON P7B 5E1 Canada. acorredo@lakeheadu.ca
[2]Clean Air Metals, 1004 Alloy Drive, Thunder Bay, ON P7B 6A5 Canada. gheggie@cleanairmetals.ca

---

The Mesoproterozoic (1,106.6 ± 1.6 Ma [1]) Current intrusion forms part of the PGE-Cu-Ni mineralized Thunder Bay North Intrusive Complex. The Current intrusion consists of a northwest-trending conduit-type body (wehrlite, lherzolite, olivine gabbronorite ± troctolite) associated with the earliest stages of the Midcontinent Rift System (MRS; [2]) that intruded Archean rocks of the Quetico Basin and is associated to the Quetico Faults System that cross the boundaries between the Quetico basin and the Wabigoon terrane in the Superior Province [3]. To date the intrusion hosts four mineralized zones (Fig. 1); the Current and Bridge Zone in the northwest, the Beaver-Cloud Zone in the middle, and the 437-Southeast Anomaly (SEA) Zone is in the southeast [4].

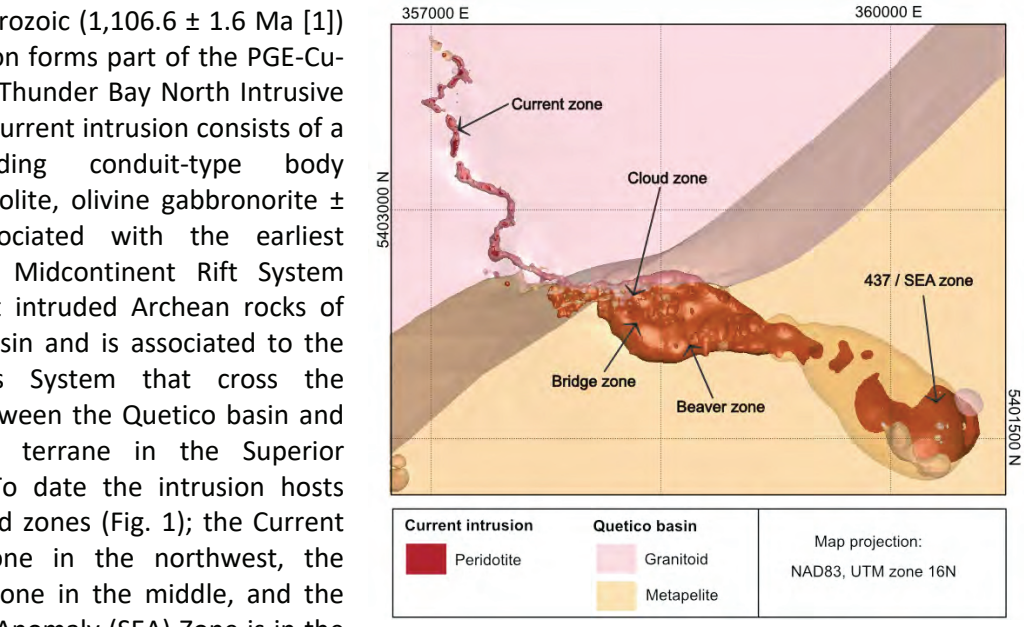


Figure 1. Schematic model of the Current intrusion and the Quetico country rock. Illustration compiled in Leapfrog using data provided by Clean Air Metals Inc.

Geochemical analysis of the intrusion reveal a well-defined primitive mantle-normalized pattern resembling ocean island basalt, characterized by LREE enrichment and small positive anomalies in Nb, La, and Ce relative to Th, suggesting no, or minimal, crustal contamination. The La/Sm_n values in samples from the Current intrusion range from 1.8 to 2.6, consistent with previous studies and suggesting the originated from an enriched mantle plume. The enriched composition of the magma in the intrusion aligns with other mineralized and unmineralized intrusions related to the MRS, including the Escape, Seagull, Lone Island intrusions, and the Nipigon Sills [5,6,7,8]. The intrusion has slightly lower Sr_i (0.7021 to 0.7043) and ε_{Nd} (-1.18 to -4.02) than the typical values of the mantle source at 1100 Ma as well as the Nipigon Sills, Seagull intrusion, and Coubran volcanics [5,6,9]. Given the absence of geochemical anomalies that indicate assimilation of the Archean crust, an enriched SCLM is suggested to have interacted with the parental magma to generate the slightly negative ε_{Nd} values. Stable isotope analysis suggest that the rocks of the intrusion underwent interactions with magmatic fluids (δ^2H from −40 to −80‰, $\delta^{18}O$ from 5.5 to 7.0‰; [10,11]), meteoric fluids (δ^2H <-80‰, $\delta^{18}O$ <5.5‰; [12]), and crustal derived fluids ($\delta^{18}O$ >7‰; Figure 2; [13,14]).

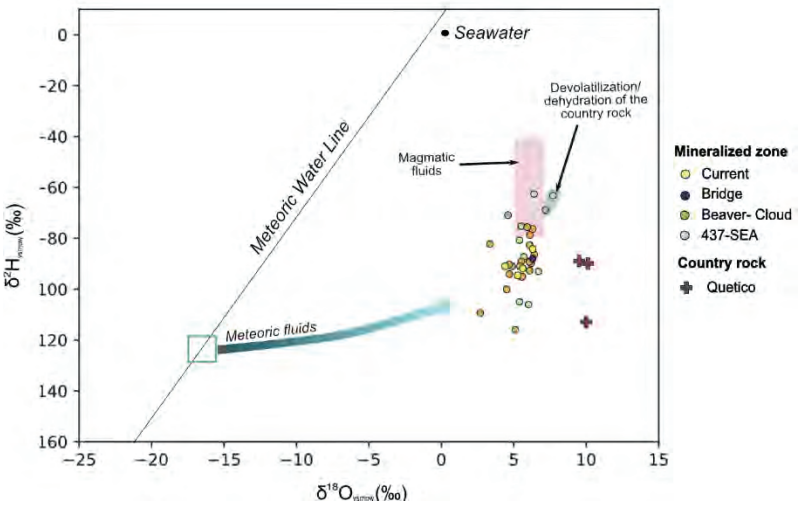


Figure 2. $\delta^{18}O$ and $\delta^{2}H$ values of bulk rock in the four mineralized zones of the Current intrusion (Current, Bridge, Beaver-Cloud, and 437-SEA) and the surrounding country rock of the Quetico basin.

The assessment of alteration intensity and micro-textural features in the intrusion identified three distinct domains, each showing varying secondary mineral assemblages. Domain A consists of antigorite, actinolite-tremolite, clinochlore, epidote, sericite, pyrite, millerite, secondary pyrrhotite, chamosite and secondary magnetite. Domain B consists mainly of lizardite-chrysotile and an increase in the modal abundances of clinochlore, epidote, sericite, pyrite, millerite, and secondary magnetite relative to Domain A. Domain C is composed of talc and carbonate minerals that have replaced the secondary minerals of Domains A and B. Domains A and B were formed by fluids with H_2O content derived from meteoric and magmatic sources. Domain A indicates high-temperature alteration processes, with the presence of antigorite suggesting temperatures exceeding 300°C [15]. In contrast, Domain B formed from fluids at lower temperatures (<300 °C; [16]), primarily due to the presence of lizardite-chrysotile. Domain C is associated with later crustal fluids with CO_2 contents below 50°C [16].

The alteration processes that have modified the Current intrusion involved the mobilization and incorporation of major elements such as Na_2O, Fe_2O_3, K_2O, and CaO in the replacement of primary silicates by secondary silicates, as well as a reduction in mineral volume during the replacement of primary sulfides by secondary sulfides and oxides.

References:

[1] Bleeker W et al. (2020) Geological Survey of Canada 8722: 7-35
[2] Woodruff L et al. (2020) Ore Geology Reviews 126: 103716
[3] Williams H (1991) Ontario Geological Survey 833-403
[4] Kuntz G et al. (2022) Princeton University 171-204
[5] Heggie G (2005) Lakehead University 365
[6] Hollings P et al. (2007b) Canadian Journal of Earth Sciences 44(8): 1111-1129
[7] Caglioti C (2023) Lakehead University 242
[8] Yahia K (2023) Lakehead University 148
[9] Cundari R (2012) Lakehead University 154
[10] Loewen M et al. (2019) Earth and Planetary Science Letters 508: 62-73
[11] Taylor H (1968) Contributions to Mineralogy and Petrology19(1): 1-71
[12] Ripley E and Al-Jassar T (1987) Economic Geology 82(1): 87-107
[13] Li H (1991) Mcmaster University 138
[14] Ripley E et al. (1993) Economic geology 88(3): 679-696
[15] Evans B (2004) International Geology Review 46(6): 479-506
[16] Barnes I et al. (1973) Economic Geology 68(3): 388-398

Sulfide percolation and drainback process in magmatic conduit system in the Huangshan-Jingerquan mineralization belt

Deng, Y.-F.[1], Xie-Yan Song[2] and Feng Yuan[1]

[1] Ore Deposit and Exploration Center (ODEC), Hefei University of Technology, Hefei 230009, Anhui, P. R. China, dengyufeng@hfut.edu.cn
[2] State Key Laboratory of Ore Deposit Geochemistry, Institute of Geochemistry, Chinese Academy of Sciences, 46th Guanshui Road, Guiyang 550002, P. R. China

---

Magma conduit systems consist of a series of flow-through dykes and sills (Barnes et al., 2016). When sulfides segregated at depth are carried by ascending mafic magmas, they would settle out in magma feeders or chambers at shallower depths as the flow velocities decreased. The differentiated sulfide rich melts in the upper magma chamber could drain back into the feeder dykes to form massive sulfide veins. The Huangshan-Jingerquan Ni-Cu metallogenic belt is located at the southern margin of the Central Asian Orogenic Belt. The total Ni metal reserve of the deposits is about a million tonnes. This makes it the largest orogenic Ni-Cu metallogenic belt worldwide (Deng et al., 2022). The Huangshandong, Huangshan, Tulaergen deposits are the biggest magmatic Ni-Cu deposits in this area, the morphology of the sulfide-bearing mafic-ultramafic complex and occurrence of the Ni-Cu sulfide orebodies in the deposits are obviously different.

The Huangshandong complex is rhombus-shaped, ~3.5 km long with a maximum width of 1.2 km. The complex was emplaced in the Gandun Formation carbonaceous slate and meta-sandstone intercalated with limestone. The Huangshandong deposit contains 90 million metric tonnes (Mt) of sulfide ores at average grades of 0.40 wt% Ni (Song et al., 2021). Several ore horizons comprised of disseminated and net-textured sulfides are located at the base of the lherzolite within the complex. A series of concave lenticular orebodies within the gabbronorite occur at the western end of the complex.

The tadpole-shaped Huangshan complex is 3.8 km long and up to 0.8 km wide. The base of the complex dips to the west to a depth of ~1000 m and becomes shallower to the east. It was emplaced into the sulfur-barren meta-sandstone and limestone of the Gandun Formation. There is an up to 50m thick thermal metamorphic aureole containing cordierite and epidote around the Huangshan complex. The Huangshan deposit contains 80.4 Mt of sulfide ores with average grades of 0.54 wt% Ni (Zhou et al., 2004). The main stratiform sulfide orebody comprised of disseminated and net-textured sulfides occurs at the base of the lherzolite, which is underlain by gabbronorite.

The small Tulaergen dyke consists of lherzolite, websterite and gabbro, and was emplaced in the Wutongwozi Formation meta-tuff and meta-sandstone. The Tulaergen deposit contains ~37 Mt of sulfide ores with average grades of 0.45 wt% Ni (Mao et al., 2008). Variably sized lenticular Ni-Cu sulfide orebodies comprised of disseminated and net-textured sulfides are situated in the central part of the lherzolite . The Ni grade is higher in the upper part of the orebodies than in the lower part. A Fe-rich massive ore vein occurs within the disseminated ores and a Cu-rich massive ore body extends from the ultramafic dyke to the wall-rock (Zhao et al., 2019).

The Ni-Cu sulfide deposits along the Huangshan-Jingerquan belt were formed in different locations at different depths in independent conduit systems. The migration and deposition processes of the sulfide liquids in these conduit systems are analogous to the model proposed by Barnes et al. (2016). We propose that some of the sulfides were deposited where the magma pathways changed direction and formed the Tulaergen sulfide-mineralized dyke in the Wutongwozi Formation at relatively deep levels (Deng et al., 2021). The negative correlations between IPGE and Pd/Ir of the Tulaergen massive ore veins suggest a differentiation between IPGE and PPGE triggered by fractional crystallization of the sulfide melt (Zhao et al., 2019). The massive ore veins embedded within the disseminated ores are likely the result of drain back of differentiated sulfide liquids along fractures within the

disseminated orebody. Whereas, other sulfide-rich liquids were carried upward into shallow magma chambers. There, the reduction in flow velocity caused the precipitation of sulfide that formed the stratiform or lenticular orebodies in the large magma chambers at relatively shallow depths, such as the Huangshan and Huangshandong complexes hosted in the Gandun Formation.

References:

[1] Deng Y-F et al (2022) Economic Geology 117: 1867-1879
[2] Song X-Y et al (2021) Lithos390-391 doi:10.1016/j.lithos.2021.106114
[3] Zhao Y (2019) Geochimica et Cosmochimica Acta 249:42-58
[4] Barnes S (2016) Ore Geology Reviews 76:296-316

Weathering of non-ore grade rock from Duluth Complex deposits: Outcomes from comprehensive pre-mining geochemical characterization

Diedrich, T.R.[1] and Theriault S.[2]

[1]MineraLogic LLC, 306 W Superior St., Suite 920, Duluth, MN USA 55802, tdiedrich@mnlogic.com
[2]MineraLogic LLC, St. Paul, MN, USA

The Duluth Complex, a large, predominantly mafic, intrusive complex in northeastern Minnesota, USA associated with the 1.1 Ga Mid-Continent Rift System, hosts several magmatic copper-nickel-cobalt and platinum group element (Cu-Ni-Co ± PGE) deposits. These deposits are generally located along the northwestern boundary of the complex, and in proximity to the Paleoproterozoic-aged metasediments of the Animikie Basin. NewRange Copper Nickel LLC ("NewRange") is currently assessing and/or engaged in development of the Mesaba and NorthMet deposits within the Duluth Complex. Complementing these efforts, NewRange has conducted an extensive and comprehensive program to characterize the environmental geochemistry of non-ore grade rock, ore, tailings, and unconsolidated surficial materials associated with the deposits. This program includes standard mine waste characterization methods, e.g., ASTM humidity cell tests (HCT); custom designed tests to provide information at different scales of evaluation; multi-faceted mineral characterization components; and field weathering tests. The results of the test program both provide a robust basis for identifying waste rock and water management strategies which would be protective of the environment during mining, and elucidate aspects of the fundamental weathering behavior of gabbroic composition rock.

Non-ore grade rocks and tailings from these deposits contain minor amounts of the iron sulfide mineral pyrrhotite, which, during weathering in the presence of oxygen, releases proton acidity through the reaction:

$$2FeS_{(po)} + 2.75O_2 + 2.5H_2O \rightarrow 2Fe^{2+} + 2SO_4^{2-} + 5H^+ \quad \textbf{(1)}$$

If the reaction continues to proceed in the presence of adequate oxygen, the iron will oxidize and, under circum-neutral pH conditions, precipitate as iron oxides, hydroxides, or oxyhydroxides, generalized as the following:

$$Fe^{2+} + ¼\ O_2 + H^+ \rightarrow Fe^{3+} + ½\ H_2O \quad (2)$$

$$Fe^{3+} + 3H_2O \rightarrow Fe(OH)_{3(s)} + 3H^+ \quad (3)$$

While rocks from the deposits *do not* contain appreciable carbonate minerals to neutralize this proton acidity, they *do* contain abundant plagioclase and olivine—both of which can neutralize the proton acidity produced during the above reactions during weathering. The environmental geochemical characterization program indicates that there are at least three distinct, but related, neutralization mechanisms active in non-ore rock and tailings from the Duluth Complex.

The first neutralization mechanism is the consumption of protons as reactants in silicate mineral dissolution reactions. Common weathering reactions for relatively reactive silicate minerals that are abundant in the complex include the following:

Plagioclase (anorthite) dissolution $CaAl_2Si_2O_{8(s)} + 2H^+ + H_2O \rightarrow Ca^{2+} + Al_2Si_2O_5(OH)_{4(s)}$ (4)

Olivine (forsterite) dissolution $Mg_2SiO_{4(s)} + 4\ H^+ \rightarrow 2Mg^{2+} + H_4SiO_4$ (5)

As shown from reactions (4) and (5), every cationic charge unit (for example, 2 cationic charge units for every mol Mg^{2+} and Ca^{2+}) produced corresponds to a proton being consumed as a reactant.

Furthermore, in the presence of atmospheric CO_2, dissolution of CO_2 into rainwater results in reactions driving towards equilibria between carbonic acid, proton acidity, and bicarbonate alkalinity:

$$H_2CO_3 \rightarrow H^+ + HCO_3^- \quad (6)$$

Weathering of silicate minerals in the presence of carbonic acid under neutral pH conditions tends to move reaction (6) toward the reaction products, resulting in accumulation of bicarbonate alkalinity in associated waters. Reaction with the accumulated alkalinity represents a second potential neutralization mechanism.

Finally, under select hydrologic conditions (low water to rock ratios), bicarbonate produced in reaction (6) could build up and eventually react with the calcium and magnesium released during reactions (4) and (5) to precipitate carbonate minerals *in situ.* This reaction leads to the third neutralization mechanism, dissolution of secondary carbonate minerals, and, further, provides a means of capturing and transforming atmospheric CO_2 into stable solid phases in the rock.

Outcomes from the environmental characterization program support the long-term effectiveness of these three mechanisms in neutralizing acidity from low sulfur rock. A subset of tests have been running for approximately 19 years, and, thus provide direct observational evidence at the multidecadal scale (Fig. 1). Furthermore, geochemical trends from these tests indicate that neutralization reactions will persist at least as long as the sulfide oxidation potential exists.

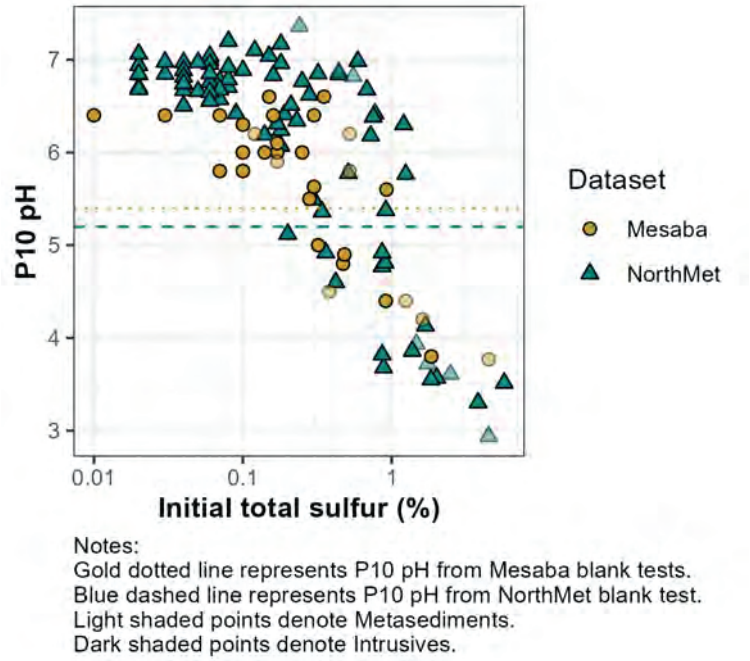


Figure 1. 10th percentile ("P10") of pH values observed over long-term kinetic testing as a function of initial sulfur content. **Each circle represents one HCT. Test durations vary, with the longest tests running for approximately 19 years. The potential to generate drainage with pH less than the blank is dependent on initial sulphur content, with all samples starting with less than approximately 0.2% sulphur maintaining a neutral pH throughout testing.**

Application of FactSage to Model the Compositional Variability of the Ni-Cu-PGE Mineralization at the Main Zone of the Tamarack Intrusive Complex

El Ghawi, A.K.[1] and Mungall, J.E.[1]

[1]Carleton University; Mineral Deposits. Lab Herzberg Laboratories 1125 Colonel By Drive, Ottawa, Ontario, Canada; Karimelghawi@cmail.carleton.ca

---

The Tamarack Intrusive Complex (1105.6 ± 1.2 Ma) is located in NE Minnesota and was emplaced during the early magmatic stage of the Midcontinental Rift System (MRS) [1]. The TIC is composed of a Dike intrusion in the north where the Ni-Cu-PGE mineralization is hosted, and a less explored Bowl intrusion in the south, (Fig. 1). The Dike area of the complex can be divided into many zones which are, from north to south, the Raptor Zone, the Main Zone, and the 164 Zone (Fig.1). Sulfide mineralization in these zones occur as disseminated (1-8 wt.% S), semi-massive (8-25 wt.% S), and massive sulfides (> 25 wt.% S), composed dominantly of pyrrhotite, pentlandite, and chalcopyrite. Massive sulfide bodies in the Main Zone are mostly hosted in the country rocks between the Fine-Grained Olivine (FGO) and Coarse-Grained Olivine (CGO) Intrusions (Fig.1). Some thin massive sulfide veins also occur in the Main Zone, crosscutting the CGO intrusion.

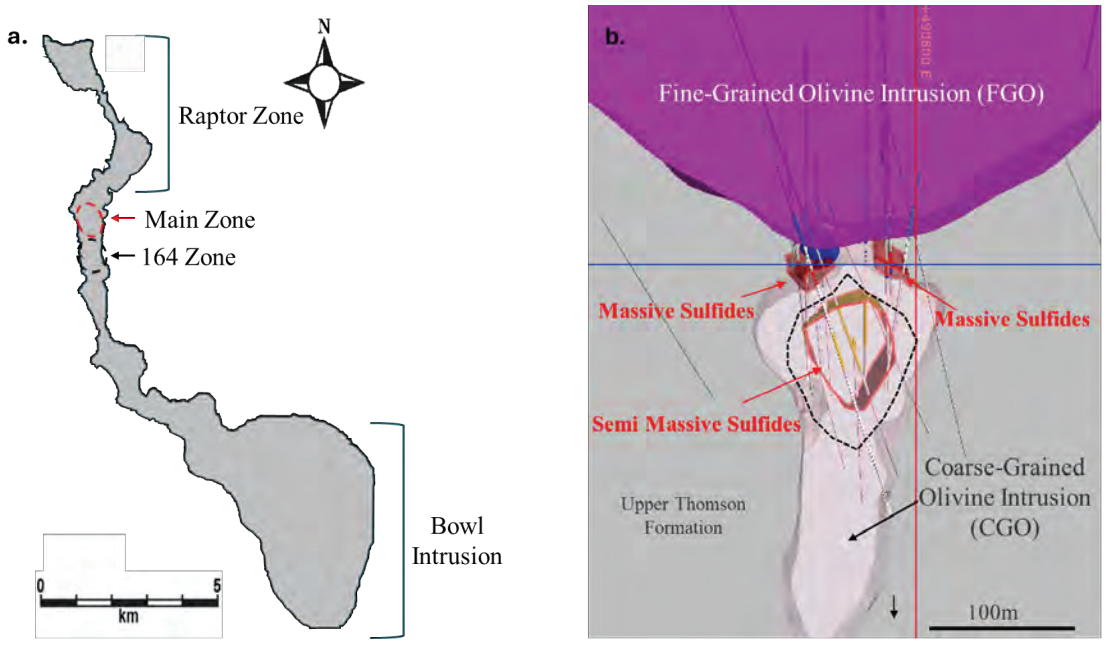


Figure 1: a) Outline of the Tamarack Intrusive Complex. b) Cross section through Main Zone, looking north. Modified after [2].

To understand the compositional variability of the sulfide mineralization at the Main Zone of the TIC, as well as the evolution of the sulfide and silicate magma, chalcophile element compositions (Ni, Cu, Pt, Pd) of sulfide-mineralized rocks have been reported, and a thermodynamic model was developed using the thermodynamic software FactSage 8.3. The FactSage software package uses the ChemSage Gibbs energy minimization routine to minimize the total Gibbs energy of a system with a given set of constraints, and with the availability of the thermodynamic database for the system of interest [3]. These databases have been developed from the optimization of data from the literature, and from new experimental results [3].

The silicate magma composition that is equilibrated with the sulfide liquid in the TIC has been inferred using FactSage. An isenthalpic assimilation-fractional crystallization model has been

followed starting with the composition of the Mamainse Point Formation, Volcanic Group 2, that is associated with the same stage that the TIC was emplaced in [4]. The contaminant that was used in this model is the Virginia Formation shale. An R-factor model was then implemented to assess the effects of varied silicate to sulfide mass ratios on the composition of the sulfides at the Main Zone of the TIC [5]. The R-factor curve passes through the disseminated sulfides, most of which occur between R = 700 and R = 1500 (Fig. 2). The semi massive sulfides are depleted in Pt and Pd compared with the disseminated sulfides. The massive sulfides that mainly occur in the country rocks are Pt and Pd poor and Ni rich, suggesting that these sulfides might be dominated by accumulated monosulfide solid solution (MSS), and there might have been a net loss of fractionated sulfide liquid from the Main Zone of the TIC (Fig.2). The sulfide melt composition calculated at an R factor equal to 900 was then inputted into FactSage and an equilibrium crystallization run was then performed. Trends of MSS and sulfide liquid were generated (Fig. 2). The sulfide melt composition at R = 900 coexists with the early crystallizing MSS at the sulfide liquidus temperature of 1038 °C. With cooling and crystallization of MSS, the sulfide liquid becomes more enriched in Pt, Pd, and Cu. Most semi massive sulfide compositions can be represented as mixtures of MSS and liquid. The extreme enrichment in Pt and Pd shown by sulfide veins cannot be explained solely in terms of MSS fractionation and will be the subject of future study.

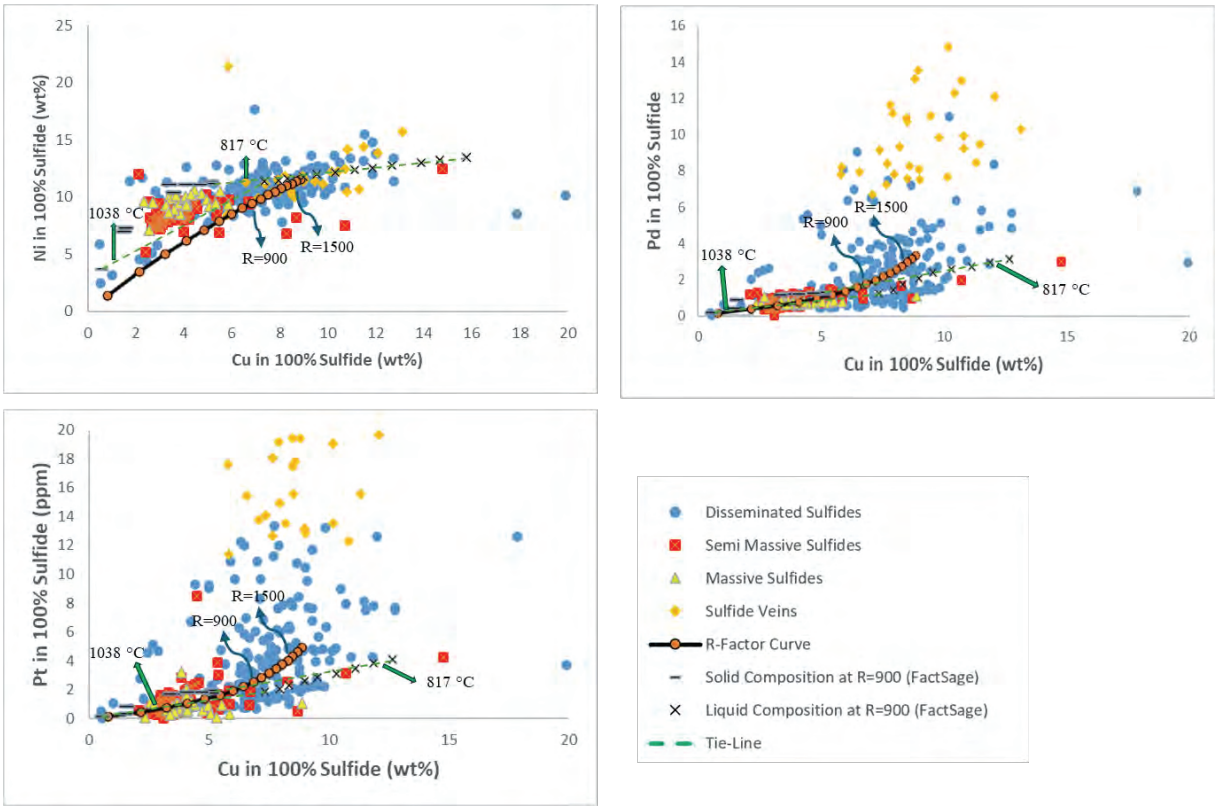


Figure 2: Variation of Ni, Pt, and Pd versus Cu in the disseminated, semi massive, massive sulfides, and sulfide veins from the Main Zone of the TIC. Concentrations are represented in 100% sulfide. The orange circles along the black curves represent sulfide compositions at different R factors. Solid and liquid compositions during equilibrium crystallization of a sulfide liquid formed at R= 900 are represented by horizontal lines and crosses, respectively. Tie-lines are represented in green dashed lines connecting the coexisting liquid and the early crystallizing solids at 1038 °C and at 817 °C.

References:

[1] Goldner B (2011) MSc Thesis: 155
[2] Talon Metals (2022) Technical Report
[3] Bale C et al. (2009) Calphad 33(2): 295-311
[4] Lightfoot P (1999) OGS 5998: 91
[5] Campbell IH and Naldrett AJ (1979) Econ Geol 74: 1503-1506

Petrophysics Applied to Magmatic Sulfide Deposits: The Physical Properties - Mineralogy Link

Enkin, R.J.[1]

[1]Geological Survey of Canada, POB 6000, Sidney, BC V8L 4B2, CANADA, randy.enkin@nrcan-rncan.gc.ca

---

Modern mineral exploration demands interpretation formed by the integration of two principal activities: geological mapping and geophysical survey collection. The linking element is the physical properties of rocks, which must be measured, compiled, and analysed. The current emphasis on critical minerals is motivating us to look deeper into previously explored regions to understand the geological settings that are conducive to discovering economic critical mineral systems.

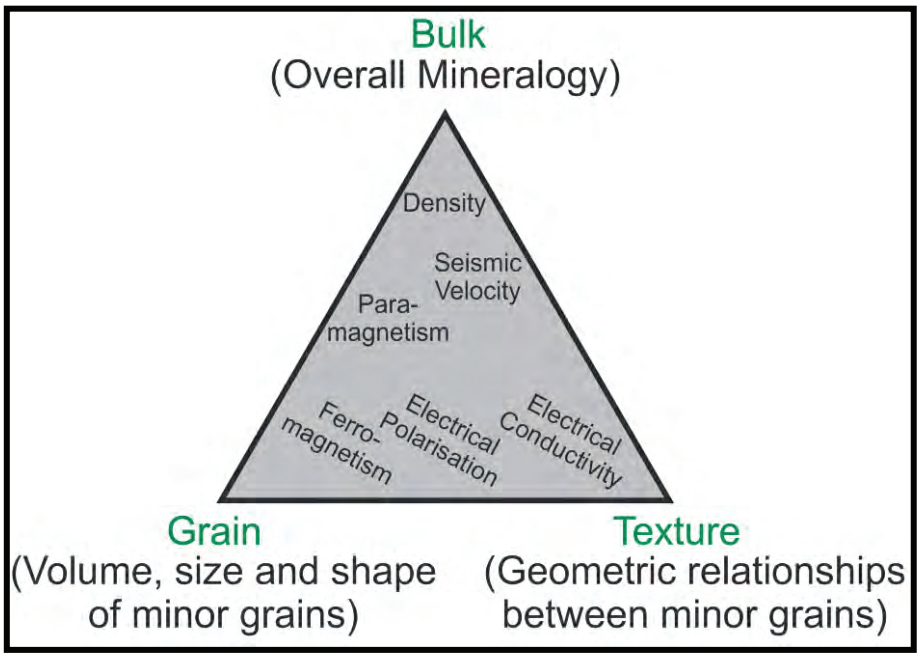


Figure 1, Conceptual framework describing the behaviour of various physical properties commonly measured by the mining industry. [1]

Physical properties are directly controlled by the bulk composition, the mineralogy, and the texture of rocks [2]. Gravity and magnetic surveys reflect density and magnetic properties, which can mostly be described by the relative amounts of three principal components of mineral families: the light minerals: quartz+feldspar+calcite, the dark minerals: ferromagnesian silicates, and magnetite. Ore minerals and porosity add and subtract density. Importantly, igneous rocks formed in the upper crust usually have a ~10:1 ratio of ferromagnesian silicates to magnetite concentration, and most subsequent geological processes lead to magnetite loss.

Electric resistivity and chargeability are controlled by permeability and ore minerals which effectively form networks of wires and capacitors, as revealed by equivalent circuit analysis of spectral impedance measurements.

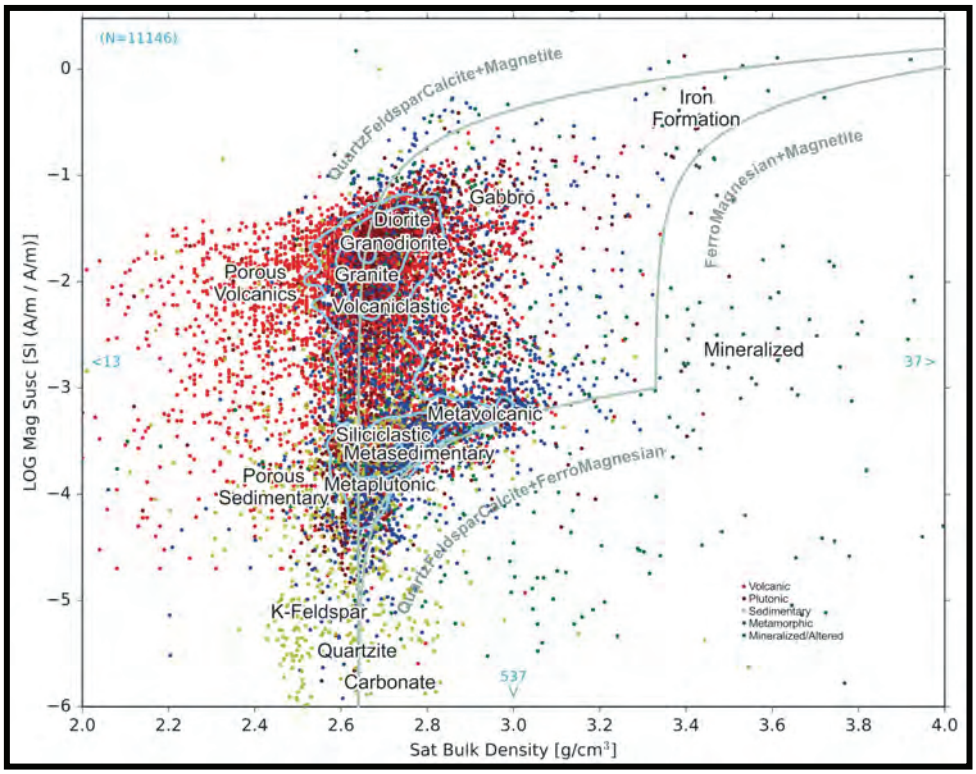


Figure 2, Henkel Plot, Density vs Log(Magnetic Susceptibility), of rocks in the Canadian Rock Physical Property Database. [3]

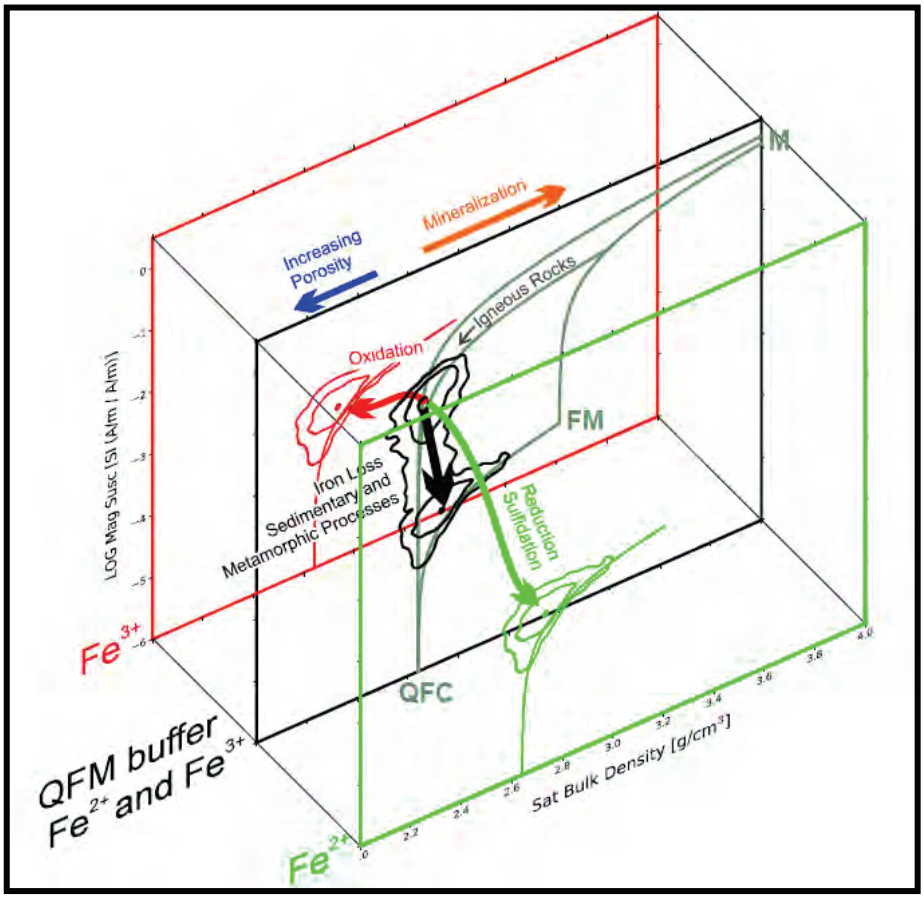


Figure 3, Igneous rocks formed in the upper-crust fall on the Magnetite Trend (FM/M~10), whereas most other geological processes are magnetite destructive. [2]

Ultramafic environments, which commonly host Ni-Cu deposits, have a distinctive set of petrophysical properties, which bears directly on their geophysical signatures [4]. Originating from deep, reduced levels, unaltered ultramafics are typically dense and paramagnetic. On hydration and serpentinization, rocks become extremely low density, and iron is rejected from ferromagnesian silicates to form high concentrations of magnetite. These rocks are extremely magnetic and usually display high Koenigsberger ratios, meaning that magnetic remanence dominates aeromagnetic surveys. Carbonation transforms rocks to dense, paramagnetic bodies. Examples from British Columbia and Ontario will illustrate these exotic trends and processes.

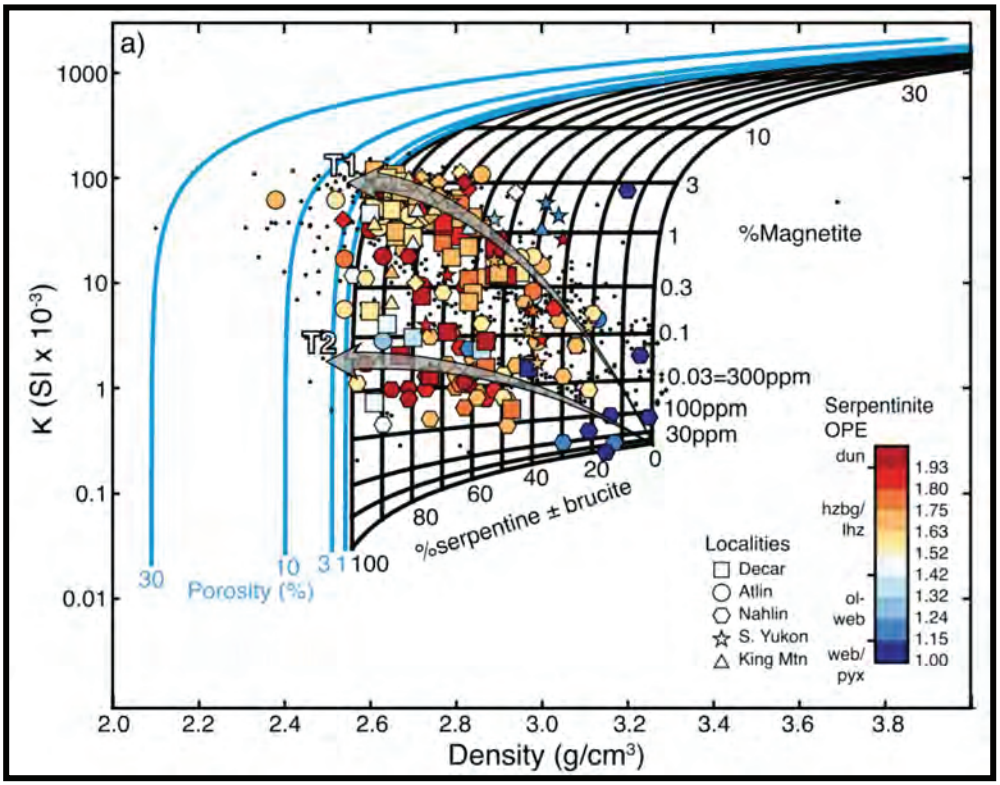


Figure 4, Henkel plot of ultramafic rocks in the Canadian Cordillera, displaying physical property changes with degree of serpentinization. [4]

Through understanding the physical properties - mineralogy link, geophysical interpretation leads to delineation of geological processes and better exploration strategies.

References:

[1] Dentith, et al. (2020), Geophysical Prospecting, 68: 178-199 doi.org/10.1111/1365-2478.12882
[2] Enkin RJ, et al. (2020), Geochemistry, Geophysics, Geosystems, 21: doi.org/10.1029/2019GC008818
[3] Enkin RJ (2018), Geological Survey of Canada Open File 8460, doi.org/10.4095/313389
[4] Cutts JA, et al. (2021), Geochemistry, Geophysics, Geosystems, 22: doi.org/10.1029/2021GC009989

Regional changes in plume-generated stress linked to MCR (Keweenawan LIP) chonolith emplacement

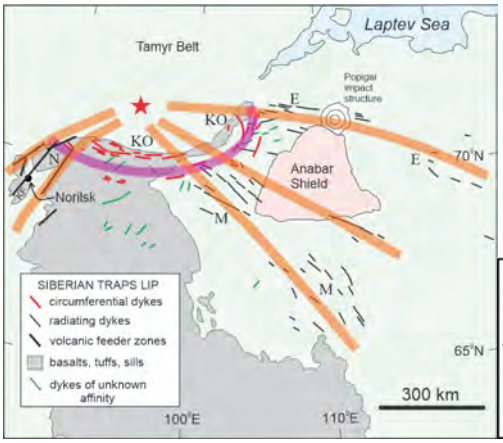
Ernst, R.E.[1], El Bilali, H.[1], Buchan, K.L.[2] and Jowitt, S.M.[3]

[1]Department of Earth Sciences, Carleton University, Ottawa K1S 5B6, Richard.Ernst@Carleton.ca.
[2]273 Fifth Ave., Ottawa K1S 2N4, Canada
[3]Nevada Bureau of Mines and Geology, University of Nevada Reno, 1664 N. Virginia Street, Reno 89503, Nevada, USA

Introduction: Changes in regional stresses contribute to the formation of many types of ore deposits. Here, we consider the role of plume-generated stresses in metallogeny, and the role of giant dyke swarms of LIPs in monitoring those stresses. We begin with our just-published analysis of the Siberian Traps LIP, its giant dyke swarms and its Norilsk-Talnakh ores [1], and then we consider the Mid-Continent Rift / Keweenawan LIP event as a second example.

Norilsk-Talnakh ores of the Siberian Traps LIP: Plume-generated 90° stress change recorded by the transition from radiating to circumferential dolerite dyke swarms of the Siberian Traps LIP may be linked to emplacement of Norilsk-Talnakh ore deposits. [2] showed that the timing of Norilsk-Talnakh Ni-Cu-PGE mineralization in the Siberian Traps LIP is associated with a 90° change in stress, which they attributed to changes in plate stresses. However, as detailed in [1], we propose that this 90° stress change associated with Norilsk-Talnakh mineralization could instead be due to changing plume dynamics as monitored by the transition from the LIP's giant radiating dolerite dyke swarm to its circumferential swarm (Fig. 1).

As noted in [1], the 90° transition from a regional radiating swarm to a circumferential swarm involves a decrease in the radial sigma 1 stress followed by an increase in a hoop-like sigma 1 stress. This implies an intervening period in which the stress is isotropic, a period that we associated with emplacement of the Norilsk-Talnakh mineralization. It is possible that this stress drop led to release of volatiles and allowed ascent and/or lateral emplacement of gas-buoyed magmatic sulphides (e.g. [3-5]).



younging ↑

Volcanic Assemblages	Mineralization	Sigma 1	Dyke Swarm
3rd: Morongovsky-Samoedsky (>251.4 Ma)	Ni-Cu-PGE (251.9-251.6 Ma)	ESE-WNW	Circumferential
Stress Transition			
2nd: Khakanchansky-Nadezhdinsky		NNW-SSE	Radiating
1st: Ivakinsky-Gudchikhinsky		NNW-SSE	Radiating

Figure 1: LEFT: Distribution of dyke swarms and volcanic feeder zones associated with the Siberian Traps LIP; modified after [6]. A generalized version of the overall radiating system of dykes and feeder zones is superimposed in orange, and a generalized version of the circumferential dykes is in light purple. Dyke sets: E = Ebekhaya; KO = Kochikha; M = Maimecha. N = Norilsk feeder zones to volcanic flows, which correlate with major fault zones, including the prominent Norilsk-Kharaelakh fault (KF). RIGHT: Timing of volcanic assemblages in the Norilsk region (younging upward), compared with the stress orientations after [2] and with the matching dyke swarm pattern from [1].

Mid-Continent Rift System (Keweenawan LIP): We consider this as a possible example of plume related stress change linked to chonolith mineralization. This major (~1112-1090 Ma) LIP event in the

Great Lakes region of North America is associated with an arcuate zone of rifting and a significant number of mineralized intrusions ("chonoliths" and 'tube-like conduits" in [7]; and "conduit type intrusions" in [8]. [8] noted two main stages in this LIP: the ~1112-1105 Ma Plateau stage, and the ~1100-1092 Ma Rift stage, followed by Late Rift and Post-Rift stages. The numerous chonoliths (conduit type intrusions) were mostly emplaced during the Plateau stage.

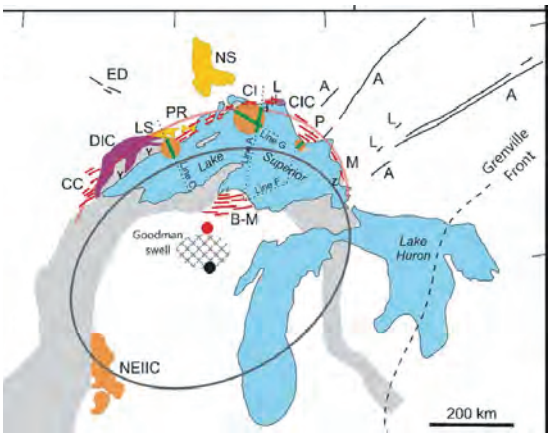


Figure 2. The 1112–1090 Ma Keweenawan LIP of the Mid-continent Rift of North America. Key elements include volcanics, sills, a circumferential dyke swarm, and exposed and buried intrusive complexes. Also shown are the older ca. 1140 Ma Abitibi dyke swarm and coeval lamprophyre dykes, which may represent a radiating dyke system, and may be related to 1150 Ma Corson diabase intrusions [9] centred just west of the figure.

Rift-parallel circumferential Keweenawan dykes from west to east: CC = Carlton County, PR = Pigeon River, CI = Copper Island, P = Pukaskwa, M = Mamainse Point. BM = Baraga-Marquette dykes. Keweenawan sills: LS = Logan, NS = Nipigon sills. Intrusive complexes: DIC = Duluth, CIC = Coldwell, NEIIC = northeastern Iowa. Ca. 1140 Ma radiating dykes: A = Abitibi, ED = Eye-Dashwa, L = lamprophyre dykes. Interpreted mid-crustal intrusive complexes are shown schematically as brown circles. The Goodman Swell has been interpreted as locating the centre of an underlying mantle plume. More details in [10].

[10] described a giant circumferential dyke swarm for the Keweenawan LIP / Midcontinent Rift (Fig. 2), analogous to a Venusian corona. The ages of Pigeon River dykes [7], which we interpret as a portion of the circumferential swarm, indicate emplacement during the Rifting stage, perhaps in association with spreading of the plume head. In our interpretation, plume head arrival and initial domal uplift may have occurred 30 my earlier at 1140-1150 Ma, associated with emplacement of the 1141 Ma radiating Abitibi swarm (Fig. 2; [11].

We speculate that the radiating stress regime at 1140 Ma associated with plume generated uplift persisted until the Plateau stage before transitioning to the circumferential stress regime associated with the Rifting stage. The chonoliths/conduit type intrusions, such as Tamarack, BIC, Eagle and Current Lake [7-8], were mostly emplaced during the Plateau stage, i.e. during our proposed transition from radiating to circumferential stresses. This is a similar timing to our interpretation for the Norilsk-Talnakh ores of the Siberian Traps LIP (Fig. 1; [1].

References:

[1] Ernst R et al. (2024) Econ Geol 119: 243–249

[2] Begg et al. (2018). Ch 1, in Mondal S and Griffin W (ed.) Processes and ore deposits of ultramafic-mafic magmas through space and time: Elsevier, p. 1–46.

[3] Lesher (2019) Can J Earth Sci 56: 756-773

[4] Yao Z-s and Mungall J (2022) E Sci Rev 227: 103964

[5] Barnes S et al. (2023) Geology 51 (11): 1027-1032

[6] Buchan K and Ernst R (2019), In: Srivastava R et al (eds.) Dyke swarms of the world – a modern perspective: Springer, p. 1–44,

[7] Bleeker W et al. (2020). In Bleeker W and Houlé M (ed.). Geol Surv Canada Open File 8722.

[8] Woodruff L et al (2020) Ore Geol Rev 126: 103716

[9] McCormick K et al (2018) Can J Earth Sci 55: 111-117

[10] Buchan K and Ernst R (2021) Gondwan Res. 100: 25–43

[11] Ernst R et al. (2018). Earth Planet Sci Lett 502: 244-252

A proposed cryptic common thread among Ni-Cu-PGE-(Au-Te) systems spanning the boundary between Laurasia and Gondwana

Fiorentini, M.[1]*, Holwell, D.[2], Blanks, D.[3], Cherdantseva, M.[1], Denyszyn, S.[4], Ince, M.[1], Vymazalova, A.[3], and Piña Garcia, R.[5]

[1]Centre for Exploration Targeting, Australian Research Council Industrial Transformation Training Centre in Critical Resources for the Future, School of Earth Sciences, University of Western Australia, Australia - marco.fiorentini@uwa.edu.au

[2]Centre for Sustainable Resource Extraction,School of Geography, Geology and Environment, University of Leicester, United Kingdom

[3]BHP Metals Exploration, United Kingdom

[4]Department of Earth Sciences, Memorial University of Newfoundland, Canada

[5]Dpto. Mineralogía y Petrología, Universidad Complutense Madrid, Spain

---

The long-lived geodynamic evolution of the boundary between Laurasia and Gondwana may have created the ideal conditions for the genesis of a trans-continental Ni-Cu-PGE-(Au-Te) mineralised belt in Europe. This working hypothesis stems from the recent understanding that orogenic processes play a fundamental role in the triggering of chemical and physical processes for the transport of metals from the metasomatised mantle through to various crustal levels.

An insight into the polyphased genetic evolution of magmatic sulfide mineral systems is provided by a series of mineralised occurrences located in the Bohemian Massif, Czech Republic. Here, a series of hydrated gabbros contain magmatic sulfides ranging in texture from disseminated to matrix and blebby. These alkaline intrusions with a markedly sodic nature host magmatic sulfide mineralisation revealing a mantle-like signature, with in-situ ð34S values ranging from -2.4 to +1.8‰. New TIMS U-Pb data pinpoint emplacement and crystallisation of these mineralised magmas at 363.9 ± 0.6 Ma, with Sm-Nd model ages pointing to involvement of a metasomatised Mesoproterozoic lithospheric mantle in a post-orogenic geodynamic framework.

Mineralised intrusions in the Bohemian Massif are strongly analogous to a series of Permo-Triassic (290-250 Ma) hydrated and carbonated ultramafic alkaline pipes containing Ni-Cu-PGE-(Te-Au) mineralisation emplaced in the lower continental crust in the Ivrea Zone, Italy. Despite the significant age difference, mineralisation in the Bohemian Massif and Ivrea Zone is similar in terms of their geochemical and isotopic characteristics, pointing to similar ore forming processes and mantle sources having operated in a syn- to post-Variscan Orogen setting. A subsequent mineralising event is recorded in the Ivrea Zone at ~200 Ma, most likely associated with the Central Atlantic Magmatic Province (CAMP). It is argued that this event reactivated and focussed lower-crustal carbonate- and metal-rich sulfide mineralisation associated with the Permo-Triassic pipes into the ~200 Ma mineralised intrusion known as La Balma Monte Capio.

Mineralised systems in the Bohemian Massif and Ivrea Zone are markedly different in size, geometry and overall metal endowment from the larger and better-known Aguablanca system in southern Spain. However, they all share distinctive geochemical and isotopic characteristics pointing to a common DNA: their association with the complex and multi-phase activation of the margin between Laurasia and Gondwana across the Variscan metallogenic belt from the Devonian to the Triassic.

The nature and localisation of the magmatic sulfide mineral systems along this belt indicate that enhanced potential for ore formation at lithospheric margins may be due not only to favourable architecture, but also to localised enhanced metal and volatile fertility. This hypothesis may explain why ore deposits along the margins of lithospheric blocks are not distributed homogeneously along their entire extension but generally form clusters. As mineral exploration is essentially a search space reduction exercise, this new understanding may prove to be important in predictive exploration targeting for new mineralised camps in Europe and elsewhere globally, as it provides a way to prioritise segments with enhanced fertility along extensive lithospheric block margins.

How exploration geologists can and should use “soft NSRs” to represent assays of Ni-Cu-PGE mineralization

Goldie, R.J.

Independent Analyst and Director, 54 Peach Willow Way, Toronto, Ontario, Canada M2J 2B6
Raymondgoldie@outlook.com

A Net Smelter Return (NSR) is the net revenue generated by a block of mineralization, less off-site costs (Goldie and Tredger [1]). Three procedures for computation of the NSRs of Ni-Cu-PGE sulphide mineralization are in common use: values calculated by accountants; mine-specific estimates prepared by mine operators, and “soft estimates” (Goldie [2]).

Soft estimates are useful in representing assays of samples taken during exploration for Ni-Cu-PGE deposits. Their computation is based on statistical analyses of the grades and metallurgical properties of ores at operating Ni-Cu-PGE mines, and the smelting and refining fees paid by those mines.

There are three reasons why exploration geologists should express assays of samples as soft estimates of NSRs: (i) representing assays as single numbers facilitates their graphical representation, such as on contour maps; (ii) the computation of soft estimates may reveal that, as is common in mineralization that is rich in PGE, the mineralization contains substances or has mineralogical issues that could lead to a smelter penalizing or even rejecting a potential mine’s products (Goldie [3]); (iii) representation of assays as single numbers not only facilitates their comprehension by the readers of company press releases, it may also reduce the chances that investors apply invalid rules-of-thumb to those assays, resulting in expensive misunderstandings.

References:

[1] Goldie R and Tredger P (1991) Geosci Canada 18:159-171

[2] Goldie R (2023) Min Economics https://doi.org/10.1007/s13563-023-00400-3

[3] Goldie R (2022) Aust Inst Mining & Metal, Int Mining Geol Conf: 222-235

Characterizing the Early (Plume) and Main (Rifting) Stages in the evolution of the Midcontinent Rift

Good, D.J.

Department of Earth Sciences, Western University, London, ON N6A 5B7, Canada, dgood3@uwo.ca

---

The mid-Proterozoic Midcontinent Rift (Keweenawan Large Igneous Province) contains the most diverse assemblage of basalt rock types for any LIP on earth. In this study, six of the eight main basalt types in the rift are compared to the global distributions of ocean plateau, ocean island basalts and continental large igneous province basalts using a combination of two sophisticated classification strategies based on high precision incompatible trace element data (after O'Neill, 2016 and Pearce et al., 2021). The two basaltic sequences that are not described here occur in the northeast quadrant of the Midcontinent Rift and were shown by Good et al. (2021) to have been derived from a metasomatically modified mantle source. Thus, they are not suitable candidates for interpretation using the classification strategies as applied here. Basalt data for the Midcontinent Rift were compiled by the author from detailed studies of trace element geochemistry at numerous sites around Lake Superior by several researchers during the past 30 years. Data for oceanic basalts were compiled by O'Neill (2016) as part of his impressive study to highlight the usefulness of calculated coefficients to characterize REE diagram patterns ($\lambda 0$, $\lambda 1$ and $\lambda 2$). Data for continental Large Igneous Provinces were compiled by Pearce et al. (2021) to show the usefulness of geochemical proxy diagrams to define which of the various petrological mechanisms operated during their formation (the LIP Print Approach).

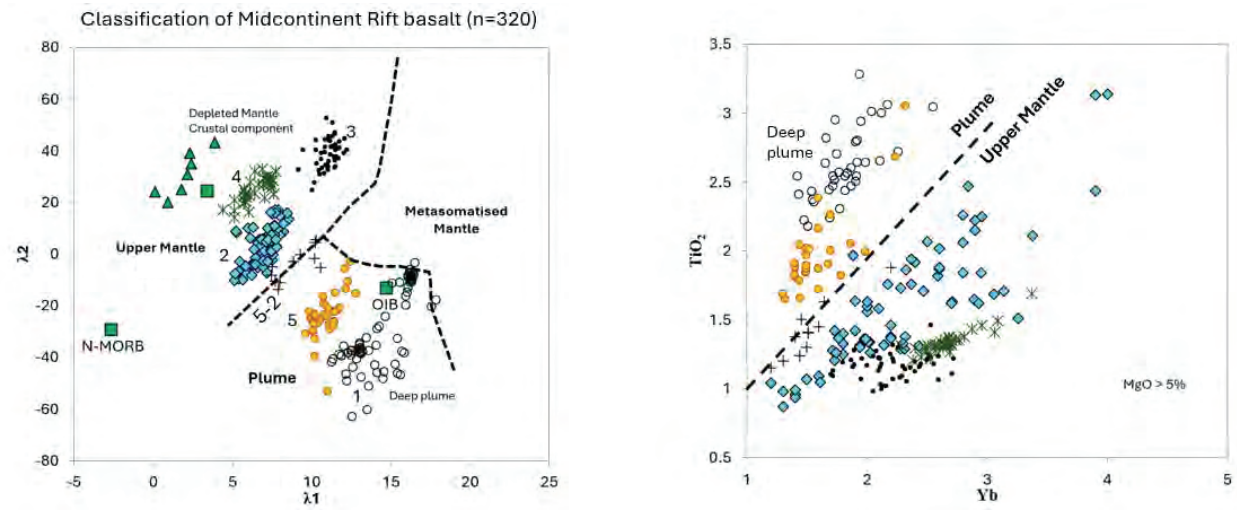


Figure 1: Discrimination boundaries for basalts sourced from different Mantle Regions plotted on the O'Neill diagram (left hand side). See text for discussion. Group 52 corresponds to basalt that shows characteristics of both plume and upper mantle source.

Taken together, these comparisons show that Midcontinent Rift data in groups 2, 3 and 4 are like ocean plateau basalts and groups 1 and 5 are like ocean island basalts. That is, data are in excellent agreement with the hypothesis that basalt in group 2 was derived by partial melting in the Upper Mantle whereas groups 5 and 1 were derived by partial melting in the Mantle Plume, but at depths below the pyrope garnet and majorite garnet stability boundaries, respectively. This and other evidence suggest Groups 3 and 4 were derived by partial melting in a subduction modified depleted mantle source. Based on these inferred origins for the various basalt units, the Midcontinent Rift exhibits spatial and temporal zonation. Spatially, the mantle plume was centred beneath the west

central portion of what is now Lake Superior. Temporally, the effects of mantle plume volcanism occurred throughout the Early Stage of the Midcontinent Rift but had vanished before the end of the Hiatus Stage. During the subsequent Main Stage of magmatism, mafic rocks were derived primarily from the Upper Mantle, presumably by decompression melting as the crust thinned during extension.

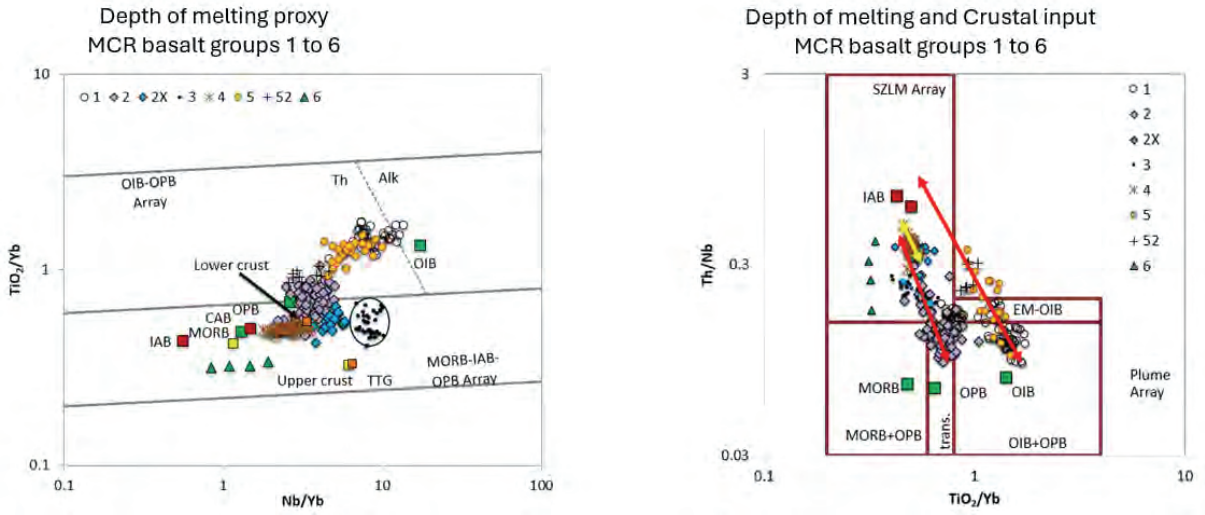


Figure 2: Midcontinent Rift basalt of groups 1 to 6 plotted in the LIP print diagrams of Pearce et al. (2021). See text for discussion.

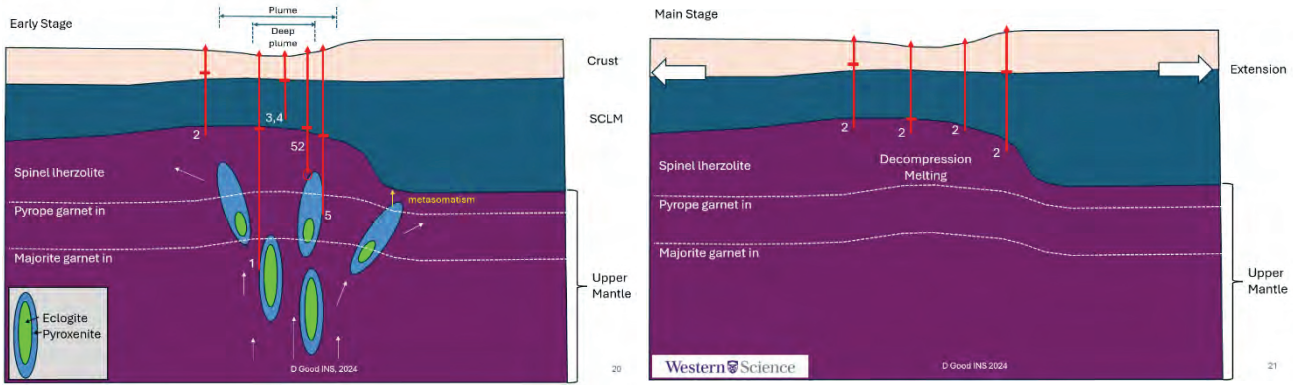


Figure 3: Model for basaltic melt source regions of the Midcontinent Rift Event: (a) During the Early Stage, most melts are generated in the mantle plume with lesser amounts generated in the overlying mantle and/or subduction modified lithospheric or asthenospheric mantle; (b) During the Main stage, most of the melts are generated by decompression melting in the upper mantle as the crust thins during extension.

References:

[1] O'Neill, H.St.C, (2016) Journal of Petrology, Vol. 57, No. 8, 1463–1508
[2] Pearce, J.A. et al., (2021) Lithos 392–393 (2021)
[3] Good, D.J. et al. (2021) Journal of Petrology, 2021-07, Vol.62 (7)

Lithospheric structure controls for large magmatic Ni-Cu discoveries

Hayward, N.[1,2]

[1]Centre for Exploration Targeting, University of Western Australia, Crawley, WA 6009, Australia.
NHayward@protonmail.com
[2]PredictOre Pty Ltd, 1/40 Victory Terrace, East Perth, WA 6009, Australia

---

To sustain the clean energy transition, society needs to increase the reserve base of green and critical mineral ore deposits containing metals such as copper (Cu), lithium (Li), nickel (Ni), cobalt (Co), rare earth elements (REE) and platinum group elements (PGE). Discovery of large new polymetallic Ni-Cu (±PGE, Co) sulfide deposits can help meet this need, but their discovery rates have declined over the last 25 years, and they present very difficult greenfield exploration targets because of their rare occurrence, very small footprints, large range in formation depths, concealment among extensive magmatic provinces, and increasing challenges for exploration land access. The fact that most recent Ni sulfide discoveries were found in magmatic provinces that had no previously known Ni-sulfide resources favours a first-mover Ni exploration strategy. The minerals industry needs improved mineral system models that more accurately predict the location of new districts (camps) and large deposits in remote and covered terrains with low data quality and availability. This study [1] demonstrates that low-cost three-dimensional lithospheric structure targeting has the power to significantly improve the accuracy and precision of targeting large magmatic Ni discoveries. It also addresses a disconnect between conceptual academic models for magmatic Ni-Cu (also Cu-Au) systems, which largely omit lithospheric structural controls on magma flux and intrusion emplacement, and the practice of explorers to empirically target proximity to lithospheric-scale fault zones for mineralised intrusions. This disconnect is exacerbated by a lack of quantitative analyses of the spatial accuracy, precision and causality of lithospheric structures that are inferred to be control ore deposition, which this study also addresses.

The 1st-order (subprovince-scale) lithospheric structure control on magmatic Ni-Cu ore distribution is widely accepted to be along the sutured edges of paleo-cratonic blocks with preserved Archean subcontinental lithospheric mantle [2]. However, 2nd- to 3rd-order controls on emplacement of district-scale mineralised intrusion clusters and individual deposits along craton edges remain poorly understood. Two alternative models previously proposed are: (i) emplacement of dyke-like intrusions in dilational jogs along strike-slip faults [3], and (ii) emplacement of intrusion clusters near intersections of transverse translithospheric faults (TLFs) [4,5]. These models invoke predominantly vertical magma transport along fault conduits with subjacent sulphide saturation. Other models invoke long-distance lateral magma transport through interconnected sill and dyke complexes and potential for distal sulphide saturation [6,7] which, if correct, would greatly increase the permissive search space.

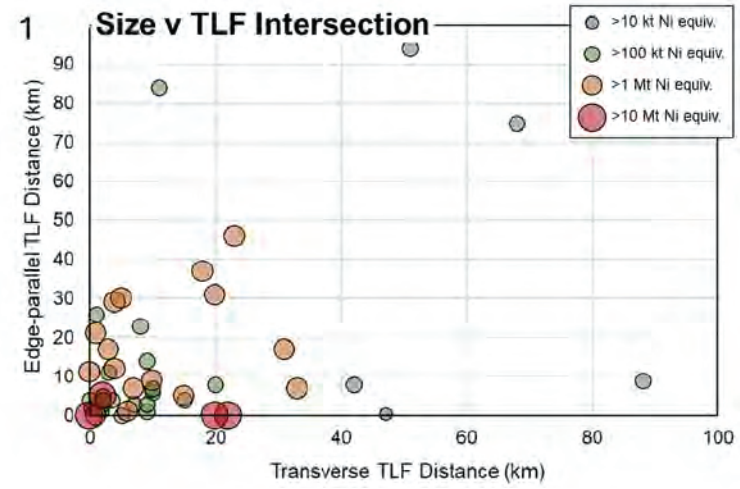
New structural interpretations and quantitative analyses were completed globally for 72 Ni deposits with >50kt Ni (equivalent) metal. This extensive sample population covers a range of magmatic Ni deposit settings from intracratonic to pericratonic and arc-related, and from Mesoarchean to Cenozoic. Six detailed case studies addressing the lithospheric structure architecture controls on giant Ni deposits will be presented for Voisey's Bay, Noril'sk-Talnakh, Kabanga, Jinchuan, West Musgrave, and the Cape Smith Belt. Less detailed examples will also be shown from the Midcontinent Rift, southern Africa, China, and western Australia.

From quantitative analysis of the 72 regional structural case studies, the 1st-order control for all large magmatic Ni-Cu deposits is observed to be ≤30 km from paleocraton edge-parallel translithospheric faults, and specifically in their hangingwall where inclined. This relationship holds for all magmatic Ni-Cu deposit settings. Furthermore, large intracontinental Ni deposits are also located ≤30 km from 2nd-order transverse translithospheric faults that intersect paleocraton edges (Fig. 1). However, for pericratonic and Archaean greenstone komatiite settings, proximity of Ni deposits to transverse

translithospheric fault intersections is not widely recognised or preserved. In one exception, clusters of komatiitic Ni deposits in the Agnew-Wiluna greenstone belt are observed to have a semi-regular spatial periodicity along strike with a mean spacing of ~22 km, and this is controlled by the intersection of local cryptic transverse rift faults [8].

Prioritising target proximity to certain translithospheric fault intersections can significantly reduce subprovince-scale search areas (~10^4-10^5 km^2) to a few prospective districts (~10^2 km^2). The largest deposits are found closest to (but rarely within) the most prominent translithospheric faults. At smaller scales, a few deposits are localised along small-scale dilational jogs in wrench faults, but this control is relatively rare. At deposit scale, controls on emplacement of mineralised channel-like flows and pipe-like intrusions (chonoliths) are typically more stratigraphic than structural, where overpressured, high temperature magmas self-generate pathways. Productive stratigraphic horizons are dominated by rheologically weak and highly fusible metasedimentary or gneissic units.

A model (Fig. 2) is proposed where the root zones of translithospheric fault intersections initially channel fertile mantle melts into the deep crust. Ascent of buoyant overpressured magmas is then dispersed up to a few 10s km lateral to inclined master fault conduits through complex dyke-sill-dyke networks in steeper hangingwall fault splays, their damage zones, and rheologically weak contacts. The extreme magma flux required to form large Ni sulfide deposits results from positive magma-deformation feedbacks and bottom-up self-organisation. Targeting translithospheric fault intersections therefore requires a more systematic bottom-up and hierarchal approach to structural mapping, where the roots of cryptic lithospheric faults are defined, and structures are rated by scale, dip, and geodynamic behaviour.



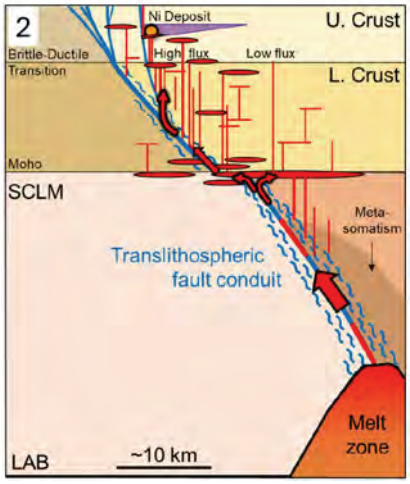


Fig. 1: Deposit size class versus distance to both edge-parallel and transverse TLFs.

Fig. 2: Concept section showing dispersal of ascending mafic-ultramafic melts through dyke-sill networks with high magma flux in hangingwall of paleocraton edge translithospheric fault zone.

References:

[1] Hayward N (2024) Submitted to Econ Geol
[2] Begg G et al (2010) Econ Geol 105: 1057-1070
[3] Lightfoot P and Evans-Lamswood D (2015) Ore Geol Rev 64: 354-386
[4] Myers J et al (2008) Can J Earth Sci 45: 909-934
[5] Begg et al (2018) Processes and Ore Deposits of Ultramafic-Mafic Magmas through Space and Time, Elsevier: 1-46
[6] Lesher C (2019) Can J Earth Sci 56: 756-773
[7] Ernst R et al (2019) J Volcanol Geotherm 384: 75-84
[8] Perring C (2016) Econ Geol 111: 1159-1185

Deep orogenic magmatic Ni and Cu sulfide systems in the Curaçá Valley, Brazil

Holwell, D.A.[1], Thompson, J.[2] , Blanks, D.E.[1], Oliver, E.[1], Porto, P.[3], Oliviera, E.[3]., Tomazoni, F.[4], Lima, A. [4], D'Altro R.,[4]., Graia, P.[4] and Sant'Ana, T.[4].

[1]Centre for Sustainable Resource Extraction, University of Leicester, UK
[2]PetraScience Consultants, Vancouver, Canada
[3]Ero Copper, Vancouver, Canada
[4]Ero Caraiba, Brazil

The magmatic sulfide ores of the Curaçá Valley, Brazil, form an unusual subgroup of intrusion-related sulfide deposits. They are Cu-rich in general, with some Ni-dominant deposits on a district scale. They are located in small, hydrous mafic-ultramafic intrusions emplaced into the lower-mid crust at around peak metamorphic conditions.

The metallogeny of the majority of known Curaçá Valley deposits are dominated Cu-sulfide deposits with abundant bornite, chalcopyrite with magnetite and hydrous silicates; phlogopite being abundant to semi massive in places. They have high Cu/Ni and Au/PGE ratios and have abundant telluride minerals. In addition, recently discovered Ni-rich deposits contain pyrrhotite, with pentlandite loops, some Co-rich pyrite, very minor chalcopyrite that is associated with phlogopite. Both deposit types are very low in IPGE (Os, Ir, Ru) and Rh.

The Cu-Au-Te signature of the Curaçá Cu deposits, with abundant hydrous phases, particularly phlogopite, is consistent with an alkaline mafic genetic model, as these metallogenic characteristics have been identified in many of intrusions worldwide and usually represent post-subduction magmatic systems [1,2]. There are (at least at present) many more Cu occurrences identified in the Valley than Ni ones, and if the district is taken as a whole, then the overall metallogenic signature is still Cu-Au-Te dominant with some Ni and PGE. However, further discoveries of Ni would change this overall mass balance.

An alternative, or possibly additional process that may have occurred is large scale sulfide liquid fractionation, where Ni-rich mss separates from Cu-rich sulfide liquid that crystallises at a lower temperature to Cu-rich iss. The general Cu-Au-Te(+Pd) signature of the Cu ores from the Curaçá Valley are entirely consistent with an iss signature, but it would imply sulfide liquid fractionation within the magmatic plumbing system on a district scale of km to tens of km. Whilst this may seem extreme, the process is clearly scalable from the mm to cm scale seen in many sulfide blebs and patches up to deposit scale such as the Cu-rich veins at Sudbury. Textural differences are striking, with the Ni ores having sulfides as disseminations, interstitial patches and net textured and massive sulfides representative of sulfide coexisting with silicate minerals. The Cu ores in stark contrast commonly show textures indicative of migrating Cu sulfide liquid, intruding as veins and breccia fills along with net-textures and insterstitial sulfides. The importance of phlogopite and other volatile-rich mineral phases with the Cu sulfide would also be consistent with a fractionated, volatile-rich sulfide liquid migrating over a wide range of distances.

It is possible that the Curaçá Valley (and the O'okiep district in South Africa), represent deep magmatic sulfide systems at the roots of orogenic belts, formed from hydrous, metasomatized mantle sources, and where sulfide liquid fraction on a km-scale can produce both Ni- and Cu-rich deposits across a district. Regardless of the preferred individual or combined model, there is clearly potential for further discoveries in this complex setting

References:

[1] Holwell DA (2019) Nat Com 3511
[2] Blanks DE (2020) Nat Com 4342

Spatial distribution, lithological associations, and geochemical signatures of Ring of Fire Intrusive Suite within the McFaulds Lake Greenstone Belt in the Superior Province: Implications for the Ni-Cu-PGE, Cr, and Fe-Ti-V Metal Endowment of the Region

Houlé, M.G.[1,2], Sappin, A.-A.[1,] Lesher, C.M.[2], Metsaranta, R.T.[3], Rayner, N.[4], and McNicoll, V.[4]

[1]Geological Survey of Canada, Lands and Minerals Sector, Natural Resources Canada, 490 Couronne Street, Québec City, QC G1K 9A9 Canada michel.houle@nrcan-rncan.gc.ca
[2]Mineral Exploration Research Centre, Harquail School of Earth Sciences, Goodman School of Mines, Laurentian University, 935 Ramsey Lake Road, Sudbury, ON P3E 2C6 Canada
[3]Earth Resources and Geoscience Mapping Section, Ontario Geological Survey, 933 Ramsey Lake Road, Sudbury, ON P3E 6B5 Canada
[4]Geological Survey of Canada, Lands and Minerals Sector, Natural Resources Canada, 601 Booth Street, Ottawa, ON K1A 0E9 Canada

---

The McFaulds Lake greenstone belt (MLGB) is an arcuate (>200km long) belt within the Superior Province in northern Ontario that records episodic volcanism and sedimentation spanning from ca. 2.83 to 2.70 Ga and has been subdivided into several tectonostratigraphic assemblages [1]. One of the dominant geological features of the Mesoarchean to Neoarchean MLGB is the semi-continuous trend of mafic to ultramafic intrusions belonging to the Ring of Fire intrusive suite (RoFIS) [2], which hosts world-class Cr deposits, a major Ni-Cu-(PGE) deposit, and potentially significant Fe-Ti-V-(P) prospects. Intrusive bodies of the RoFIS occur within almost all volcanic-dominated supracrustal rock assemblages.

The RoFIS has been subdivided into two subsuites based on their spatial distribution, lithological associations, geochemical signatures, and mineralization styles: the Ekwan River (ERSS) and Koper Lake (KLSS) subsuites [3, 4]. Although the mafic to ultramafic intrusive bodies of these subsuites have similar emplacement/crystallization ages (KLSS = 2732.9 to 2735.5 Ma vs. ERSS = 2732.6 to 2734.1 Ma), they are significantly different in many respects: 1) the KLSS is spatially much more restricted than the ERSS; 2) the KLSS is composed of dunite, peridotite, chromitite, pyroxenite, and gabbro, whereas the ERSS is composed of abundant gabbro and ferrogabbro with lesser anorthosite and rare pyroxenite and does not contain any olivine-rich ultramafic rocks; 3) the KLSS typically hosts Cr and Ni-Cu-(PGE) mineralization (e.g., mainly within the Esker intrusive Complex), whereas the ERSS typically hosts Fe-Ti-V-(P) mineralization (e.g., Big Mac and Thunderbird intrusions); and 4) the KLSS (higher MgO, Ni and Cr) and ERSS (higher FeO_T, Ti and V) have clear differences in their geochemical trends indicating a distinct geochemical evolution (Fig. 1). Furthermore, ERSS ferrogabbro locally intrudes KLSS units, however, the opposite relationship is also observed at one locality. The magmatic evolution is still being debated, but the above observations suggest temporally overlapping but discrete ultramafic-dominated (KLSS) and mafic-dominated (ERSS) intrusions with complex contact relationships, rather than a single, large, tectonically dismembered layered ultramafic-mafic intrusion, as previously suggested [2]. A newly recognized intrusive body in the area contains olivine-rich ultramafic rocks and chromitite seams, like other members of KLSS, but both are enriched in Fe relative to rocks of the KLSS. This highlights the presence of several types of oxide-rich mineralization within the RoFIS. These include high Cr and low Fe chromitite seams typically associated with most of the Esker intrusive complex, intermediate Cr and Fe chromitite seams sporadically associated with parts of the Esker intrusive complex, and high Fe and low Cr magnetitite seams typically associated with EKSS's intrusive bodies.

Regardless of their origin, the exceptional metal endowments, and the wide diversity of mineral deposit types within the mafic and ultramafic rocks of the RoFIS, including Cr, Ni-Cu-(PGE), and Fe-Ti-V-(P) mineralization, of the McFaulds Lake greenstone belt highlight the likelihood of discovering additional mineral resources elsewhere within the Superior Province and other frontier areas throughout the Canadian Shield.

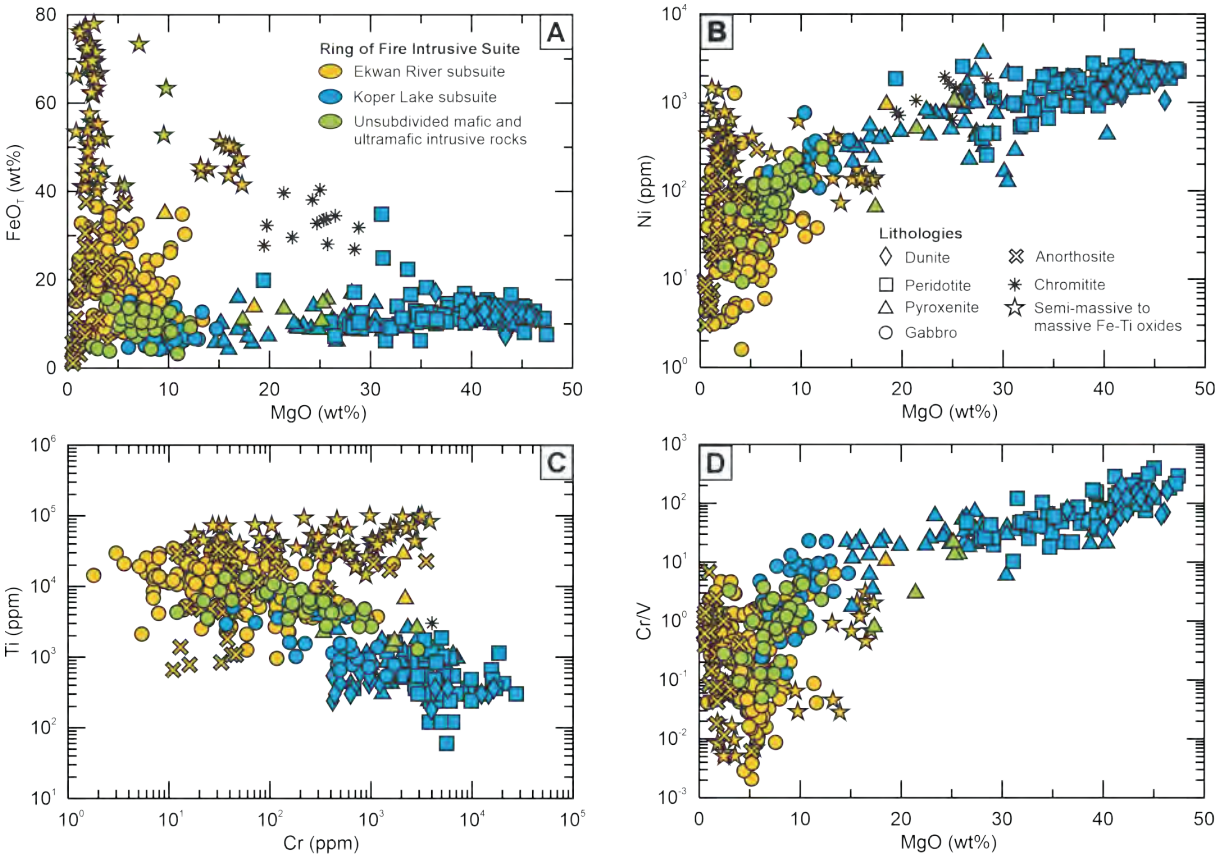


Figure 1: Binary plots of major and trace elements (anhydrous and normalized to 100%) of the mafic to ultramafic intrusions within the Koper Lake and Ekwan River subsuites of the Ring of Fire intrusive suite. A) FeOT versus MgO. B) Ni versus MgO. C) Ti versus Cr. D) Cr/V versus MgO. Data are from [5, 6, and Houlé, unpublished data].

References:

[1] Metsaranta RT and Houlé MG (2020) Open File Rep 6359:360p.
[2] Mungall JE et al. (2011) Proc GAC-MAC-SEG-SGA Ann Meeting Ottawa 2011:148
[3] Houlé MG et al. (2018) Open File Rep 8589:441-448
[4] Houlé MG et al. (2020) Open File Rep 8722:141-163
[5] Kuzmich B et al. (2015) Open File Rep 7856:115-123
[6] Metsaranta RT (2017) Ont Geol Surv Misc Rel Data 347

Spatial distribution of mafic and ultramafic units in the Canadian north: Implications for critical minerals (Ni, Cu, Co, PGE) potential

Houlé, M.G.[1,2], Bédard, M.-P.[1], Lesher, C.M.[2], and Sappin, A.-A.[1]

[1]Geological Survey of Canada, Lands and Minerals Sector, Natural Resources Canada, 490 Couronne Street, Québec City, QC G1K 9A9 Canada; michel.houle@nrcan-rncan.gc.ca
[2]Mineral Exploration Research Centre, Harquail School of Earth Sciences, Goodman School of Mines, Laurentian University, 935 Ramsey Lake Road, Sudbury, ON P3E 2C6 Canada

---

The transition to low-carbon economy that is taking place in Canada and elsewhere around the world is driving renewed interest in critical minerals, especially in battery minerals, like Ni and Co. Canada is one of the world's leading magmatic sulfide Ni producers, as attested by the presence of at least 5 world-class Ni mining districts (e.g., Sudbury-ON, Thompson-MB, Raglan/Expo-QC, Voisey's Bay-NL, and Lynn Lake-MB). These Ni-Cu-Co-(PGE) deposits are associated mainly with magmatic mafic-ultramafic mineral systems. Canada contains a very large number of mafic and ultramafic units across the country, but their total abundance is unknown and of these, only a handful are partially to well characterized. As example, a recent global compilation has reported only 52 layered intrusions in Canada [1]. Thus, an extensive compilation of mafic and ultramafic unit area is currently underway by the Geological Survey of Canada (GSC) to aid in identifying historic and future mineral resources (**Fig. 1**).

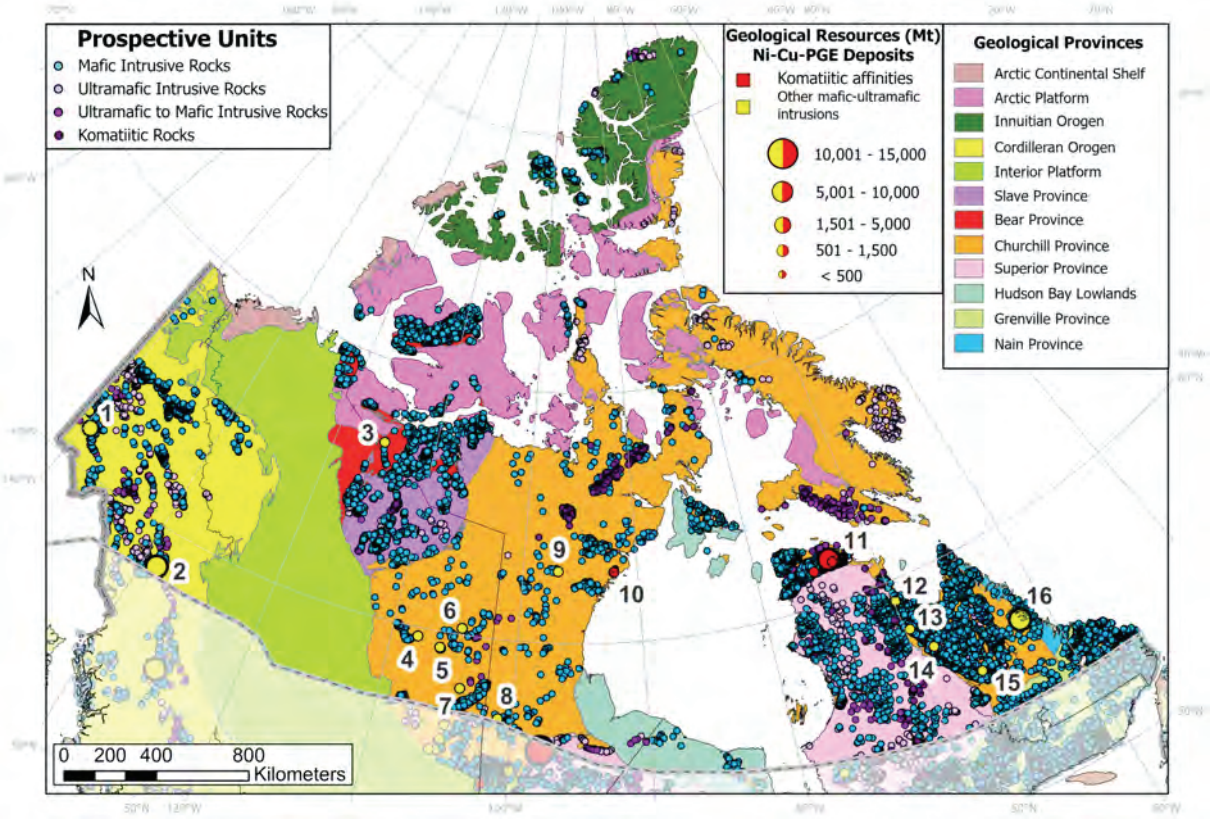


Figure 1. Distribution of mafic and ultramafic units within northern Canada. Grey dashed line represents the approximate boundary of GEM-GeoNorth area (north of ~54° N latitude). Geological provinces are from [2]. Ni-Cu-Co-(PGE) deposits: 1 = Canalask/Wellgreen, 2 = Turnagain, 3 = Muskox, 4 = Dinty, 5 = Axis/Currie/Rea, 6 = Nickel King, 7 = West Bear, 8 = Lynn Lake, 9 = Ferguson Lake, 10 = Rankin Inlet, 11 = Raglan Nickel Belt – Raglan and Expo horizons, 12 = Hope Advance sector, 13 = Chrysler-Erickson sector, 14 = Redcliff sector, 15 = Blue Lake sector, and 16 = Voisey's Bay.

The first step in this compilation is a large-scale spatial inventory of mafic and ultramafic units. To date, over fifteen thousand units have been catalogued north of ~54° N latitude (within the GEM-GeoNorth area), based on geological maps available at scales ranging from large scale (1:500,000 to

1:63,360) to more detailed scale (1:5,000 or less), in the vicinity of known and historic Ni-Cu-(PGE) deposits, and where areas of interest have been identified due to the preponderance of mafic-ultramafic units or nickel showings. Within the GEM-GeoNorth area, the largest proportions of mafic and ultramafic bodies are related to three major Proterozoic Large Igneous Provinces (LIPs) worldwide: the Franklin LIP (~0.72 Ga), the Mackenzie LIP (~1.27 Ga), and the Circum-Superior LIP (~1.88 Ga), which exhibit quite variable metal endowments [3]. Thus far, no deposits have been found in the Franklin LIP, only small Ni-Cu-(PGE) and Cr deposits have been identified in the Mackenzie LIP (e.g., Muskox), whereas world-class mining districts occur within the Circum-Superior LIP (e.g., Raglan, Thompson). Because of the size of the Muskox intrusion (over 120 km long), its worldwide recognition, and the historical work done by the GSC in 1960s [4], this prospective unit will receive a special attention within the framework of this compilation.

In the Canadian context, magmatic Ni-Cu-Co-(PGE) deposits with variable abundances of sulfides/alloys and metal ratios have formed throughout geological time (Mesoarchean to Cenozoic), from a wide range of parental magmas (komatiitic to quartz dioritic), in a wide range of tectonic settings (extensional to convergent), so none of these attributes are particularly critical exploration variables. Almost all the historic and current Canadian production comes from large mining districts (e.g., Sudbury, Thompson, Voisey's Bay, Raglan, and Lynn Lake), all of which still have significant large brownfield potential. However, several other regions have excellent greenfields potential, as evidenced by the presence of many historic and recently discovered Ni-Cu-Co-(PGE) deposits. The preliminary results of the GSC compilation indicate, for example, that more than 50 Ni-Cu-Co-(PGE) deposits occur north of ~54° N latitude, including Triassic flood basalt-related subvolcanic intrusions (e.g., Wellgreen, Canalask) and Jurassic plutonic zoned/composite complexes (e.g., Turnagain) within the Cordillera Province; Neoarchean norite- and gabbro-related intrusions (e.g., Nickel King, Ferguson Lake), Paleoproterozoic komatiite-related (e.g., Rankin Inlet) and gabbro-related (e.g., Lynn Lake) intrusions within the Western Churchill; Paleoproterozoic volcanic (e.g., Raglan) and subvolcanic (e.g., Expo Ungava) komatiitic basalt-related lava channels and channelized dikes within the Central Churchill; Paleoproterozoic volcanic-subvolcanic picritic to komatiitic basalt-related intrusions, differentiated ultramafic to mafic sills, and glomeroporphyritic gabbroic sills within the Eastern Churchill; and Mesoproterozoic plutonic troctolitic (e.g., Voisey's Bay) intrusions within the Nain Province. The degree of preservation of these deposits ranges from essentially unmetamorphosed and undeformed (e.g., Voisey's Bay) through low-grade metamorphosed with very localized deformation (e.g., Raglan) to medium- and high-grade metamorphosed with widespread deformation (e.g., Ferguson Lake, Thompson).

Overall, the ubiquitous distribution of ultramafic and mafic units highlighted by this compilation indicates that there is not only significant potential for the discovery of additional Ni-Cu-Co-(PGE) mineralization in traditional and established mining camps, but also has tremendous potential for the discovery of new Ni-Cu-Co-(PGE) and Cr-PGE deposits in under-explored regions of Canada.

References:

[1] Smith WD and Maier WD (2021) Earth Sci Rev 220:1-36

[2] Wheeler JO et al (1996) GSC A Map Series 1860A

[3] Ernst RE (2014) Larg Ign Prov; Camb Univ Press: 667

[4] Scoates JS and Scoates RFJ (2024) Lithos 474-475: 1-40

Copper and komatiitic magmatism – source of copper in the Sakatti Cu-Ni-PGE deposit in northern Finland

Höytiä, H.[1,2], Peltonen P.[1], Halkoaho, T.[3], Makkonen, H.V.[3,5] and Virtanen, V.J.[1,5]

[1]Department of Geosciences and Geography, P.O. Box 64, FI-00014 University of Helsinki, Finland
[2]Anglo American plc (AA Sakatti Mining Oy), Tuohiaavantie 2, FI-99600 Sodankylä, Finland
[3]Geological Survey of Finland, P.O. Box 1237, FI-70211 Kuopio, Finland
[4] Geological Survey of Finland, Vuorimiehentie 2K, FI-02150 Espoo
[5]Suomen Malmitutkimus Oy, Kuopio, Finland
[6]Institut des Sciences de la Terre d'Orléans, UMR 7327, CNRS/Université d'Orléans/BRGM, Orléans, France

---

Copper is an important commodity in most of the magmatic Ni-Cu-platinum group element (PGE) sulfide deposits. Several nickel camps and deposits, e.g. Noril'sk (Russia), Sudbury and Raglan (Canada), and Jinchuan (China), host individual mineralizations and mineralization types that are more enriched in Cu compared to Ni. Host rocks of these Cu-enriched Ni-deposits vary from mafic (derived from tholeiitic parental magmas) to ultramafic (derived from ferropicritic or komatiitic basaltic parental magmas) and they bear evidence of variable, but generally high silicate/sulfide mass ratios (R factor) from c. 100 to > 1000 during their formation [1.Important Cu-enrichment mechanisms also include mantle source with low Ni/Cu, fractional crystallization of segregated sulfide phase, assimilation of Cu from external source, and post-magmatic modification of sulfides by fluids.

Sakatti is a Cu-Ni-PGE deposit in the Paleoproterozoic c. 2.5-1.8 Ga Central Greenstone Belt (CLGB) in northern Finland with total reported resources of 44.4 Mt @ 1.9% Cu, 0.96 % Ni, 0.05% Co, 0.64 g/t Pt, 0.49 g/t Pd and 0.33 g/t Au [2]. The deposit was discovered by Anglo American Plc in 2009 and can be sub-divided into six distinct ore types: 1) Ni-rich massive ore, 2) Cu-rich massive ore, 3) Ni-Cu interstitial ore in gabbronorites, 4) Cu-rich disseminated ore, 5) Cu-PGE-rich stockwork vein ore, and 6) Py-rich massive ore. The mineral assemblage consists of chalcopyrite, pyrrhotite, pentlandite, pyrite and Ni-Pt-Pd tellurides of the melonite-merenskyite-moncheite series. The sulfide phase shows evident fractionation from Ni-rich monosulfide solid solution (mss) to Cu-rich intermediate sulfide solid solution (iss) [3, 4]. Bulk of the sulfides in Sakatti show narrow range of $\delta^{34}S$, between +2 and +4 ‰, indicating non-magmatic source of sulfur for much of the deposit. The Sakatti sulfide deposit is underlain by argillaceous sediments with thick anhydrite-gypsum intervals, some of which, are in direct contact with the cumulates and show prominent magma-country interaction.

The sulfide ores in Sakatti are hosted by chonolith-style magma conduit composed of ortho-, meso- and adcumulates, pegmatoidal gabbronorites and fine-grained komatiitic rocks. These are derived from a komatiitic parental magma in equilibrium with Fo_{92-93} olivine (c. 19–21 wt. % MgO). Olivine in the Sakatti deposit contains relatively high Ni contents (2500–3500 ppm), which can be due orthopyroxene fractionation in the lower crust en route to surface [5]. Typical mineral assemblage contains olivine + chromite ± orthopyroxene ± clinopyroxene ± plagioclase. All host rocks show one to two orders of magnitude enrichment in LREE compared to that of chondrite. The age of the ultramafic magmatism is constrained to c. 2054 Ma [6], which corresponds to a global Ni-Cu-PGE mineralizing event with coeval ages in e.g. Bushveld (South Africa), Mirabela (Brazil) and Elanskii (Ukraine) complexes, related to the final break-up of the supercontinent Kenorland.

With R factor modelling it is not possible to achieve the observed low Ni/Cu ratio at Sakatti. The same is true also with the N factor (zone refining) or with the multistage upgrading modelling. Therefore, four other processes that could account for the anomalously high Cu-content and low Ni/Cu of Sakatti are discussed: 1) Magma generation from Cu-enriched metasomatized mantle source 2) removal of Ni-rich mss at depth, 3) Assimilation of copper from country rocks, and 4) post-magmatic upgrade of the Cu grades.

[1] Cu-enriched mantle source is commonly attributed to metasomatized mantle. Uncontaminated CLGB komatiites have MREE-enriched hump-shaped patterns, reflecting limited marks of metasomatized source at the time of their separation [7]. Mantle source alone contributing the copper contents in Sakatti is doubtful, as the degrees of partial melting for parental melts are high (c. 15-25 %) [5, 7].

[2] Brownscombe et al. [3] proposed that the primary mss was segregated at earlier stage and the Cu-rich portion of it was re-assimilated and injected into the current host cumulates by later magmas that did not equilibrate with the sulfides, possibly due to a kinetically controlled process, similar to that proposed for varying metal tenors in the Raglan deposits [8]. However, the most primitive olivine cumulates also host the most primitive mss, indicating that host magma took part to the sulfide segregation to some degree. R factors for Sakatti are generally low (50–100) and the modelled Ni/Cu values are generally much higher than the ones observed, therefore indicating that there must be additional processes contributing to the varying Ni/Cu ratios. However, an alternating option could arise from computational simulations, where Ni/Cu ratios between 1.9 and 0.4 ratios can be produced for sulfides during closed fractional crystallization scenario depending on the initial sulfur content of the parental magma [5].

[3] Magma-sulfate interaction textures, positive $\delta^{34}S$, elevated Fe^{3+} contents in chromite [9] and similarity in REE-patterns between cumulates and sulfate rocks indicate that Sakatti host rocks have assimilated their sulfate-bearing country rocks during ascent and/or in-situ. However, most of the seemingly unaltered sulfate sediments bear very low Cu contents, and besides, regionally potential assimilants have Cu contents typically below 150 ppm [10, 11]. Yet copper collection during assimilation could be facilitated by oxidized magma, coexisting magmatic fluid(s) [12] and formation of xenomelts [13], which would form as a response to assimilation of carbonate-sulfate sediments.

[4] Re-Os [14], U-Pb [6], Pb-Pb, and Cu isotope results [15] point towards later remobilization of the Cu-rich portions of the ore. However, no obvious alteration patterns resulting from late hydrothermal fluids are found in the deposit. Age constraint for post-magmatic modification spans from c. 1.9 to 1.8 Ga [6, 14], which include ages of the numerous Au and IOCG (Iron-Oxide -Copper-Gold) deposits within the CLGB [16], suggesting mobility of copper during this period. Massive sulfide ores, however, pose a strong chemical buffer, which means they are not easily extensively affected by fluid activity.

The discussed processes are not mutually exclusive and could have contributed to the high Cu budget. The available data indicates that processes 2) and 4) were the dominant controls of Cu.

[1] Burrows D and Lesher M (2012) Econ Geol 16:515–552
[2] Anglo American Ore Reserves and Mineral Resources Report (2022)
[3] Brownscombe W et al. (2015) Min Dep of Finland:211–252
[4] Fröhlich F et al. (2021) Can Min 59:1485–1510
[5] Virtanen V et al. (in review)
[6] Höytiä et al. (in review)
[7] Hanski E and Kamenetsky V (2013) Chem Geol 343:25–37
[8] Li Y and Mungall J (2022) Econ Geol 117:1131–1148
[9] Silventoinen S (2020) M.Sc. thesis Uni Helsinki, 95 p.
[10] Haverinen J (2020). M.Sc. thesis, Uni Helsinki, 82 p
[11] Köykkä J et al. (2019) Precamb Res 331:105364
[12] Iacono-Marziano G et al. (2017) Ore Geol Rev 90:399–413
[13] Lesher C (2017) Ore Geol Rev 90:465–484
[14] Moilanen M et al. (2021) Ore Geol Rev 132:104044
[15] Höytiä H et al. (2023) 14th Int Pt Symposium Abs Vol:235–236
[16] Niiranen T (2005) PhD thesis synopsis D6, Uni Helsinki, 27 p.

The Koperberg Suite of the Okiep Copper District - an overlooked target for magmatic nickel sulphides in a convergent margin system

Hunt J.P.[1], van Schalkwyk L.[1], Smart E.[1] and Benhura C.[1]

[1]Orion Minerals, 16 North Road, Dunkeld West, Randburg 2196, South Africa,
johnpaul.hunt@orionminerals.com.au

The Okiep Copper District (OCD) is the oldest formal mining district in South Africa dating back to 1852, having produced 2.2 Mt of Cu from 32 mines and 70% of this total having been mined from just 5 mines. It is located in the Bushmanland Subprovince of the Namaqua Sector of the Namaqua-Natal Metamorphic Province (NNMP) which is younger than but broadly contemporaneous with the Grenville-Kibaran orogenies associated with the amalgamation of the Rodinia supercontinent (Figure 1). Steep northwards subduction occurred to the south of the NNMP. Roll-back of the subducting slab causing dextral trans-tensional extension in the continental back-arc environment, where the Bushmanland Subprovince is presently located. Metamorphic grade, in general, increases from amphibolite facies in the north to upper granulite facies in the south. Namaquan orogenesis occurred in two episiodes: the Okiepian Episode (1180-1210 Ma) involving crustal shortening and the intrusion of large volumes of granitic sheets (now granite gneiss); and the Klondikean Episode (1020-1040 Ma) involving mafic underplating, ultra-high-temperature metamorphism, granitic sheets, dextral transtension, constrictional fabrics, and crustal thinning [1] and importantly the intrusion of the Koperberg Suite.

The Koperberg Suite is by volume predominantly anorthositic with associated jotunite, biotite diorite, leuconorite, norite, hypersthenite, and glimmerite intruded as discrete magmatic events. It intruded as ENE and ESE oriented, irregular and discontinuous dykes, sills and plugs into an overwhelmingly granulite-facies granite-gneiss terrane, which were commonly focused within kinked anticlines

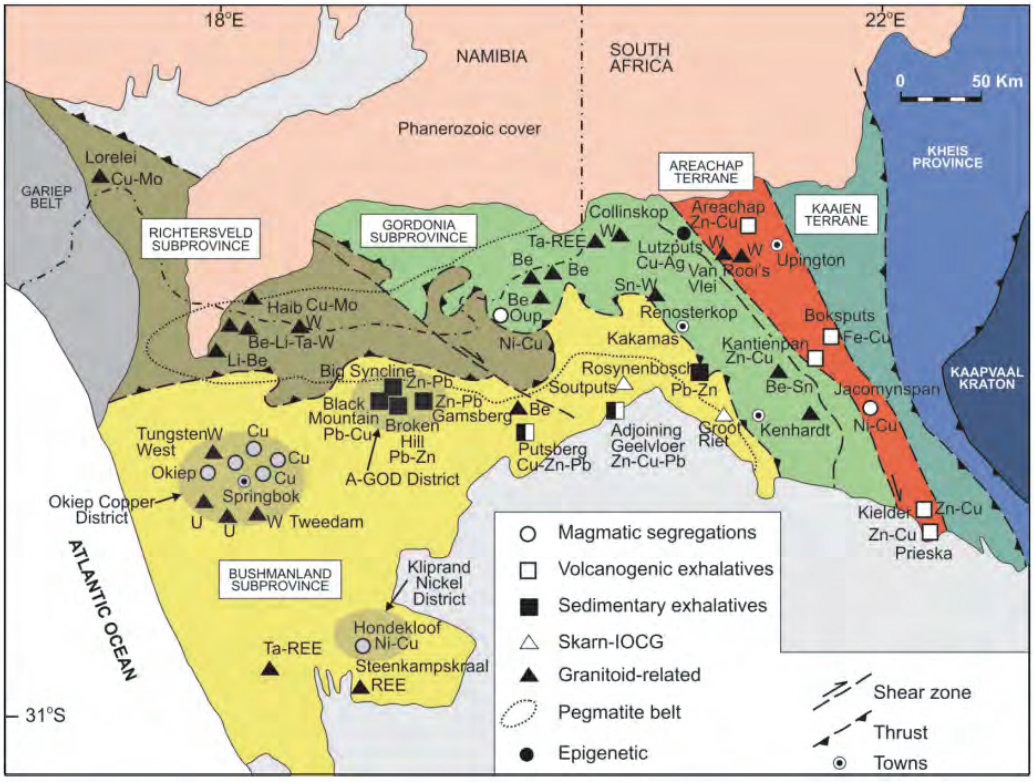


Figure 2. Distribution of ore deposits and mining districts in the various Subprovinces and Terranes of the Namaqua Sector of the Namaqua-Natal Metamorphic Province. The Okiep Copper District is located in the

northern portion of the Bushmanland Supbprovince, with the Kliprand Nickel District located approximately 150km to the southeast [2].

known as ‘steep structures’. The quartzites and metapelites of the Khurisberg Subgroup have historically been a potentially lithological control with the majority of known mineralised intrusions occurring stratigraphically above this horizon.

It has long been established that the sequence of intrusion is from felsic to mafic: anorthosite was the earliest intruded magma, followed by ferrodiorites, then norites, and ultimately orthopyroxenites (hypersthenites) and magnetitites. The majority of mineralisation is associated with the increasingly more mafic lithotypes, the majority being hosted by magnetitite, orthopyroxenite and norite, then ferrodiorite, and only a small proportion of mineralisation being hosted by anorthosite.

The Koperberg Suite ores are grouped based on the main sulphide assemblage [3], namely the:
1. Carolusberg-type ore: the most abundant type characterised by a bn-mgt (± cp) assemblage
2. Narrap-type ore: characterised by a typical iss assemblage (cp + po ± pn),
3. Hoit-type ore: an intermediate assemblage characterised by a bn-cp

It had long been held that the overwhelmingly abundant bn-mgt assemblage within the OCD was a consequence of post-magmatic oxidation of a primary sulphide assemblage as represented by the Narrap type, however, recent trace element and isotopic studies suggest this not to be the case [3]. Oxidation of the magma liquid and the corresponding immiscible sulphide liquid occurs with progressive crystallisation and fractionation of Fe^{2+}-rich phases and post-magmatic oxidation of the sulphide is not supported by textural and geochemical observations.

The Hondekloof Ni-Cu deposit is located approximately 150km SE of the OCD in the Kliprand Nickel District (KND). This gabbronorite-hosted basal massive sulphide mineralisation is part of a larger suite of intrusives including anorthosite, norite, quartz norite, diorite, glimmerite, and an earlier extensively developed charno-enderbite. The mineralisation assemblage of magnetic pyrrhotite with minor exsolved cobaltian pentlandite, chalcopyrite as well as pyrite is typical of orthomagmatic Ni-Cu-Co bearing sulphide bodies derived from a typical mss assemblage [4]. On the basis of petrological and petrochemical similarities, the gabbronorite host is correlated with a pre-Koperberg Suite “two pyroxene granulite” of the OCD, effectively having an identical gabbronoritic mineralogy and chemistry. This mafic unit was historically regarded as being unmineralized and therefore avoided.

A two-stage model was proposed [4] which is simplified as follows:
Stage 1. an early nickeliferous mss sulphide liquid was extracted from the magma chamber associated with pre- to syn-tectonic gabbronorites.
Stage 2. renewed tectonism and compression of the magma chamber resulted in the extraction of first an anorthositic suite, followed by increasingly more mafic assemblages and ultimately the most hypermelanic phases and the low-S, high-mgt, cupriferous residual iss sulphide liquid from the base of the magma chamber.

The exploration implications for the OCD is that the historical exploration and exploitation has concentrated on bn-mgt rich ores, traced on surface and followed down to depth, or efficiently mapped by magnetic geophysical surveys. The distribution of “two-pyroxene granulites” has been mapped but entirely disregarded until now. A number of known deposits have elevated Ni concentrations, such as Okiep East and Narap Mine, and it is noted that these are in proximity to increased occurrences of two-pyroxene granulites. Modern transient electromagnetic (TEM) surveys have only recently been completed and map a number of discrete anomalies both in proximity to Koperberg Suite intrusives and distinct from them. At two localities, Ezelsfontein East and Nous, both located within the OCD, drilling confirmed the presence of massive and disseminated Ni-Cu sulphide, establishing proof of concept and opening up the OCD to new aspects in its exploration potential.

References:

[1] Dewey J et al. (2006) Precam Res 150(3-4), 173–182
[2] Rozendaal A et al. (2017) SAJG 120(1), 153–186
[3] Marima E (2022) Unpubl. MSc Univ. Rhodes 120p
[4] Hamman J N et al. (1996) SAJG 99(2), 153-16

A multi-methodological approach: Combining textural observations and geochronology to study the J-M Reef Package and its Hanging Wall, Stillwater Complex, Montana

Jenkins, M.C.[1*], Corson, S.[2], Geraghty[2], E., Kamo S.L. [3], Lowers, H.[4], and Mungall, J.E.[5]

[1]U.S. Geological Survey, Geology, Minerals, Energy, and Geophysics Science Center, Spokane, Washington, USA
*mcjenkins@usgs.gov
[2]Sibanye-Stillwater, Columbus, Montana, USA
[3]Jack Satterly Geochronology Laboratory, University of Toronto, Toronto, Ontario, Canada
[4]U.S. Geological Survey, Geology, Geophysics, and Geochemistry Science Center, Denver, Colorado, USA
[5]Department of Earth Sciences, Carleton University, Ottawa, Ontario, Canada

---

The J-M Reef is a world-class platinum-group element (PGE) deposit hosted in the 2.709 Ga Stillwater Complex in Montana, USA [1, 2]. The J-M Reef is the accumulation of PGE-enriched sulfide minerals located in the Anorthosite subzone I (ASZI) of the Troctolite-Anorthosite zone I in the Lower Banded series of the complex (Fig. 1A). Anorthosite subzone I is comprised of anorthosites, troctolites, peridotites, and norite adcumulates and heteradcumulates. The cumulates that host economic J-M Reef sulfide mineralization are generally coarse-grained to pegmatoidal in texture and may be any of the rock types found in ASZI. These coarse-grained rocks are called the Reef Package (Fig. 1B). The top of the Reef Package is marked by a textural discontinuity between the coarse-grained cumulates and relatively fine-grained cumulates in the hanging wall. The surface that marks the top of the Reef Package is informally called the hanging wall contact and economic PGE mineralization is not found above this contact [3]. The sulfide mineralization that makes up the J-M Reef may not always be present; therefore, tracing the reef location during mine development can be challenging [1]. The hanging wall contact can always be identified in drill core and underground workings even where the J-M Reef is not present making this contact an important marker horizon during mining.

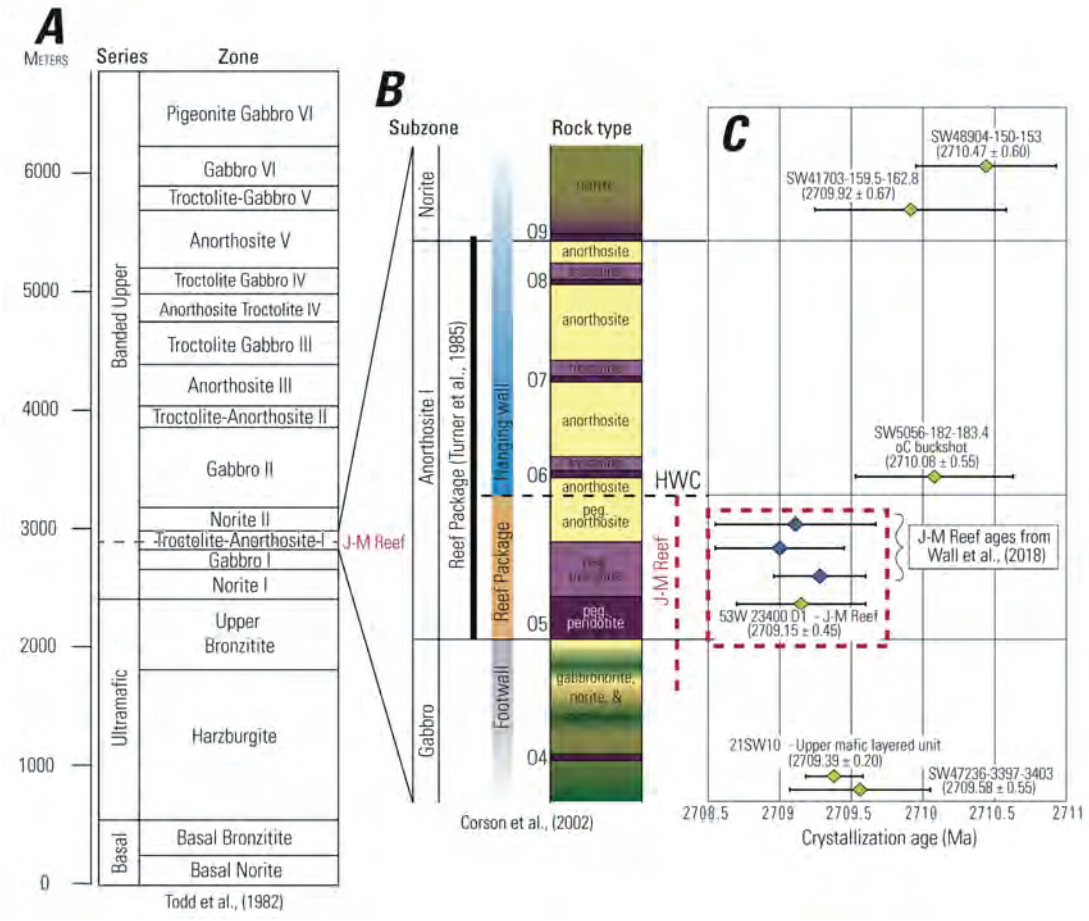


Figure 3. 1A) Stratigraphic section showing the series and zone nomenclature for the Stillwater Complex [4]. 1B) Stratigraphic section showing the subzones of Troctolite-Anorthosite zone I [3, 5, 6]. The general location of the hanging wall contact (HWC) is shown as a dashed line. 1C) Preliminary U-Pb zircon ages (yellow) and published zircon ages of the J-M Reef from Wall et al. (2018; blue) [2]. Zircon mean ages are shown as points and error bars correspond to 2σ.

Electron backscattered diffraction was used to investigate the microtextural change at the hanging wall contact from four intersections. In general, the results show that rocks in the hanging wall are characterized by finer crystal sizes and a well-developed B-type fabric typical of cumulates from layered mafic intrusions (Fig. 2) [7]. In contrast, the rocks that host the J-M Reef are found to be coarse-grained and do not have a strong rock fabric indicating that they likely crystallized under conditions where crystal settling, compaction, or magmatic flow did not impact the orientations of the crystals. Instead, the Reef Package may have crystallized *in situ* where crystals grew to impingement without a preferred orientation. These findings do not resolve the origin of the hanging wall contact as it could plausibly represent either a resumption of normal layered mafic intrusion petrogenetic processes like crystal settling and/or compaction or it could represent a pre-existing cumulate layer that acted as an aquitard to the magma that formed the Reef Package.

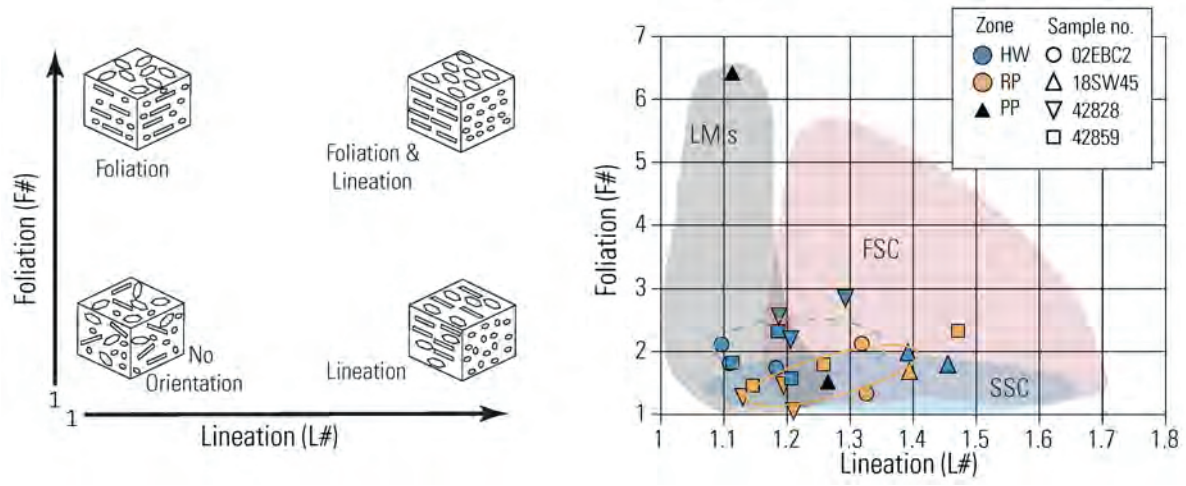


Figure 4. Bivariate plots showing rock fabrics from the hanging wall (HW) and Reef Package (RP) based on the foliation number (F#) vs the lineation number (L#) defined as the ratios of the maximum eigen value divided by the intermediate eigen value for the crystallographic axes. The F# is equal to e1/e2 for the (010) plane and the L# is equal to the e1/e2 for the [100] direction. Stillwater cumulates from the Picket Pin (PP) area are shown as solid black triangles. The shaded fields show where data from other layered mafic intrusions (LMIs), fast spreading centers (FSC), and slow spreading centers (SSC) plot on the diagram [3, 7].

To test the hypothesis that the hanging wall contact represented a cumulate layer that existed prior to the emplacement of the magma that formed the Reef Package, high-precision chemical abrasion-isotope dilution thermal ionization mass spectrometry (CA-ID-TIMS) zircon U-Pb dating was used to determine the age of rocks below, above, and within the Reef Package (Fig. 1B). The mean ages of zircons below the Reef Package are approximately the same as those in the Reef Package. In contrast, mean ages from zircons in the hanging wall are older than the Reef Package—including one substantially older sample (SW48904-150-153) from Norite subzone (Fig. 1B). These results support the hypothesis that the hanging wall contact represents the base of a pre-existing cumulate layer that caused the magma that formed the J-M Reef Package to pool at the level of the Reef Package. The zircon ages are consistent with out-of-sequence CA-ID-TIMs zircon ages that have been reported from Stillwater [2] and the Bushveld [8, 9] complexes. The age results do not place firm constraints on the origin of the J-M Reef deposit as either the hydromagmatic model [10] or orthomagmatic

model [11] could plausibly form the reef with or without the presence of an overlying igneous aquitard layer.

References:

[1] Jenkins et al. (2020) Econ Geol 115: 1799-1826
[2] Wall et al. (2018) J Petrol 59: 153-190
[3] Jenkins et al. (2022) J Petrol 63: egac053
[4] Todd et al. (1982) Econ Geol 77: 1454-1480
[5] Turner et al. (1985) Mont Bur Min Geol 92: 210-230
[6] Corson et al. (2002) 9th Plat Symp 101-102
[7] Cheadle and Gee (2017) Elem 13: 409-414
[8] Mungall et al. (2016) N Comm 7: 13385
[9] Scoates et al. (2021) J Petrol 62: egaa107
[10] Boudreau (1999) J Petrol 40: 755-772
[11] Jenkins et al. (2021) Precambr Res 367: 106457

Note: Any use of trade, firm, or product names is for descriptive purposes only and does not imply endorsement by the U.S. Government.

Nickel-copper-platinum group elements potential of mafic and ultramafic intrusions in northwestern Ontario

Jonsson, J.[1], Malegus, P.[1], Churchley, S.[1], Price, R.[1]

[1]Resident Geologist Program, Ontario Geological Survey, Ministry of Mines, Suite B002, 435 James Street South, Thunder Bay, ON P7E 6S7 Canada

---

Globally, magmatic sulphide deposits host significant resources of nickel, copper, cobalt and platinum group elements (PGE). These deposits occur as concentrations of sulphide minerals hosted within mafic to ultramafic intrusive rocks and are widespread across Ontario, occurring in every Precambrian geologic terrane. Ontario is home to 10 operating mines in magmatic sulphide deposits: 9 within the Paleoproterozoic Sudbury Igneous Complex and one within the Neoarchean Lac des Iles Complex.

In 1999, Operation Treasure Hunt was initiated by the Ontario Government to stimulate mineral exploration by acquiring new airborne geophysical data, surficial and bedrock geochemical data, and development of new methods. In 2003, following completion of the Operation Treasure Hunt project, the Ontario Geological Survey published a report that assessed 109 mafic to ultramafic intrusions across Ontario [2]. The purpose of this part of Operation Treasure Hunt was to characterize and publish data for intrusions known to be prospective for PGE-dominated magmatic sulphide mineralization. Many of the intrusions studied during Operation Treasure Hunt were host to significant known mineralization, including current and past-producing mines, and several of these intrusions are the focus of ongoing mineral exploration.

Despite the work by Vaillancourt et al. [2], there are hundreds of mafic to ultramafic intrusions in Ontario that have not been systematically assessed for magmatic sulphide mineralization potential. Many of these intrusions have favourable characteristics for potentially containing magmatic sulphide deposits, including geophysical anomalies (e.g., magnetic, conductivity), overburden geochemical anomalies and known sulphide mineralization.

In 2023, the Resident Geologist Program of the Ontario Geological Survey initiated a project to systematically characterize geochemistry of a subset of mafic-ultramafic intrusions in northwestern Ontario that largely have not been subject to significant historical evaluation by academic researchers, government surveys, or mineral exploration companies. Evaluating the geochemistry of mafic to ultramafic intrusions can provide insight into the magma history, tectonic setting and potential for economic metal endowment. Factors that may influence metal endowment, that can be determined from the examination of geochemical data, include determining magma source characteristics, the timing of sulphur saturation and the degree of interaction of the magma(s) with their country rocks. Careful evaluation of physical characteristics and whole-rock geochemistry can inform future mineral exploration and/or the development of models for the emplacement of mafic to ultramafic intrusions and any hosted mineralization.

Initial sample collection and analytical work took place during 2023. Areas of interest are shown in Figure 1, and include the Red Lake, Onaman–Tashota, and Heaven Lake greenstone belts. In this display, we provide examples of preliminary results and interpretations from areas targeted in the first year of field work, including the Trout Bay intrusion (Red Lake greenstone belt), Westwood intrusion (northeast of the Lumby Lake greenstone belt), and the Big Ghee Lake intrusion (south of the Shebandowan greenstone belt).

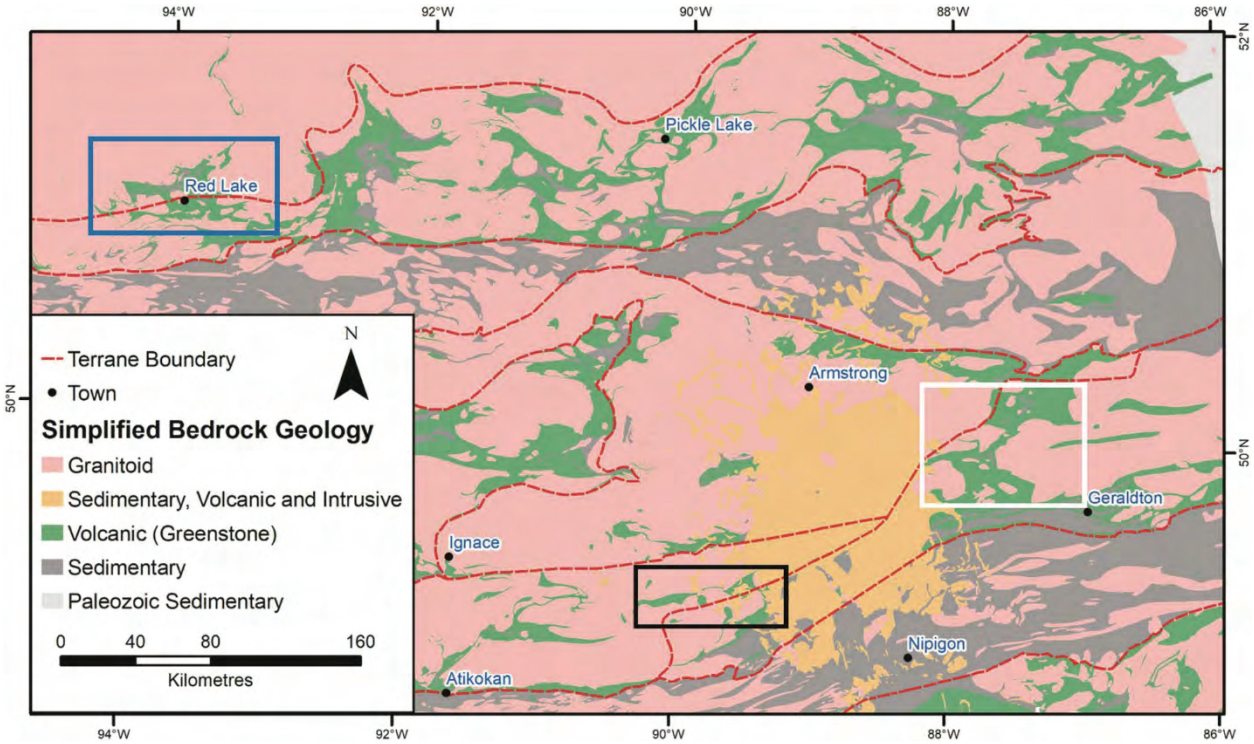


Figure 1. Simplified bedrock geology map of a portion of northwestern Ontario, showing project target areas: Red Lake greenstone belt (outlined in blue); Heaven Lake greenstone belt (outlined in black); and Onaman–Tashota greenstone belt (outlined in white). Regional geology modified from Ontario Geological Survey [1].

References

[1] Ontario Geological Survey 2011. 1:250 000 scale bedrock geology of Ontario; Ontario Geological Survey, Miscellaneous Release—Data 126 – Revision 1.

[2] Vaillancourt, C., Sproule, R.A., MacDonald, C.A. and Lesher, C.M. 2003. Investigation of mafic-ultramafic intrusions in Ontario and implications for platinum group element mineralization: Operation Treasure Hunt; Ontario Geological Survey, Open File Report 6102, 335p.

Petrogenesis of the mineralized horizons in the Offset and Creek zones, Lac des Iles Complex, N. Ontario

Jonsson, J.[1], Hollings, P.[1], Brzozowski, M.[1], Bain, W.[1], Djon, L.[2]

[1]Department of Geology, Lakehead University, 955 Oliver Road Thunder Bay, ON P7B 5E1 Canada
[2]Impala Canada, 69 Yonge Street, Suite 700 Toronto, ON M5E 1K3 Canada

---

The Lac des Iles Complex is a Neoarchean (2.69 Ga; D.W. Davis cited in Stone et al., 2003) polyphase mafic-ultramafic complex located in the Marmion terrane of the Superior Province, 85 km north of Thunder Bay, Ontario, Canada. The intrusive complex can be subdivided into two discrete subcomplexes: the ultramafic-dominated North Lac des Iles Complex and the mafic-dominated South Lac des Iles Complex (SLDIC). The SLDIC has been subdivided into four intrusive series, termed the gabbronorite, breccia, norite, and diorite series (Decharte et al., 2018). To date, economic Pd-rich mineralization has been discovered in both the breccia and norite series, and occurs proximal to the contacts between the breccia and gabbronorite series and between the breccia and norite series. The objectives of this study are to i) evaluate the mechanisms of formation of the mineralized horizons near the contact between the breccia and norite domains in the Offset and Creek zones of the SLDIC, ii) evaluate the role that crustal contamination played in this process, and iii) assess the tectonic setting in which the SLDIC formed.

The breccia and norite series are both composed of varitextured, brecciated, and equigranular leucocratic-melanocratic norites and gabbronorites, and their altered equivalents. The breccia series contains a greater proportion of brecciated and varitextured rocks, while the norite series contains a greater proportion of equigranular rocks. All pre-alteration lithologies are essentially plagioclase-orthopyroxene cumulates with varyingly minor quantities of interstitial clinopyroxene, biotite, magnetite, chalcopyrite, pentlandite, and pyrrhotite. Variable degrees of hydrothermal alteration are indicated by the presence of tremolite-actinolite and talc (after pyroxenes), chlorite and sericite (after plagioclase), and pyrite (after pyrrhotite). Although the breccia and norite series are mineralogically similar, the breccia series is generally more leucocratic (i.e., higher plagioclase/pyroxene ratio) than the norite series.

Neodymium isotopic evidence indicates that the Offset and Creek Zone magmas were crustally contaminated. ε_{Nd} values of 19 analyzed samples range from +0.38 to -3.47 (median = -2.13), which is consistently more negative than the ε_{Nd} value of +2.24 expected in an uncontaminated mantle-derived magma that crystallized at 2.69 Ga. The crustal contaminant that imparted the negative ε_{Nd} values is unlikely to be the tonalitic gneiss that hosts the SLDIC, as the ε_{Nd} value of one reported tonalitic gneiss sample is -1.77 (Brugmann et al., 1997). The lack of correlation between ε_{Nd} and geochemical or spatial variations suggests that variable crustal contamination was not the cause of the geochemical variability observed within the Offset and Creek Zones. Samples from both the breccia and norite series have similar trace-element chemistry, including enriched LILE/LREE patterns, flat HREE patterns, and pronounced negative Nb anomalies. Although these characteristics can be caused by assimilation of crustal material, it is more likely that they are the result of formation of the parental magma in a magmatic arc. Evidence for this interpretation includes low Nb/Yb ratios, high Ba/Th ratios, low Th content, and the lack of correlation between geochemical variability and Nd isotopic variability.

Evidence from S isotopes of sulfide minerals and whole-rock geochemistry suggests that the addition of crustal S was not necessary in the formation of the Pd-rich mineralization within the Offset and Creek zones. $\delta^{34}S$ values of 54 crystals from 17 samples range from -0.37‰ to +3.28‰ VCDT (median = +1.11‰), with values from 52 of 54 crystals falling in the expected range of mantle-derived sulfur (0 ± 2‰; Seal, 2006). Based on the association of low Cu/Pd ratios with high Pd values, Offset and Creek zone ores formed at high R factors, which were likely high enough to cause the PGE

enrichment without incorporation of crustal sulfur. The higher degree of Pd enrichment in the Offset Zone compared to the Creek Zone was likely due to a greater amount of sulfide liquid in the Offset Zone that also underwent higher R factors; the distribution of sulfide liquid and magma flow may have been influenced by primary structural constraints on the geometry of the intrusion. No evidence was found for significant low-temperature remobilization of chalcophile elements, including the PGEs.

The compositional variability observed within the breccia and norite domains suggests that both domains formed via multiple pulses of compositionally similar magma. The proximity of mineralization to the interpreted feeder conduits suggests that the distribution of mineralization is largely the result of PGMs/Pd-rich pentlandite crystallizing as the magma transitioned from the feeder structure outwards into the periphery of the intrusive complex. This process may have repeated several times as successive magma pulses infiltrated the partially crystallized intrusive complex, resulting in the redistribution of ores in brecciated zones.

References:

Brugmann, G.E., Reischmann, T., Naldrett, A.J., and Sutcliffe, S.H., 1997. Roots of an Archean volcanic arc complex: the Lac des Iles area in Ontario, Canada. Precambrian Research, vol. 81, p. 223-239.
Decharte, D., Hofton, T., Marrs, G., Olson, S., Peck, D., Perusse, C., Roney, C., Taylor, S., Thibodeau, D., and Young, B., 2018. Feasibility study for Lac des Iles mine incorporating underground mining of the Roby Zone. North American Palladium, NI 43-101 Technical Report, 435p.
Seal, R.R., 2006. Sulfur isotope geochemistry of sulfide minerals. Reviews in Mineralogy and Geochemistry, vol. 61, p. 633-677.
Stone, D., Lavigne, M.J., Schnieders, B., Scott, J., and Wagner, D., 2003. Regional geology of the Lac des Iles area, in Summary of Field Work and Other Activities 2003. Ontario Geological Survey, Open File Report 6120, p. 15-1 to 15-25.

Quantum full tensor magnetic gradiometry to better define conduit type Ni-Cu-PGE targets

Kaski, K.[1], Smith, J.[1], Tschirhart, Victoria[1], Heggie, G., Enkin, R.[1]

[1]Natural Resources Canada, Geological Survey of Canada, 601 Booth Street, Ottawa, ON K1A 0E8

Magmatic Ni-Cu-PGE sulfide deposits are frequently associated with small conduit-type intrusions. These deposit types are challenging exploration targets due to their limited size, absence of distinct alteration halo or distant footprint, complex and variable morphology, and unpredictable depositional sites of sulfides [1]. Additionally, mafic rocks often retain significant remanent magnetization, which, if overlooked, can lead to inaccurate modelling and targeting of these deposits. The dwindling number of new Ni discoveries over the last decade highlights the necessity for the development and implementation of novel methods to facilitate improved detection and targeting of these deposit types at the regional to deposit scales.

Traditional airborne Total Magnetic Intensity (TMI) data is the most used and cost-effective surveying method for identifying and delineating intrusions which can host nickel deposits. Although there is incredible value in TMI data there are challenges with data interpretation including issues of non-uniqueness, scalar measurements, and the inability of TMI to differentiate remanence from the induced field. The full tensor magnetic gradiometry (FTMG) technique, which measures the full magnetic gradient tensor at each measurement point, overcomes many of these limitations and offers numerous advantages including: (a) superior resolution of near-field sources, (b) enhanced detectability at low-magnetic latitudes, (c) automatic removal of the regional field and diurnal variations, and (d) additional target information from a single flight line. FTMG can therefore provide improved discrimination of magnetic sources and a more complete picture of the subsurface magnetic properties. Commercialized quantum FTMG sensors currently use Superconducting Quantum Interference Device (SQUID) technology and due to their size and strict temperature requirements are most appropriate for large-scale airborne surveys. With SQUID sensors being unsuitable for ground and uncrewed aerial vehicle (UAV) surveys a new generation of compact, rugged diamond-based quantum magnetometers are in development and offer an alternative FTMG technology for ground and UAV surveying.

Although quantum FTMG offers significant advantages in sensitivity and the opportunity for improved targeting of ore deposits, its widespread adoption by the mining industry has been hindered, in part, by a lack of capabilities and expertise in the areas of data handling and interpretation. As part of a larger collaborative research project, the Geological Survey of Canda (GSC) with Defense Research and Development Canada, aim to de-risk quantum magnetic gradiometer use across Canada through the field testing and validation of quantum FTMG systems and comparing them with traditional total magnetic field systems and non-quantum FTMG systems. As part of this project, the GSC is undertaking a comprehensive study on the Ni-Cu-PGE bearing Escape and Current Intrusions of the Thunder Bay North Intrusive Complex which present as complicated magnetic signals that are strongly affected by remanent magnetization.

Here we present preliminary results from the processing of TMI data (Fig. 1) provided by Clean Air Metals Inc. and compare this with newly acquired SQUID FTMG data. Unconstrained (Fig. 2) and constrained magnetic susceptibility inversions derived from both datasets are presented to examine the 3D geometry and extent of the Ni-Cu-PGE mineralized mafic-ultramafic intrusions. Magnetization vector inversions (MVI) are also presented and offer additional insights into the extent and strength of remanent magnetization developed in association with these intrusions. Physical rock properties

of the intrusions are used to further validate the MVI models and gain insights into the processes controlling the localization of remanent magnetization.

This study marks the first instance of generating publicly accessible quantum FTMG data covering critical mineral deposits in Canada. Ultimately, the aim is to enhance exploration capabilities by validating tools applicable to critical metal deposits, whose intricate geophysical characteristics pose challenges for conventional geophysical techniques.

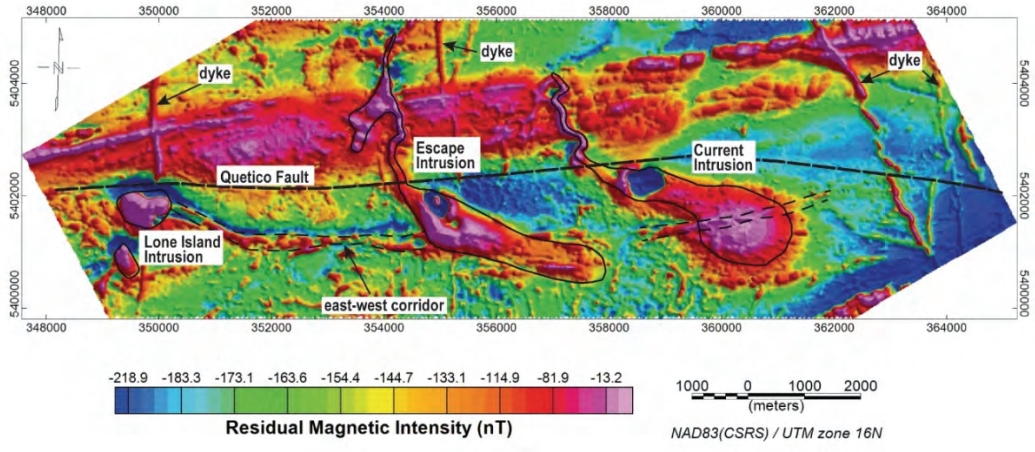


Figure 5. Residual magnetic intensity of the Escape and Current Intrusions of the Thunder Bay North Intrusive Complex.

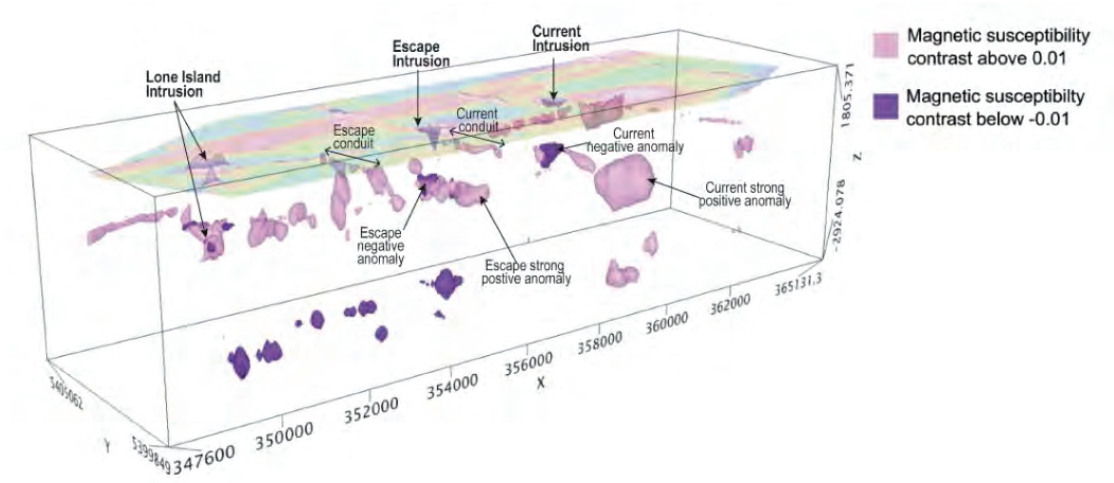


Figure 6. Unconstrained inversion results representing highest modelled magnetic susceptibility contrasts in the Escape and Current Intrusions of the Thunder Bay North Intrusive Complex.

References:

[1] Barnes, S.J., 2023. Lithogeochemistry in exploration for intrusion-hosted magmatic Ni–Cu–Co deposits. Geochemistry: Exploration, Environment, Analysis, 23(1), pp.geochem2022-025.

Exploration-Based Classification Scheme for Magmatic Ni-Cu-(PGE) Systems

Lesher C.M.[1] and Houlé M.G.[2,1]

[1] Mineral Exploration Research Centre, Harquail School of Earth Sciences, Goodman School of Mines, Laurentian University, Sudbury, ON P3E 2C6, Canada, mlesher@laurentian.ca
[2] Geological Survey of Canada, Lands and Minerals Sector, Natural Resources Canada, 490 Couronne Street, Québec City, QC G1K 9A9, Canada

---

Magmatic Ni-Cu-Co-(PGE) deposits have typically been classified on the basis of age, magma type, and tectonic setting [e.g., 1] or cumulus mineralogy [2], but they formed throughout geological time (Mesoarchean to Cenozoic) from a wide range of parental magmas (komatiitic to quartz dioritic) with different cumulus mineralogy in a wide range of tectonic settings (extensional to convergent), so none of these attributes are particularly useful exploration variables. A more useful classification is based on the nature of the host units: 1) impact melt sheets, 2) differentiated layered mafic-ultramafic intrusions, 3) channelized mafic-ultramafic lavas/sills/dikes, 4) differentiated/zoned mafic-ultramafic pipes/plugs/stocks, and 5) orogenic peridotites, each of which is fundamentally different:

Group	Subgroup	Setting	Examples
Group 1 Impact melt sheets	**A** Exogenetic (external S ± metals)	Impact structure	Sudbury ON
	B Endogenetic (internal metals ± S)		Morokweng SA
Group 2 Differentiated layered mafic-ultramafic intrusions	**A** Layered differentiated intrusions	Primarily large igneous province	Bushveld SA, Great Dyke ZI, Muskox NU, Stillwater MT
	B Composite differentiated intrusions		Duluth MN, Montcalm ON
	C Weakly layered differentiated intrusions		Americano do Brasil BR, Bird River MB, Kotalahti FI
Group 3 Channelized mafic-ultramafic flows/sills/dikes	**A** Flows	Primarily large igneous province	Alexo ON, Kambalda WA, Perseverance WA, Raglan QC
	B Sills		Dumont QC, Jinchuan CH, Mt Keith AU, Namew Lake SK, Norilsk RU, Pechenga RU, Thompson MB
	C Dikes		Eagle MI, Eagle's Nest ON, Expo-Méquillon QC, Hongquiling CH, Huangshan CH, Limae CH, Voisey's Bay NL, Qingkuangshan CH
	D Chonoliths		Kalatongke CH, Limoeiro BR, Mirabella BR, Nebo-Babel WA, Nkomati (Uitkomst) SA, Savannah WA, Tamarack MN
Group 4 Differentiated/zoned mafic-ultramafic pipes/plugs/stocks	**A** Zoned composite	Convergent	Duke Island AK, Giant Mascot BC, Mordor AU, Xiarihamu CH
	B Zoned non-composite		Jingbulake CH, Lynn Lake "EL" MB, Gordon Lake ON,
	C Unzoned composite		Aguablanca SP, Lynn Lake "A" MB, Turnagain BC
	D Unzoned non-composite		Lynn Lake "FLGC" MB, Hitura-Vammala FI
Group 5 Orogenic peridotites	**A** Ophiolite complexes	Oceanic crust/ mantle	Acoje PH, Baptiste (Decar) BC, Potosí CU, Oman, Shetland UK, Troodos CY
	B Peridotite massifs		Ivrea-Verbano IT

Group 1 impact melt sheets thus far include only one example with economic Ni-Cu-PGE mineralization, the 1850 Ma, 260 km-diameter Sudbury (ON) structure [see e.g., 3]. The 146 Ma, 80 km-diameter Morokweng (SA) structure contains subeconomic Fe-Ni-Co sulfide nodules and veins that appear to be derived in part from the impactor [e.g., 4]. No other impact structures with Ni-Cu-

PGE mineralization have been identified [e.g., 5], most likely because they were too small to generate enough impact melt and/or lacked the abundant economic (e.g., Shakespeare) to subeconomic (e.g., Nipissing and East Bull Lake Intrusive Suites) Cu-Ni-PGE mineralization in the target rocks at Sudbury.

Group 2 differentiated layered intrusions commonly host sub- to uneconomic reef-type PGE-(Cu)-(Ni) mineralization (e.g., Centre Hill ON, Romeo II QC), but sometimes contain economic reef-type PGE-(Cu)-(Ni) mineralization (e.g., Bushveld Merensky and UG-2 reefs, Stillwater J-M reef, Great Dyke MSZ) and where they do contain Ni-Cu-(PGE) mineralization it is normally low-grade (e.g., Duluth Complex, Muskox). Because they are A) periodically replenished and well-differentiated magma chambers (e.g., Bushveld), B) composite differentiated intrusions (e.g., Duluth), or C), weakly layered differentiated intrusions they are only rarely/locally dynamic enough to generate high-grade Ni-Cu-(PGE) mineralization.

Group 3 channelized mafic-ultramafic flows/sills/dikes include some of the world's largest, highest-grade Ni-Cu-(PGE) deposits/camps (e.g., Raglan, Thompson, Kambalda, Jinchuan, Norilsk-Talnakh) and many small high-grade deposits (e.g., Eagle, Tamarack, Eagle's Nest). They are typically enriched in olivine or Opx, poorly to weakly differentiated, and interpreted to have formed at high magma fluxes, enhancing thermomechanical erosion of S-bearing country rocks and upgrading of metal contents in sulfide xenomelts. In low-grade deposits, Ni-Co-IPGE in olivine can be redistributed into sulfides during serpentinization (e.g., Dumont, Mt Keith).

Group 4 differentiated/zoned mafic-ultramafic pipes/plugs/stocks have typically been subdivided based on their cumulus mineralogy into: Opx-poor (e.g., Uralian-Alaskan type), Opx-rich (e.g., Giant Mascot-type), Gabbroic, and Noritic [e.g., 2], but those characteristics also apply to many deposits in Group 3. Most are zoned and/or multiphase, representing relatively low magma fluxes. They can contain economic mineralization (e.g., Aguablanca, Giant Mascot, Lynn Lake, Xiarihamu), but typically have low tonnages, grades, and tenors.

Group 5 ophiolites and peridotite massifs (AKA orogenic peridotites) often contain subeconomic to economic abundances of Cr ± PGE mineralization, and typically only contain currently economic abundances of Ni after being lateritized [6]. However, the sparse amounts of Ni-Cu-(PGE) may be "upgraded" by liberation of Ni-Co-IPGE during serpentinization of olivine under fO_2 conditions that favour stabilization of Ni sulfides and/or Ni ± Pt ± Ir-Os alloys (e.g., Decar).

Each group exhibits variations in form, degree of olivine/Opx accumulation, and degree of differentiation, sometimes hampering classification into Groups 2, 3, and 4. They also exhibit variations in original (and current) orientations, compositions, and degrees of zoning/differentiation/layering/brecciation. They also formed from a wide range of magma types, some derived from depleted peridotitic mantle (undepleted in PGE relative to Ni-Cu-Co) and some derived from fertilized pyroxenitic mantle (depleted in PGE relative to Ni-Cu-Co). The single most important element to generating high-grade and high-tonnage deposits appears to be high magma flux, but lower-grade and lower tonnage deposits can form at lower magma fluxes.

References:

[1] Naldrett AJ (2004) Springer: 728 pp.
[2] Nixon GT et al. (2015) Geol Surv Canada OF7856: 17-34
[3] Lightfoot PC (2016) Elsevier: 680 pp.
[4] Hart RJ et al. (2002) EPSL 198: 49-62
[5] James S et al. (2022) Energy Geosci 3: 136-146
[6] Golightly JP (2010) SEG Spec Publ 15: 451–485

Thermodynamic constraints on the generation of cubanite-rich magmatic sulfides

Maghdour-Mashhour, R.[1], Mungall, J.[1]

[1]Department of Earth Sciences, Carleton University, 2115 Herzberg Laboratories, Ottawa, Ontario K1S 5B6, Canada

---

Nickel (Ni) and Copper (Cu) are paramount for advancing sustainability and enhancing human well-being, serving as indispensable elements in modern technology and pivotal components in green energy solutions. We launched a study of Ni-Cu ore deposits from the Keweenawan Large Igneous Province (LIP) to unravel their intricate geochemical and thermodynamic conditions, crucial for understanding their genesis and optimizing ore extraction methods, thereby bolstering industrial efficiency and sustainability.

The Keweenawan LIP, emplaced within the ca. 1.1 Ga Mid-Continent Rift (MCR), comprises by mafic-ultramafic intrusions and flood basalts extending across Lake Superior in Ontario and Minnesota [1]. The MCR preserves a broad array of magmatic sulfide deposits in a relatively unmetamorphosed state, offering a unique opportunity for detailed study and understanding of primary processes that are commonly obscured by later metamorphism.

MCR deposits exhibit variable concentrations of cubanite ($CuFe_2S_3$) alongside the more prevalent chalcopyrite ($CuFeS_2$). Cubanite content ranges widely from less than 1% to as high as 80% of the Cu sulfide mode [2], posing a major metallurgical challenge. The presence of cubanite prolongs flotation circuit processing times, necessitating a delicate balance between efficiency and optimization to separate Cu sulfides from tails effectively [3]. The occurrence of cubanite and chalcopyrite cannot be inferred from Cu-Ni-S assay and must be observed petrographically. Our primary aim is an innovative approach to mitigate cubanite prevalence within the circuit by precisely identifying cubanite-rich geometallurgical zones exclusively through assay databases, thereby circumventing the need for costly petrography and SEM analyses.

The first essential step is to comprehend the thermodynamic controls imposed by intensive parameters, including oxygen and sulfur fugacity (fO_2 and fS_2), which contribute to the stability of cubanite in a system where silicate melt, and sulfide melt are in equilibrium. Subsequently, we explore the required parental magma chemical composition and intensive variables necessary at elevated temperatures to ensure the stability of cubanite as the system cools down to lower temperatures.

To address these questions, we utilized FactSage 8.3 to model the evolution of a cubanite-favorable anhydrous magmatic closed system initially comprising ~15 wt% sulfide liquid and ~85% silicate melt at the liquidus temperature. Re-equilibration of the model system to lower temperatures allowed us to determine the conditions required at the liquidus that would result in the development of cubanite-rich sulfide assemblages upon cooling to near ambient temperatures. Our investigation yielded novel findings that cubanite stability is achieved at log fS_2 of -14, log fO_2 of -37, and a temperature of 270 degrees Celsius. These conditions correspond to a low-temperature ambient state, akin to a parental magma composition with log fS_2 of -0.7 and log fO_2 of -7.2 at the liquidus temperature indicating a condition slightly more reduced than the Quartz-Fayalite-Magnetite (QFM) buffer (ΔQFM -1).

We have also uncovered a diverse array of model cubanite-bearing low-temperature assemblages, including various combinations of pentlandite, pyrrhotite, chalcopyrite, talnakhite, and mooihoekite. Whereas the abundances of pentlandite, pyrrhotite, and chalcopyrite display a wide spectrum of sensitivity to fO_2 and fS_2, our findings reveal five distinct assemblages—incorporating chalcopyrite, talnakhite, and mooihoekite—that showcase high sensitivity to even two decimal points of shifts in fO_2 and fS_2. As fO_2 decreases and fS_2 increases, these assemblages undergo transitioning from chalcopyrite to talnakhite and ultimately to mooihoekite.

It is noteworthy that cubanite exhibits stability even in hydrous systems, albeit under extremely reduced conditions. For some cubanite-bearing assemblages, such as those with mooihoekite, cubanite stability necessitates an exceptionally reduced environment, with ΔQFM reaching as low as -3.3 and log fS_2 dropping to -2.5.

As our study progresses, our next phase entails conducting quantitative and qualitative mineral classification through petrography and SEM X-ray mapping of representative samples sourced from Ni-Cu deposits spanning distinct intrusions across the Mid-Continent Rift (MCR). Our aim is to compare sulfide paragenesis within cubanite-rich domains across the MCR with thermodynamically generated model compositions and assemblages provided by FactSage. Additionally, we will incorporate geochemical insights to establish a link between bulk rock assay data and the presence of cubanite in the Ni-Cu deposits. This approach will enable us to delineate geometallurgical domains potentially requiring modified beneficiation circuits.

References:

[1] Taranovic et al. (2015) Can Min 24(2): 347
[2] Ripley and Alawi (1986) Lithos, 212: 16-31
[3] Muzinda et al. (2018) Min Eng, 125: 34-41

Constraining the Sunday Lake mineralization: A Ni-Cu-PGE deposit

Mexia, K.[1], Hollings, P. [1]

[1]Department of Geology, Lakehead University, 955 Oliver Road, Thunder Bay, On P7B 1J4, Canada
kmexiad@lakeheadu.ca

The Sunday Lake Intrusion (SLI) is located 25 km north of Thunder Bay, Ontario, and hosts Ni-Cu-PGE mineralization. It has been dated at 1109.0±1.3 [1], and as such is related to the plateau stage of the ~1115 to 1106 Ma Midcontinent Rift System (MRS; [2], [3]). The SLI is a tabular shaped intrusion emplaced in Archean rocks of the Quetico Basin that becomes more tube-like to the northwest where it is hosted by Archean granitoids. It is emplaced along the Crock Fault, which is interpreted to be a splay of the main Quetico Fault [3]. It varies from 350 meters to 1000 meters in thickness. The intrusion consists of mafic-ultramafic layers divided into three series: the Upper Gabbro Series, the Lower Gabbro Series, and the Ultramafic Series (Fig 1.) [3].

Reef-style sulphide mineralization (2-10 vol.%) is present in the lower zones of the intrusion, consisting of disseminated to blebby chalcopyrite-pyrrhotite-pyrite-cubanite in an olivine melagabbro (Fig. 2). The Ultramafic series mineralization shows a laterally extensive 20 meters thicks layer with enrichment in Cu-Pt, Pd and Au at levels of 3-10 g/t Pt+Pd+Au [3]. The main objective of this project is to characterize the paragenetic sequence of the Sunday Lake Intrusion and to study the effects of crustal contamination on mineralization.

This project utilizes two representative drill holes from which a total of 71 samples were collected. A total of thirty polished thin sections were generated for petrographic studies. Rocks were classified based on relative proportions of olivine, clinopyroxene, and plagioclase with modal rock names such as melagabbro, olivine melagabbro, and wehrlites. Downhole diagrams of trace and major elements vary within the layered intrusion, but both plume-like compositions (Fig. 3A), and evidence for contamination by host rocks (Fig. 3B). Variation in composition suggest other geological processes such as episodes of melt re-injection, contamination, assimilation, and fractional crystallization. These processes likely lead to the generation of sulphides and further precipitation. Sixteen samples have been sent for Sm-Nd and Rb-Sr isotope studies to assess the paragenetic history of the Sunday Lake Intrusion mineralization.

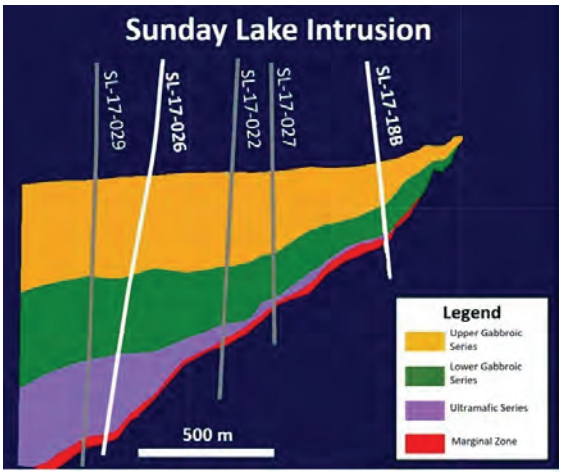


Figure 1. Cross section of the Sunday Lake Intrusion showing lithologies.

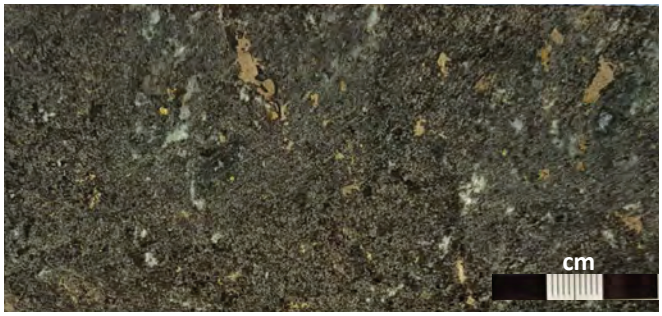


Figure 2. Photograph of sample SL23KM41 showing an olivine melagabbro with disseminated and blebby sulphides.

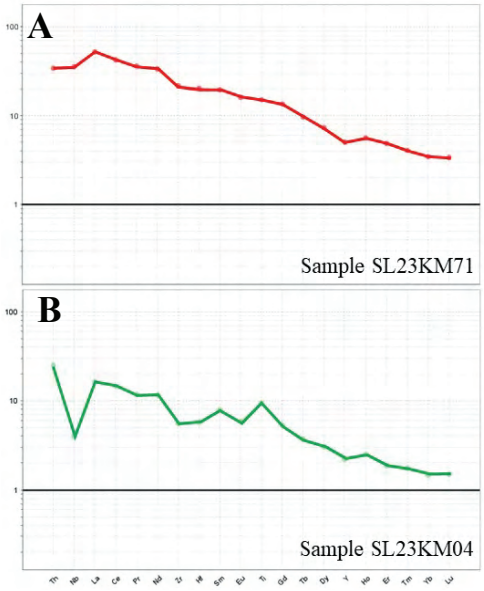


Figure 3. Primitive mantle normalized REE spider diagram of two samples. A: Sample showing a plume-like trend. B: Sample suggesting an interaction with the host rock. Normalising values from [5].

References:

[1] Bleeker, W., et al. "The Midcontinent Rift and its mineral systems: Overview and temporal constraints of Ni-Cu-PGE mineralized intrusions." Targeted Geoscience Initiative 5 (2020): 7-35.
[2] Heaman, L. M., Easton, R. M., Hart, T. R., MacDonald, C. A., Hollings, P., & Smyk, M. (2007). Further refinement to the timing of Mesoproterozoic magmatism, Lake Nipigon region, Ontario. Canadian Journal of Earth Sciences, 44(8), 1055-1086.
[3] Flank, S. (2017). The Petrography, Geochemistry and Stratigraphy of the Sunday Lake Intrusion, Jacques Township, Ontario. School of graduate studies.
[4] Woodruff, L. G., Schulz, K. J., Nicholson, S. W., & Dicken, C. L. (2020). Mineral deposits of the Mesoproterozoic Midcontinent Rift system in the Lake Superior region–a space and time classification. Ore Geology Reviews, 126, 103716.
[5] Sun, S. S., & McDonough, W. F. (1989). Chemical and isotopic systematics of oceanic basalts: implications for mantle composition and processes. Geological Society, London, Special Publications, 42(1), 313-345.
[6] Miller, J.D. (2020). Report on the Petrography, Geochemistry, and Lithostratigraphy of DDH SL10-026 from the Southern Sunday Lake Intrusion. JDM GeoConsulting.

Primitive arc magmatism and the development of magmatic Ni-Cu-PGE mineralization in Alaskan-type ultramafic-mafic intrusions

Milidragovic, D.[1,2], Nixon, G.T.[3], Spence, D.W.[2], Nott, J.A.[2], Goan, I.R.[2], Scoates, J.S.[2]

[1]Geological Survey of Canada-Pacific; 1500-605 Robson St., Vancouver, BC, V6B 5J3; dejan.milidragovic@nrcan-rncan.gc.ca [2]Pacific Centre for Isotopic and Geochemical Research; Department of Earth, Ocean and Atmospheric Sciences; University of British Columbia [3]British Columbia Geological Survey

---

Zoned ultramafic-mafic plutonic rocks in convergent margin settings represent trans-crustal magmatic feeders [1,2] to coeval, and better studied, arc volcanoes. Arc lavas, which are on average basaltic to andesitic, represent differentiated and largely degassed magmatic products [3,4] and only rarely provide a clear glimpse into the earliest stages of arc magma evolution [5,6,7]. The study of lower- to mid-crustal arc cumulates, which include high-temperature liquidus lithologies, is complimentary and necessary to establish a holistic understanding of arc magmatism and mantle-crust metal transfer.

Ultramafic-mafic convergent margin intrusions are typically composed of rocks comprised of variable proportions of olivine ±Cr-spinel, clinopyroxene, amphibole, and magnetite. Plagioclase is volumetrically minor and appears relatively late in the crystallization sequence, consistent with high parental magma water contents. The absence of orthopyroxene distinguishes the predominantly abundant class of “Alaskan-type” intrusions (e.g., Tulameen, Polaris, Turnagain), which are the focus of this presentation, from orthopyroxene-rich “Giant Mascot–type” intrusions [8].

Alaskan-type intrusions have long been recognized for their platinum group element (PGE) potential, hosted principally within micrometer-size platinum group metal (PGM) inclusions (e.g., laurite, isoferroplatinum, tetraferroplatinum) in thin chromite-rich horizons and massive schlieren occurring in dunite. Alaskan-type intrusions may also host significant magmatic Ni-Cu-PGE sulfide mineralization in dunite and wehrlite (e.g., Turnagain [9]) and notable palladium-subgroup PGE (PPGE) concentrations may occur in association with Cu-rich sulfides (e.g., chalcopyrite ±bornite) in more evolved clinopyroxene- and hornblende-rich rock types [10,11]. The mineralization style and potential in Alaskan-type intrusions is a reflection of the interplay between: 1) degree of country rock assimilation during emplacement and differentiation, and 2) the oxidation state of the primary, mantle-derived melts.

Evolution of oxidized arc magmas [12] through assimilation of either S-rich or relatively reduced country rock favours early sulfide saturation and formation of magmatic Ni-Cu-PGE sulfides in high-temperature dunite and wehrlite. At Turnagain, assimilation of country rocks is indicated by the isotopic composition of sulfides, which show non-uniform $\delta^{34}S$ values (+4.2 to -12.3 ‰ [13,14]) that are largely intermediate between those of the depleted mantle (-1.28 [15]) and surrounding phyllite (-11.6 to -20.1 [13,14]).

Magmatic chalcopyrite from the Polaris Alaskan-type intrusion has uniform near-chondritic sulfur isotope compositions ($\delta^{34}S$ =-0.19 +0.48/-0.32‰) that are markedly lighter than those of the country rocks ($\delta^{34}S$ = +7.4 +1.3/-1.7), indicating that the evolution of primitive mantle-derived magma(s) occurred without appreciable country rock assimilation [16]. The differentiation of primitive arc magma without contamination from country rocks favours crystallization of PGM in association with chromite-bearing dunite and immiscibility of Cu-PPGE-Au-rich sulfide from the more differentiated clinopyroxene, magnetite ±hornblende-saturated magmas. In principle, the nature of PGM (i.e., Pt-enriched vs. IPGE-enriched) and the onset of sulfide immiscibility in systems not affected by country rock assimilation are governed by the oxidation state of the primary magma, and by extension, the oxidation state of the sub-arc mantle wedge. The predominance of Pt-alloys, such as those observed at the Tulameen intrusion, indicates moderately oxidized parental magmas (log $f(O_2)$ <FMQ+2),

where Pt is likely to be near saturation [17]. In contrast, the absence of Pt-alloys and predominance of Ir-Ru-Os alloys and laurite (e.g., Polaris) indicates strongly oxidized parental magmas (log $f(O_2)$ ≥FMQ+2) [11]. In the absence of country rock assimilation, sulfide immiscibility may be attained through reduction in the oxidation state of the magma, most likely triggered by magnetite fractionation [18]. The oxidation of the FeS component in the melt to form magnetite (e.g., $6\ FeS_{\ melt} + 4O_2 = 2\ Fe_3O_{4\ magnetite} + 3S_2$ [19,20]) is consistent with the Cu-rich character of the earliest formed immiscible magmatic sulfides at both Tulameen and Polaris [10,11].

The diverse magmatic Ni-Cu-PGE mineralization styles of Alaskan-type intrusions reflect the complexity of arc magmatism. Key controlling factors include: 1) first-order differences in the oxidation state of the sub-arc mantle that may relate to the composition and nature of the subducted oceanic crust [16,21], and 2) the composition and volume of crust that is assimilated during magma ascent and emplacement.

References:

[1] Cashman K V et al. (2017) Science 355: 9
[2] Spence D W et al. (2024) Lithos 474-475: 107578
[3] Müntener, O and Ulmer P (2018) Am J Sci 318: 64-89
[4] Ding S et al. (2023) Geochem Geophys Geosys 24: e2022GC010552
[5] Russell J K and Snyder L D (1997) Can Min 35, 521-541
[6] Milidragovic D et al. (2016) Earth Planet Sci Lett 454: 65-77
[7] Till C B (2017) Am Min 102: 931-947
[8] Nixon G T et al. (2015) GSC Open File 7856: 17-34
[9] Mudd G and Jowitt S (2014) Econ Geol 109: 1813-1841
[10] Nixon G T et al. (2020) GSC Open File 8722: 197-218
[11] Milidragovic D et al. (2021) Can Min 59: 1627-1660
[12] Cottrell E et al. (2022) Geophys Monogr 266, 33-61
[13] Scheel J E (2007) UBC MSc thesis, 201 p
[14] Jackson-Brown S (2017) UBC MSc thesis, 272 p
[15] Labidi J et al. (2013) Nature 501: 208-211
[16] Milidragovic D et al. (2023) Earth Planet Sci Lett 620: 118337
[17] Borisov A and Palme H (2000) Am Mineral 85: 1665-1673
[18] Jenner F E et al. (2010) J Petrol 51: 2445-2464
[19] Wohlgemuth-Ueberwasser C C et al. (2013) Min Dep 48: 115-127
[20] Lesher C M (2017) Ore Geol Rev 90: 465-484
[21] Canil D and Fellows S A (2017) Earth Planet Sci Lett 470: 73-86

Stratigraphy of the Grasset Ultramafic Complex and its Ni-Cu-(PGE) mineralization, Abitibi Greenstone Belt, Superior Province, Canada.

Milier, K.[1], Houlé M.G.[2] and Saumur B.M.[1]

[1]Université du Québec à Montréal (UQAM), Département des sciences de la Terre et de l'Atmosphère, 201 avenue du Président Kennedy, Montréal, QC H2X3Y7, Canada.
[2]Geological Survey of Canada, Lands and Minerals Sector, Natural Resources Canada, 490 Couronne Street, Québec City, QC G1K 9A9 Canada

---

In the Abitibi Greenstone Belt (AGB), komatiitic rocks are prospective for Ni-Cu-PGE mineralization. Most of these occur within the Kidd-Munro and Tisdale assemblage located in the southern parts of the AGB [1]. The Grasset Ultramafic Complex (GUC) of the northern AGB is a notable exception, as it hosts one of the largest Type I komatiitic Ni-(Cu)-(PGE) deposits in the entire Abitibi. [1]. Located in the Harricana-Turgeon area, the GUC is an 8 kilometre long ultramafic corridor (Fig. 1A) within the volcano-sedimentary Manthet Group interpreted as part of the Deloro assemblage (2734-2724 Ma). The country rocks mostly consist of felsic to mafic volcanic rocks with gabbroic sills and graphitic mudstones. The GUC occurs within felsic volcanic and graphitic sediments that may contain semi-massive to massive sedimentary sulfides intervals. However, it can crosscut the local stratigraphy. The GUC consists of thick ultramafic cumulate bodies (Fig. 1B, C) and komatiitic lava flows within the GUC central area (Fig. 1C). Both host Ni-(Cu-PGE) mineralization, such as that observed in the GUC central area and in the southern end of the GUC. The latter hosts the Grasset deposit.

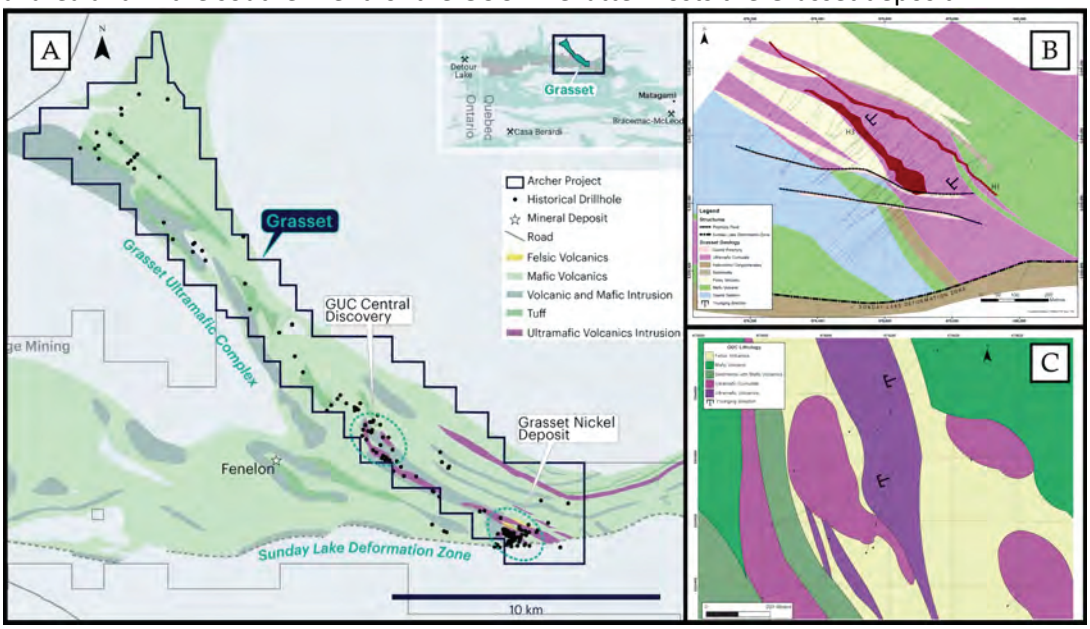


Figure 7 A) Simplified geological map of the GUC area [2]. B) Geological map of the Grasset area [3]. C) Geological map of the GUC central area [4].

The Grasset deposit consists of a peridotitic body (Fig. 1A) dipping to the southwest, cut by the Sunday Lake fault to the southeast (Fig. 1A, B), and dominated by olivine meso- to orthocumulate with lesser intervals of olivine adcumulate. The ultramafic rocks have undergone a significant degree of talc-serpentine-carbonate alteration, and primary mineral assemblages have been completely obliterated. The ultramafic body does not exhibit much lithological variation, especially in its central portions where it occurs as a homogenous olivine cumulate unit. Toward the northwest, the ultramafic splits into two bodies interleaved with felsic volcanics (Fig. 1A). The lower and upper contacts within the country rocks are sharp and gradually shifts from pyroxenite (Fig. 2B) to peridotite. Locally, relicts of "olivine hopper crystal" crescumulates (Fig. 2A) occurs within the cumulate body. Three Ni-Cu-(PGE) mineralized horizons (H1, H2, H3) occurs at different levels of the Grasset ultramafic body. H1 occurs along the basal contact between the ultramafic and the footwall rocks (Fig. 2B) and consists of disseminated to net-textured and semi-massive to massive sulfides. H2

is very sparse and cannot be confidently defined as a clear mineralized horizon. H3, the main horizon, occurs in the upper part of the Grasset ultramafic unit. Its thickness can be up to 55 m, consisting of several intervals from disseminated, to heavy disseminated and net-textured sulfides (Fig. 2C) with rare massive sulfide intervals. Sulfide assemblages of H3 and H1 differ. H3 is largely composed of pyrrhotite (Po) ≈ pentlandite (Pn) >> chalcopyrite (Cpy), With pyrite (Py) occasionally replacing Po. In contrast, H1 exhibits a more common magmatic sulfide paragenesis of Po **>>** Pn >> Cpy. However, when normalized to 100% sulfide, H3 average grade is 15.1% Ni, 1.4% Cu, 0.31% Co and 12.1 ppm Pt+Pd, whereas H1 tenors are lower showing an average grade of 7.6% Ni, 1.0% Cu, 0.15% Co and 5 ppm Pt+Pd. Despite these tenor variations, H1 and H3 show similar Ni/Cu (8-11) and Pd/Pt ratios (1.8-2.0).

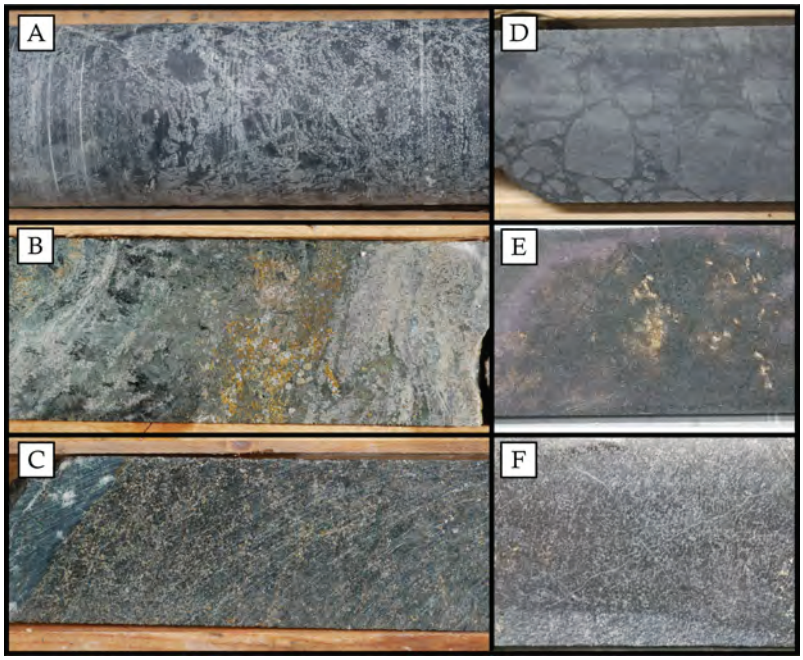


Figure 2: A) Relict of hopper crystal in an olivine crescumulate. B) H1 disseminated sulfides within the pyroxenite in contact with the hornfelsed footwall felsic tuff (Right). C) H3 net-textured sulfides. D) Komatiitic flow top breccia. E) Disseminated sulfides within the olivine cumulate of a komatiitic flow. F) Olivine mesocumulate of the poorly differentiated cumulate, note the presence of elongated olivine.

The GUC central area is composed of a series of komatiitic flows and thick cumulate ultramafic bodies dipping to the west. These komatiitic flows occur between the felsic volcanics and graphitic sediments (Fig. 1C). The flows consist of several flow top breccias (Fig. 2D) underlain by olivine ortho- to mesocumulates (Fig. 2E) that progressively decrease in thickness toward the stratigraphic top. The earliest flows, at the base of the sequence, appear to contain the bulk of the Ni-(Cu)-(PGE) mineralization in this area. This mineralization occurs at the bottom of the olivine cumulate with disseminated (Fig. 2E) to net-textured and massive sulfides. The thick ultramafic cumulates (Fig. 2F) are poorly differentiated bodies, composed of olivine ortho- to mesocumulate. These ultramafic bodies do not show clear field evidence of intrusive relationships, but they occur at varying local stratigraphic levels. They exhibit sparse disseminated sulfides, but rarely massive sulfides at the basal contact.

In conclusion, the GUC is a komatiitic sequence consisting of extrusive komatiitic flows and thick olivine cumulate bodies. The system could thus host both Type I and II komatiite-associated mineralization. The GUC could represent a volcanic-subvolcanic komatiitic succession where extrusive facies are more likely to be found in the GUC central area. The extrusive or intrusive origin of Grasset remains unclear at this stage. However, the occurrence of crescumulate and several Ni-(Cu)-PGE horizons suggests the existence of several ultramafic subunits within the Grasset unit. The Grasset deposit highlights the potential for new Ni discoveries hosted in the Deloro assemblage and for similar discoveries in underexplored area such as the northern parts of the AGB.

References:

[1] Houlé MG et al. (2017). Rev in Econ Geol 19: 103-132
[2] Archer Exploration (2023). Corporate presentation
[3] Tucker MJ et al (2019). Proc 15th SGA Biennial Meeting 2: 497-500
[4] Balmoral Ressources Ltd (2020). Roundup

Geochemistry of Camp Lake Block Lac des Iles Palladium Mine, N. Ontario, Canada

Njipmo Ngoko, B.[1], Hollings, P.[1], Djon, L.[2] and Hamilton, M.[3]

[1]Department of Geology, Lakehead University, 955 Oliver Road, Thunder Bay, ON P7B 5E1 Canada. bnjipmo@lakeheadu.ca
[2]impalacanada, 69 Yonge Street, Suite 700, Toronto ON, Canada M5E 1K3 Canada. lionneldjon@gmail.com
[3]Jack Satterly Geochronology Laboratory, University of Toronto, 22 Russell Street, Toronto, ON M5S 3B1, Canada

---

The Archean Lac des Iles suite is located just north of the Wabigoon-Quetico boundary [1], approximately 90 kilometers north of Thunder Bay in Northwestern Ontario. This suite of intrusions includes discrete mafic and ultramafic complexes associated with sanukitoids, which were emplaced along deep-seated regional faults [2]. Among these, only the Lac des Iles Complex hosts economically significant palladium deposits, specifically at the Lac des Iles mine. The complex is divided into two parts: North Lac des Iles and South Lac des Iles. The North Lac des Iles mainly comprises ultramafic rocks such as websterite, clinopyroxenite, wherlite, lherzolite, dunite, and peridotite [3]. In contrast, South Lac des Iles is primarily composed of mafic rocks such as gabbro, gabbronorite, norites, and melanorite [4] and is the main host of the Roby, Offset, and Camp Lake zones. This study focuses on the Camp Lake zone, the deepest part of the palladium deposit, recently highlighted by exploration drilling. The aim is to characterize the petrological, geochronological, and geochemical attributes of the Camp Lake zone and compare these with those of the Roby and Offset zones.

Four main petrographic subtypes have been identified within the Camp Lake zone: leucogabbronorites, mesogabbronorites, melagabbronorites, and norite. The rock textures are generally equigranular or varitextured. Petrographic studies show these rocks mainly consist of a mixture of pyroxenes and plagioclase. The pyroxenes predominantly comprise orthopyroxene with minor clinopyroxene, which are partially to completely replaced by amphiboles (cummingtonite, actinolite, and tremolite). The plagioclase is weakly to moderately altered and generally retains its original habit. The Camp Lake rocks exhibit magmatic sulfide contents ranging from 0.5% to 3%, dominated by pyrrhotite, pentlandite, and chalcopyrite, with minor pyrite. Sulfide minerals often occur as blebs or disseminated grains intergrown with silicate minerals.

A new zircon U-Pb age was acquired for the mineralized Camp Lake rocks, yielding an emplacement age of 2690.56 ± 0.80 Ma [5], closely similar to that of the Roby and Offset deposits [6]. Geochemical analysis of the Camp Lake Zone rocks shows enrichment in LREE (La/Sm_n ranging from 1.29 to 7.75, with a median of 3.30), unfractionated HREE (Gd/Yb_n ranging from 0.56 to 1.49, with a median of 0.88), and a negative Nb anomaly. These values are similar to those of the Roby and Offset zones and are consistent with a subduction zone setting [7]. Also, similar to the Roby-Offset deposits, PGE values in Camp Lake range between 1.0 g/t and 3.0 g/t, with variations in the rocks increasing with Cu and Ni content. However, Camp Lake is distinguished by higher proportions of pyrrhotite compared to chalcopyrite and lower Pd/Pt and Cu/Pd ratios than the other zones. Data show that the Camp Lake zone exhibits lower $\delta^{34}S$ values, ranging from (-1.1‰ to +0.3‰), while the Roby and Offset zones show wider variations ranging from (-0.37 to +3.28‰) [8]. This observation suggests that the sulfur in the Camp Lake zone is of mantle origin and that the sulfide was less affected by hydrothermal processes, leading to more limited sulfide alteration.

References:
[1]. Lavigne, M.J., & Michaud, M.J. (2001). The Lac des Iles Palladium Deposit, Ontario, Canada. Economic Geology. Volume 10, pages 1-17.
[2]. Impala Canada. (2017). Technical Report on the Lac des Iles Palladium Mine. Impala Canada.

[3]. Djon, L., Smith, M., Johnson, R., & Brown, T. (2017). Canadian Journal of Earth Sciences, 54, 1234-1250.
[4]. Gomwe, T. (2008). Geology and Mineralization of the Lac des Iles Complex. In: Platinum-Group Elements in Magmatic Ore Deposits. Springer, pp. 123-145.
[5]. Hamilton, M.A., 2024. Report on U-Pb CA-ID-TIMS geochronology of diorite and gabbro samples from Lac des Iles – related intrusions at Wakinoo, Buck Lake, Demars Lake, and Dog River, NW Ontario. Unpublished report prepared for Prof. P. Hollings, Department of Geology, Lakehead University, Ontario. 14p.
[6]. Peck, D., Houle, M.G., & Smith, M.P. (2016). Economic Geology, 111, 833-858.
[7]. Peck, D., Houle, M. G., et Smith, M. P. (2016) Geology, Petrology, and Controls on PGE Mineralization of the Southern Roby and Twilight Zones, Lac des Iles Mine, Canada, p. 43
[8]. Jonsson, J. (2023). Petrogenesis of mineralized horizons in the Offset and Creek zones, Lac des Iles Complex, N. Ontario, pages 146-168.

Hf-Nd-Pb isotopic evidence for variable impact devolatilization in the Sudbury Igneous Complex and its relevance for Ni-Cu-(PGE) sulfide ore formation

Peters, D.[1], Lesher C.M.[1] and Pattison E.[1]

[1] Laurentian University, Sudbury, ON P3E 2C6, Canada, dpeters@laurentian.ca

---

The Sudbury Igneous Complex (SIC), generally believed to be the remnant of a large, 1850 Ma bolide impact, hosts one of the world's largest magmatic Ni-Cu-(PGE) sulfide mining camps. It consists of i) the Main Mass, the crystallization product of the impact melt sheet), ii) underlying discontinuous lenses of variably mineralized magmatic and anatectic breccias, iii) radial and concentric, variable mineralized quartz dioritic offset dikes, and iv) overlying fallback/suevitic breccias. The ultimate source for all metals and sulfur is the immediate target rocks melted during the impact event, but the timing and mechanisms of ore formation are still being debated.

Most current models assume that all metals and sulfur completely dissolved in the impact melt sheet and subsequently exsolved and sank toward the bottom, where they accumulated in local embayments or troughs, either by convective currents [1, 2] and/or gravity-driven density flows [3]. However, this process is slow and difficult to reconcile with the observed heterogeneities in the Pb>S>Os isotopic compositions of the sulfide ores around the SIC [4, 5, 6] and would require an initially heterogeneous impact melt sheet from which the sulfide ores subsequently exsolved. An alternative model is that significant amounts of Pb [7] and S [8], as well as Zn-Cd-Rb-Cs [9] and other volatile elements were volatilized during the impact event, followed by localized thermomechanical erosion of S ± metal-bearing footwall rocks by the superheated impact melt sheet [3, 10], forming local sulfide xenomelts, which then accumulated in local embayments and troughs [3].

Impact devolatilization would have left volatile elements such as Pb and S more susceptible to post-impact modifications by thermomechanical erosion, whereas more refractory elements such as Hf or Nd [11] would have been largely preserved during impact, making them less susceptible to post-impact modifications. Characterising the Hf-Nd-Pb isotopic composition of the Main Mass (the crystallized impact melt sheet) therefore presents an excellent opportunity to better understand i) the characteristics of the initial impact melt sheet, ii) post-impact contamination processes, and iii) formation of the sulfide ores associated with the SIC.

Preliminary results of Hf isotope analysis on zircons by LA-MC-ICP-MS from four Main Mass transects across the North Range of the SIC show a narrow range in Hf isotope compositions (εHf_{1850Ma} between -8 and -12, Figure 1A), similar to previously published data for the South Range of the SIC [12]. Similarly, literature data for whole-rock Nd isotope compositions across the North Range [13, 14] also show a narrow range (εNd_{1850Ma} between -7 and -9, Figure 1B), which suggests effective vertical and lateral homogenization of the initial impact melt across the North Range prior to crystallization. Lead isotope compositions on the other hand, while being relatively homogeneous throughout the Granophyre, Quartz Gabbro and Felsic Norite ($\Delta^{207}Pb/^{204}Pb$ between 300 and 450), become more variable towards the base of the Main Mass, especially within the Mafic Norite ($\Delta^{207}Pb/^{204}Pb$ between 100 and 400, Figure 1C) [7, 15]. The greater Pb isotopic variability in the Mafic Norite can be attributed to the greater susceptibility of Pb to post-impact contamination by thermomechanical erosion, which would have been most significant at the base of the melt sheet. The decoupling of the more variable Pb isotopes from the more homogenous Hf and Nd isotopic compositions within the Mafic Norite therefore provides strong evidence for impact devolatilization of Pb>S>>Os>Nd>Hf. Although a contribution from the impact melt sheet cannot be entirely excluded, the current Hf-Nd-Pb isotopic evidence from the Main Mass favours a model in which the sulfide ores dominantly formed at the base by local thermomechanical erosion of S-bearing footwall rocks. Additional analyses of Nd and Pb isotopic compositions of the Main Mass across the North Range are in progress to confirm the results.

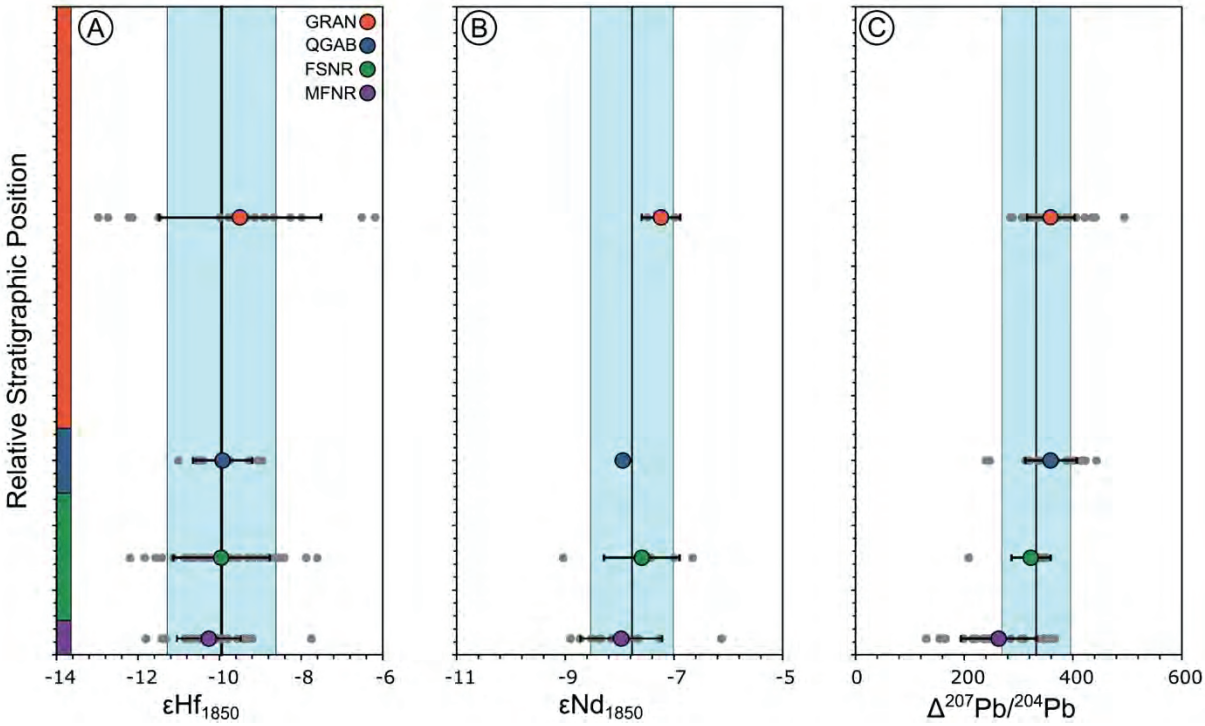


Figure 1: Stratigraphic variations in Hf, Nd, and Pb isotopic compositions throughout the North Range Main Mass of the Sudbury Igneous Complex. Individual analyses are shown in grey, unit averages (±1σ) in the colour of the respective lithology. Black lines and shaded blue squares show the overall average (±1σ) for the North Range Main Mass. **A.** εHf_{1850Ma} variations throughout the North Range Main Mass. **B.** εNd_{1850Ma} variations throughout the North Range Main Mass. **C.** $\Delta^{207}Pb/^{204}Pb$ variations throughout the North Range Main Mass. Hf data are from this study, Nd data are from [13, 14], Pb data are from [7, 15]. For calculation of $\Delta^{207}Pb/^{204}Pb$ see [7]. GRAN – Granophyre, QGAB – Quartz Gabbro, FSNR – Felsic Norite, MFNR – Mafic Norite

References:

[1] Lightfoot P et al. (2001) Econ Geol 96: 1855-1875
[2] Zieg M and Marsh B (2005) GSA Bulletin 117: 1427-1450
[3] Wang Y et al. (2022) Econ Geol 117: 1-28
[4] Darling J et al. (2012) GCA 99: 1-17
[5] Ripley E et al. (2015) Econ Geol 110: 1125-1135
[6] Morgan J et al. (2002) GCA 66: 273-290
[7] McNamara G et al. (2017) Econ Geol 112: 569-590
[8] Lesher C (2019) GAC-MAC 42: 130-131
[9] Kamber B and Shoenberg R (2020) EPSL 544: 116356
[10] Prevec S and Cawthorn R (2002) JGR 107: B8 2176
[11] Lodders K (2003) Astrophysics Journal 591: 1220-1247
[12] Kenny G. et al. (2017) GCA 215: 317-336
[13] Faggart B et al. (1985) Science 230: 436-439
[14] Dickin A et al. (1996) GCA 60: 1605-1613
[15] Dickin A et al. (1999) GSA Special Paper 339: 361-371

Deformation in mafic protoliths: Impacts from late faults on Ni-Cu-PGE mineralization at Lac des Iles Mine, Canada

Peterzon, J.[1], Phillips, N.[1], Hollings, P.[2], and Djon, M.L.[2]

[1]Lakehead University, 955 Oliver Road, Thunder Bay ON. P7B 5E1, Canada; jpeterzo@lakeheadu.ca
[2]Impala Canada, 69 Yonge Street, Suite 700 Toronto ON. M5E 1K3, Canada

---

Fault zones are complex structures that serve as permeable pathways through the upper crust; however, the impact of host lithology on damage zone development remains poorly understood. The development of fault cores and damage zones is typically controlled by the strength and composition of the protolith, conditions of deformation, and fluid chemistry [1], this is particularly true for faults hosted in mafic lithologies where damage zones control hydration in mafic crust. Permeability is significantly enhanced in damage zones due to the high density of fractures and is diminished in fault cores when a clay rich gouge is present. Faults therefore may act as conduits or barriers for fluid flow depending on the proportion of fault core to damage zone [2]. Trapped mineralization may be offset or remobilized by later faulting.

This study investigates the deformation and alteration geochemistry footprint of late faults within the mafic-ultramafic intrusions at the Lac des Iles mine (Figure 1). The 2,689 +/- 1.0 Ma Lac des Iles Complex (LDIC) [3] is a series of intrusive bodies hosted within the ~3.01 – 2.68 Ga granite-greenstone Marmion terrane of the Superior Province, Canada. Ni-Cu-PGE mineralization has been offset, and depleted in areas surrounding the fault zone, including the damage zone and fault core, by the reverse Offset Fault and hypothesized reverse Camp Lake Fault. Palladium depletion is hypothesized to be from fluid flow through the fault damage zones.

Fracture densities from the hanging wall of each fault were measured to determine the damage zone and fault core width in both gabbronorites and tonalites (Figure 2). Tonalites have a higher fracture density than the gabbronorites, suggesting fluid flow would be more effective in felsic protoliths, which in turn may contribute to metal remobilization, implying that host rock lithology has a strong control over fault zone structure, mineralization, and alteration assemblages. Metal contents display depletions in areas surrounding faults, and show a strong correlation with fracture density measurements. It is likely that a frictionally weak, chlorite rich fault core likely impeded the development of a more fracture dense damage zone in the gabbronorites, as opposed to a silica-rich brecciated fault core in the tonalites. Deformation conditions of the Camp Lake and Offset Fault zones were studied through scanning electron microscopy (SEM) and electron microprobe analyses. Preliminary results from this support our hypothesis of a silicified fault core in tonalites (Figure 3) and a chlorite-rich fault core in gabbronorites and reveal three generations of chlorite growth: pre-faulting at ~350°C, syn-faulting at ~150 – 200°C, and post-faulting at ~150°C [4] (Figure 4). We aim to highlight the importance of fluid-rock interactions in the development of fault core and damage zone structures in mafic protoliths, and their associated impact on Ni-Cu-PGE mineralization.

References:

[1] Caine et al. (1996) Geology, 24 (11): 1025-1028

[2] Faulkner et al. (2010) Journal of Structural Geology, 32 (11): 1557-1575

[3] Djon et al. (2018) Economic Geology, 113 (3): 741-767

[4] Wiewóra and Weiss (1990) Clay Minerals, 25: 83-92

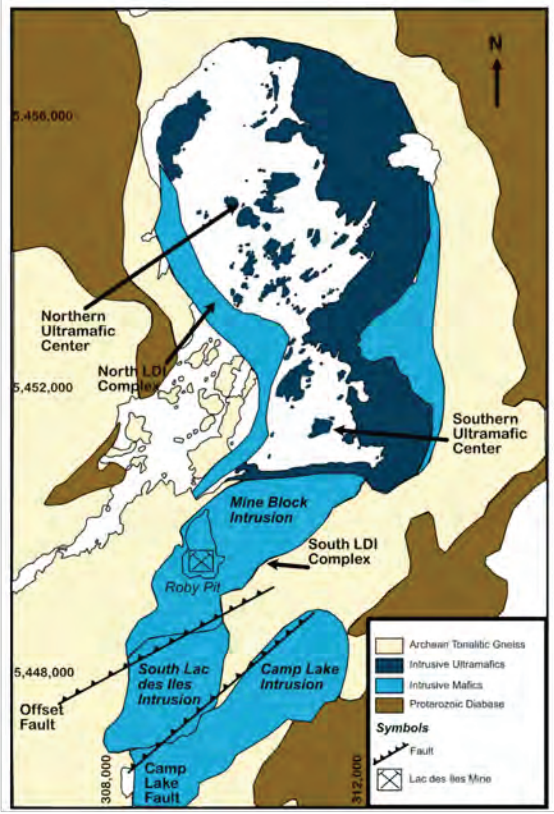


Figure 1) Local geology of the Lac des Iles Intrusion with faults in study. Modified from Djon et al., (2018).

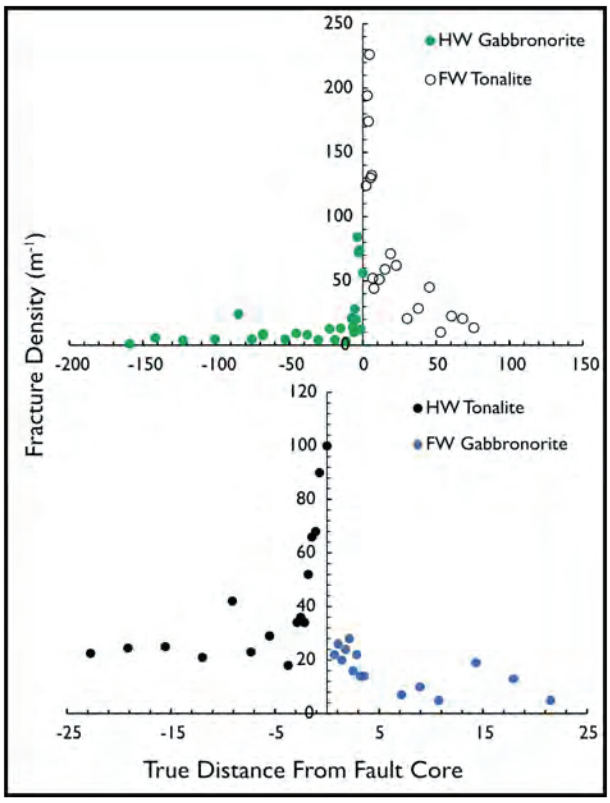


Figure 2) Fracture density with true distance from fault core.

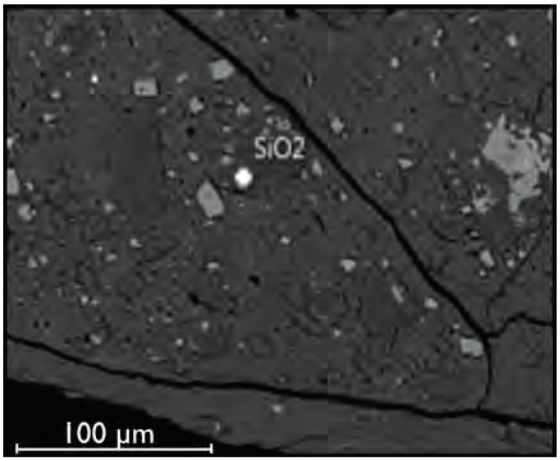


Figure 3) SEM image of typical quartz rich fault core.

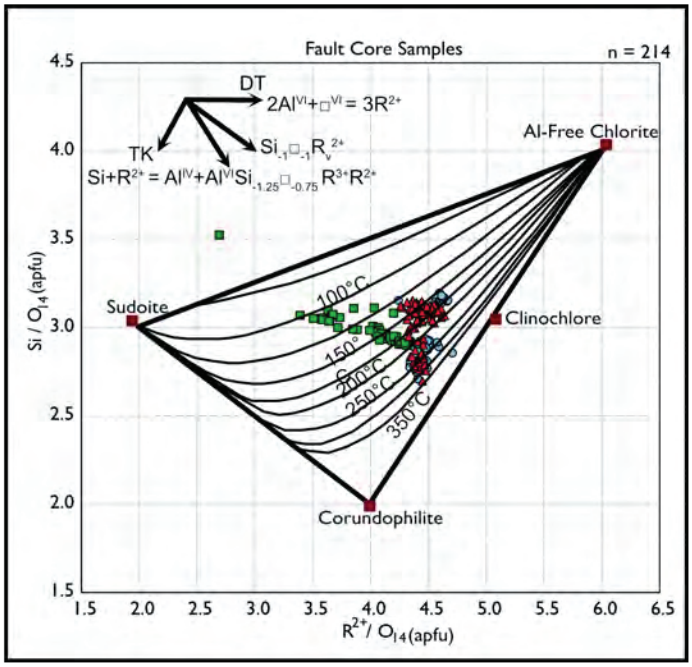


Figure 4) Results of EMPA on fault core chlorite samples plotted on R^{2+} - Si diagram after Wiewióra and Weiss (1990).

Formation of euhedral silicate megacrysts within magmatic massive sulfides

Raisch, D.[1], Staude S.[1], Fernandez, V. [2] and Markl G.[1]

[1]Department of Geosciences, University of Tübingen, Schnarrenbergstrasse 94-96, D-72076 Tübingen, Germany
[2]Natural History Museum, Cromwell Road, London, SW7 5BD, United Kingdom
Corresponding author: Dominic.raisch@uni-tuebingen.de

In the magmatic massive sulfide ore from Nova-Bollinger (Western Australia), large (up to 10 cm) silicate crystals, completely enclosed in massive sulfides, are common where sulfides infiltrate older silicate rocks. This texture could provide a new insight into the infiltration and the role of the magmatic sulfides in the nucleation and growth processes of these crystals. At Nova-Bollinger, the megacrysts consist of pyroxene, garnet and plagioclase (Fig. 1) and are typically observed in association with emulsion-textured sulfides at the sulfide infiltration front from the orebody into the silicate rocks. The infiltrated country rock itself consists of amphibolite- to granulite-facies metamorphosed mafic granulite [2] with an assemblage of plagioclase, pyroxene, amphibole ± garnet. Infiltration of hot sulfide melt caused parts of the country rock to incongruently melt producing both tonalitic melt and peritectic orthopyroxene and garnet. While the peritectic silicates formed margins at the contact between the sulfides and the country rock, the newly formed immiscible buoyant silicate melt formed an upward counterflow through the descending, denser sulfide melt, resulting in the formation of an emulsion [1, 3].

The assemblage of the country rock may contain the same minerals as the megacrysts of the emulsion texture, but they are clearly distinguishable both optically and chemically. Garnet, for example, is only occasionally present in the immediate country rock depicting a mostly poikilitic morphology with rarely any euhedral crystals larger than 800 µm, in contrast to the up to 6 cm euhedral and sometimes even skeletal garnet of the emulsion texture. In addition, the garnet and pyroxene megacrysts of the emulsion texture show distinct negative Eu-anomalies (Eu/Eu*= 0,17 for both minerals) with a strong depletion in light REE (Fig. 2) and in some cases display round multi-sulfide inclusions, as visible by computed tomography scans. Both characteristics are missing in the country rock counterparts as well as in the gabbroic host silicate melt. These observations argue for a magmatic origin of to the megacrysts via crystallisation from the silicate melt portion of the emulsion texture. The large grain size may be the result of the constant movement of the emulsion (to keep it stabilized [REF]), where the constant bumping of silicate melt droplets onto the growing crystals provides enough material to garnet, pyroxene or plagioclase to allow them grow to megacrysts within this emulsion. Once the movement of the melts decreases, the immiscible melts can separate, leaving the megacrysts behind in massive sulfides. While plagioclase coexists with garnet and pyroxene, pyroxene and garnet never coexist as megacrysts, which may be due to a temperature effect. This is based on the observation that pyroxene is mostly associated with mono-sulfide solid solution, which records temperatures up to 1100°C [4], whereas garnet is associated with intermediate sulfide solid solution, which starts to crystallise at temperatures around 880°C [4].

Besides other magmatic Ni-Cu sulfide deposits (i.e., Kambalda, Western Australia [1]), partly skeletal megacrysts are also found associated with emulsion textures of anatectic sedimentary exhalative deposits in massive sulfides (e.g. cordierite, pyroxene, and feldspar from the granulite-facies Silberberg deposit in Germany, [5]).

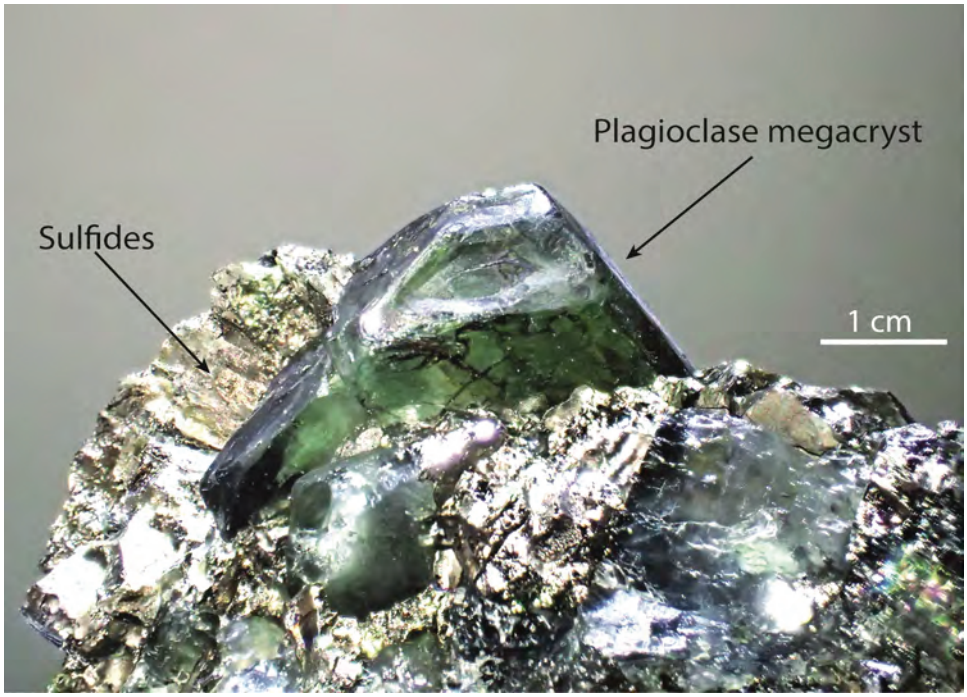


Figure 8 Plagioclase megacrysts in massive sulfides from Nova-Bollinger.

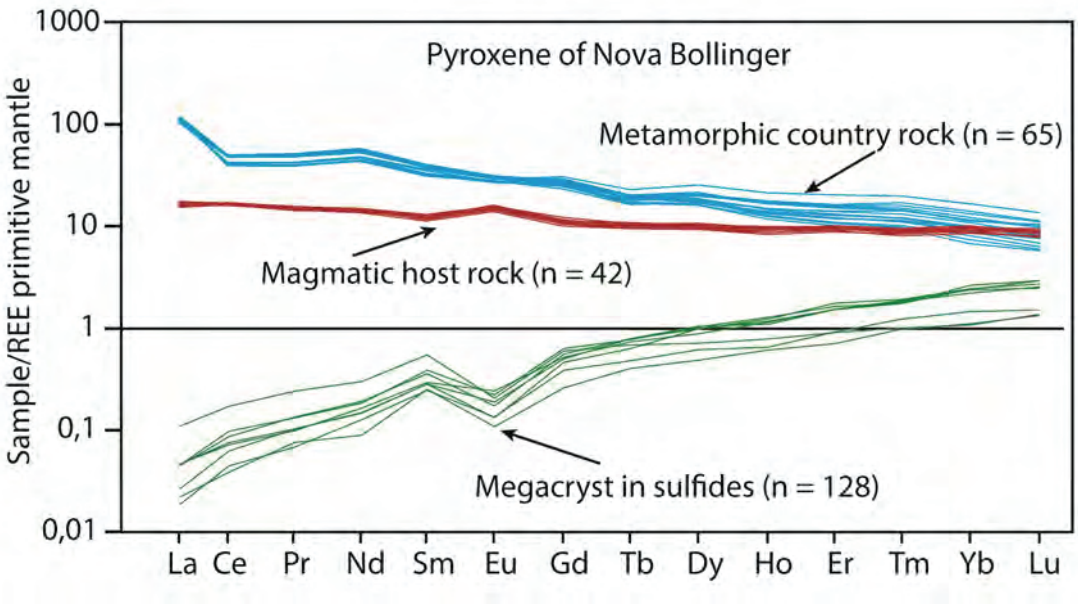


Figure 9 Primitive mantle normalized [6] REE-pattern of orthopyroxene from Nova-Bollinger.

References:

[1] Staude S et al. (2017) Ore Geol Rev 90:446-464
[2] Clark C et al. (2014) Precambrian Res 204:1-21
[3] Barnes S et al. (2018) Ore Geol Rev 101:629-651
[4] Craig JR & Kullerud G (1969) Soc Eco Geo Monogr 4:344-358
[5] Staude et al. (2023) Miner Deposita 58:987-1003
[6] Lyubetskaya T & Korenaga J (2007) Solid Earth 112

Applying Magnetic Vector Inversion (MVI) on Aeromagnetic Data in the Thunder Bay Region of the Mid-Continent Rift

Riahi, S.[1], Mungall J.E.[1], Ernst, R.E[1]

[1]Department of Earth Sciences, Carleton University, Ottawa, Ontario, Canada,
Shokouhriahinajafaba@cunet.carleton.ca

The research presented here applies the Magnetic Vector Inversion (MVI) technique to aeromagnetic datasets of the region surrounding Thunder Bay. The intrusions related to the Mid-Continent Rift contain several deposits containing high-grade mineralization zones that are abundant in platinum (Pt), palladium (Pd), copper (Cu), and nickel (Ni). Given the pivotal role of geophysical data in mineral exploration and the proven efficacy of magnetic data in delineating mineralized zones, our aim is to deepen the understanding of the geological attributes and the potential for mineralization in the Thunder Bay region deposit by applying MVI.

Aeromagnetic Data Acquisition:

The aeromagnetic data was used in this pilot study obtained from the USGS website [1], representing compilations of previously published survey data from various geological surveys and organizations. These

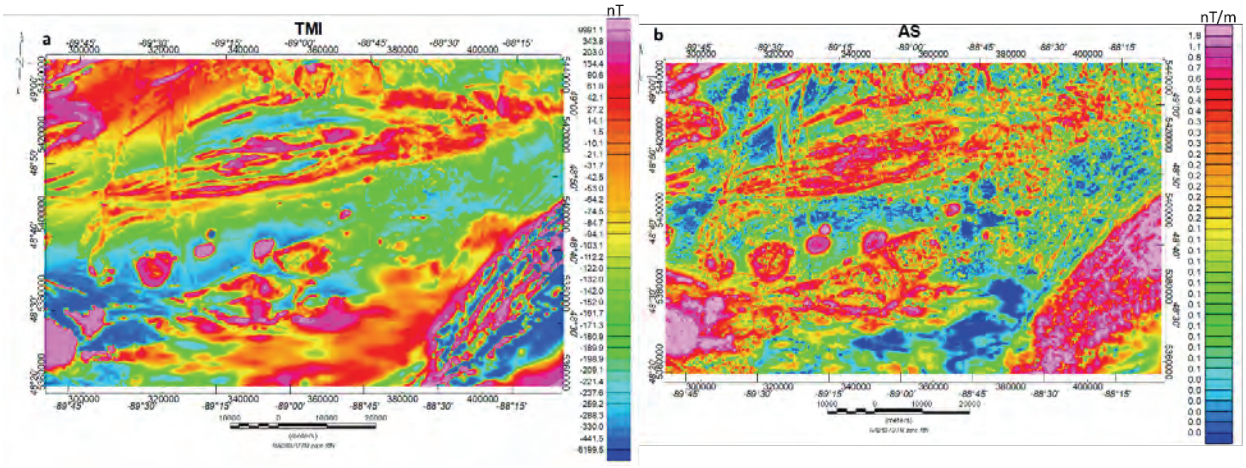


Figure 1. TMI and analytic signal (AS) of the area including the Current Lake and Escape Lake areas.

compilations, produced using industry-standard techniques, were analytically continued to a surface drape of 150 m and 300 m above ground and gridded to 250 m and 500 m cell size, respectively. They offer consistent datasets suitable for onshore geology mapping and magnetic modeling extending across the lake shore [1]. Total Magnetic intensity (TMI) data of the study area and the analytic signal (AS), with the magnetic units are shown in Figure 1.

Magnetic Vector Inversion (MVI):

Magnetization vector inversion (MVI) is employed to replicate the distribution of magnetization vectors within subsurface blocks [2-4]. This technique involves calculating the overall distribution of magnetization vectors from the components within each underground block. MVI enables the simultaneous analysis of complex geological scenarios, such as the overlay of multiple sources with

diverse remanent magnetization directions, and facilitates the complete retrieval of magnetization vector data [5-8].

All modeling and comparisons in the examples presented herein were conducted using the Geosoft VOXI Earth Modeling system. The aeromagnetic dataset was inverted to generate 3D voxel MVI susceptibility models employing the Geosoft VOXI Earth Modeling system (Fig. 2). Strong magnetic anisotropy is evident in the southwest corner of the region. Future efforts will focus on high-resolution exploration data sets over recognized chonoliths including Tamarack and Current Lake to seek distinctive magnetic vector characteristics of these small but valuable intrusions.

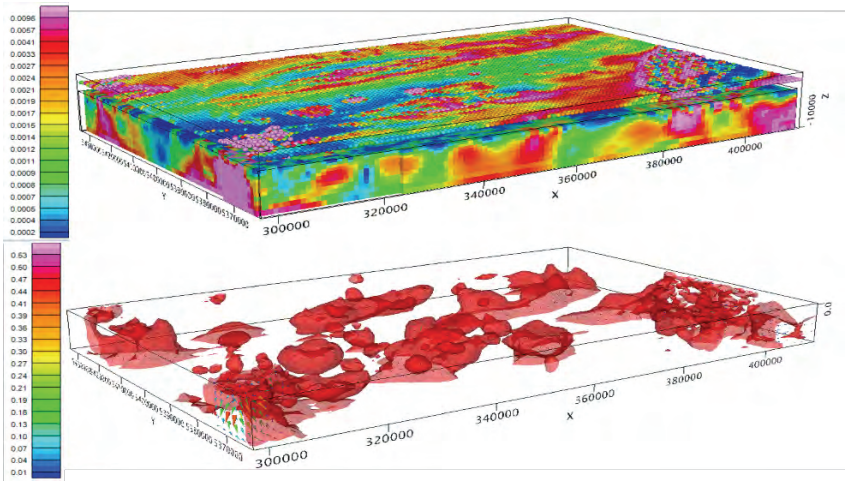


Fig 2. 3D MVI VOXEL model and MVI vectors, the above color bar gives the susceptibility in SI. The axes are in meters. The lower color bar gives the normalized amplitude in SI.

References:

[1] Anderson, E.D., and Grauch, V.J.S. (2018), Updated aeromagnetic and gravity anomaly compilations and elevation-bathymetry models over Lake Superior: U.S. Geological Survey data release, https://doi.org/10.5066/F7F18X8S.
[2] Wang, M.Y., Di, Q.Y., Xu, K., Wang, R. (2004), Magnetization vector inversion equations and forward and inversed 2-D model study, Chinese Journal of Geophysics, 47, 601‑609.
[3] Lelievre, P.G. & Oldenburg, D.W. (2009), A 3D total magnetization inversion applicable when significant, complicated remanence is present, *Geophysics,* 74, L21‑L30.
[4] Ellis, R.G., de Wet, B., Macleod, I.N., (2012), Inversion of magnetic data for remanent and induced sources, in *ASEG Extended Abstracts*, pp. 1‑4.
[5] Kubota, R., Uchiyama, A. (2005), Three-dimensional magnetization vector inversion of a seamount, Earth, Planets and Space, 57, 691‑699.
[6] MacLeod, I.N., Ellis, R.G. (2016), Quantitative magnetization vector inversion, in ASEG Extended Abstracts, pp. 1‑6.
[7] Liu, S., Hu, X., Zhang, H., Geng, M. & Zuo, B. (2017), 3D magnetization vector inversion of magnetic data: improving and comparing methods, Pure and Applied Geophysics, 174, 4421‑4444.
[8] Ghalehnoee, M.H., Ansari, A. (2022), Compact magnetization vector inversion, Geophysical Journal International, 228, 1‑16.

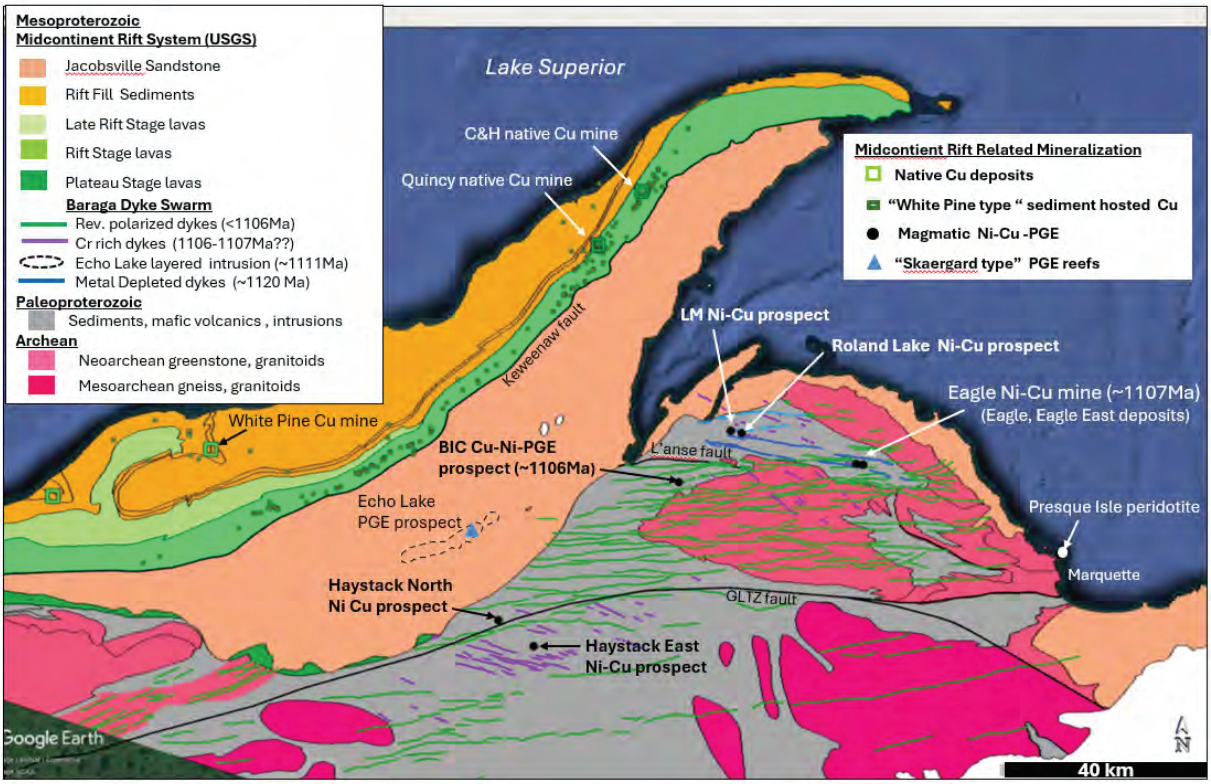
Potential links between the Midcontinent Rift (MCR) related Baraga-Marquette dyke swarm and early MCR related magmatic Ni-Cu sulfide deposits in Michigan, USA.

Rossell, D.M.[1*], Strandlie, J.[2]

1Talon Metals, Tamarack, MN, USA
2 Eagle Mines, Marquette, MI, USA
*rossell@talonmetals.com

The~1100Ma Midcontinent Rift (MCR) system can be traced across the central United States and Canada as a ~2000km long gravity high, but the only surface exposures of the volcanics, intrusions and sediments that make up the MCR are in the Lake Superior region. Despite the large extent of the MCR, historic MCR related mineral production has been almost exclusively from the portion of the MCR in Michigan. The MCR related mineral deposits shown in Figure 1, range from the famous Keweenaw volcanic hosted Native Cu deposits and the large "White Pine type" sediment hosted chalcocite deposits to the Eagle magmatic Ni-Cu sulfide mine, the only currently producing Ni mine in the USA.

In contrast to many Large Igneous Provinces which are relatively short-lived events of a few million years or less, the main period of MCR related magmatism spans ~20my [1]. The USGS [1] subdivides MCR volcanism into two main phases, an Early Plateau Stage (~1112-1105Ma) which largely occurred during a period of reversed magnetic polarity and later Rift stages (~1102-1090Ma) which occurred during a period of normal magnetic polarity



.

Figure 10 Geology map of the Western portion of the Upper Peninsula of Michigan, USA showing the distribution of dykes of the Baraga Dyke swarm and the various types of mineral deposits and prospects associated with the MCR (modified from Michigan Geologic Survey state geology map).

The Baraga dyke swarm is located on the south side of the MCR in the western portion of the Upper Peninsula of Michigan , USA (fig. 1). The dyke swarm is comprised of more than 100 mafic-ultramafic

dykes wide enough (+10m) to be visible in proprietary high resolution airborne magnetic data sets (the dykes shown in figure 1), and likely hundreds more, to thin to be discernible from airborne data, but frequently intersected in drilling in the area. The dykes can be divided into three types based on geochronology, magnetic polarity, orientation and chemistry that are referred to in figure 1 as the "metal depleted", "Cr Rich", and "Reversely Polarized" dykes The oldest known dykes within the dyke swarm are the "Metal Depleted "dykes, which are only recognized as a pair of east-west trending dykes on the north and south side of the Eagle Ni-Cu mine. These two gabbroic dykes have very different trace element chemistry from all the other dykes in the Baraga-Marquette swarm (most notably having below detection limits PGE contents) and are the only dated dykes (1120Ma+/-4my [2]). The youngest known dykes are the "reversely polarized" set of gabbroic dykes that have distinctive ophitic to sub-ophitic textures, generally East-West orientations, high TiO2 contents , mantle like Cu/Zr ratios and the highest Pd contents of any of the dyke sets. Although, all attempts to date these dykes have been unsuccessful, they cross-cut both the East Eagle intrusion dated at 1107.3+/-3.7ma [3] and the BIC intrusions dated at 1106.2+/- 1.3Ma [4]. Despite the cross cutting relationships, Paleomagnetic data suggests they might be similar in age to the Eagle intrusions [5].

The third type of dykes making up the Baraga-Marquette dyke swarm are a NW-SE trending set of dykes that range from centimetres to >70m in width. Although they have a wide range of MgO contents, the sampled dykes all have much higher Cr contents(>500ppm) than the other two types of dykes. The are often amygdaloidal, Cr Rich dykes typically do not have visible sulfides, but do resemble the amygdaloidal pyroxenite margins of the well mineralized olivine cumulates that host mineralization in the Eagle and Eagle East deposits. The Ni-Cu-PGE mineralized, pipe like conduits at Eagle, Eagle East and BIC also align closely with Cr Rich dykes, suggesting a potential temporal and genetic relationship (feeder dykes). The pronounced 30-40 degree change in orientation between the likely similar aged, reversely polarized dykes and Cr Rich dykes might indicate a change in the orientation of the regional stress fields associated with the emplacement of the mineralized intrusions.

References:

[1] Woodruff, L et al. (2020) Ore Geol. Rev. 126
[2] Dunlop, M (2013) Indiana Univ. MSc thesis (93p.)
[3] Ding X et al. (2010) Geochem. Geophys. Geosyst. v.11(3)
[4] Bleeker W et al. (2020) personal communication
[5] Foucher M (2018) Michigan Tech. Univ. PhD dissertation (173p.)

Texture and composition of Fe-Ti oxides of the Neoarchean Big Mac mafic intrusion and its implication for Fe-Ti-V-(P) mineralization in the McFaulds Lake greenstone belt, Superior Province, Canada

Sappin, A.-A.[1], Houlé, M.G.[1,2*], Metsaranta, R.T. [3], and Lesher, C.M.[2]

[1]Geological Survey of Canada, Lands and Minerals Sector, Natural Resources Canada, 490 Couronne Street, Québec City, QC G1K 9A9 Canada anne-aurelie.sappin@nrcan-rncan.gc.ca
[2]Mineral Exploration Research Centre, Harquail School of Earth Sciences, Goodman School of Mines, Laurentian University, 935 Ramsey Lake Road, Sudbury, ON P3E 2C6 Canada
[3]Earth Resources and Geoscience Mapping Section, Ontario Geological Survey, 933 Ramsey Lake Road, Sudbury, ON P3E 6B5 Canada
* Presenter

The McFaulds Lake greenstone belt (MLGB), also known as the "Ring of Fire" area, is a region with great potential for orthomagmatic Cr-platinum-group element (PGE), Ni-Cu-(PGE), and Fe-Ti-V-(P) mineralization, as attested by the discovery of the world-class Black Thor – Big Daddy – Black Horse – Black Creek – Blackbird Cr-(PGE) system, the Eagle's Nest Ni-Cu-(PGE) deposit, and the Thunderbird, Butler West, Butler East, and Big Mac Fe-Ti-V-(P) prospects. Most of the mafic-ultramafic intrusions hosting orthomagmatic mineralization in the area belong to the ca. 2736-2732 Ma Ring of Fire intrusive suite (RoFIS) (e.g., [1], [2]). This suite includes mafic and ultramafic-dominated intrusions associated with Cr-(PGE) and Ni-Cu-(PGE) mineralization (Koper Lake subsuite) and mafic-dominated intrusions associated with Fe-Ti-V-(P) mineralization (Ekwan River subsuite) [2]. The latter are the most abundant, but also more widespread geographically.

The Big Mac intrusion is the largest intrusion belonging to the Ekwan River subsuite. It forms a broadly layered, subconcordant sill, and comprises various flavors of gabbro (± Fe-Ti oxides), minor anorthosite, and rare pyroxenite. These lithologies exhibit partially preserved cumulate textures composed mostly of plagioclase and clinopyroxene (almost completely altered to amphibole) with local magnetite and ilmenite, apatite, and Fe-Ni-Cu sulfides. Fe-Ti oxide mineralization in the Big Mac intrusion occurs as massive (> 80% Fe-Ti oxides) to semi-massive (40 to 80% Fe-Ti oxides) magnetite-ilmenite layers, net-textured (20 to 35% Fe-Ti oxides) to patchy net-textured (10 to 25% Fe-Ti oxides), and locally as millimeter- to a few centimeter-thick stringers (Fig. 1). Massive to semi-massive Fe-Ti oxide layers are mainly located in the northern part of the intrusion, whereas patchy to net-textured oxides are more widespread throughout. All lithologies typically contain at least several percent disseminated Fe-Ti oxides (< 10%). Based on whole-rock geochemical data, the best mineralized interval (9.5 m thick) has an average composition of 68 wt.% FeO_t, 17 wt.% TiO_2, and 0.48 wt.% V_2O_5. The Big Mac sill also contains disseminated pyrrhotite, pentlandite, pyrite, and chalcopyrite (< 10% sulfides) throughout the intrusion, and millimeter-thick stringers of chalcopyrite, pyrite, and pyrrhotite. In the northern part of the intrusion, the semi-massive to massive magnetite layers contain patchy net-textured pyrrhotite, pentlandite, pyrite, and chalcopyrite (10 to 20% sulfides; Fig. 1E-F) with up to 1.6% Ni_{100} (Ni at 100% sulfides) and 1.8% Cu_{100}.

Fe-Ti oxides are well preserved in the Big Mac intrusion and their chemical composition can be used to characterize the internal stratigraphy, to determine which parts are more prospective for V and P mineralization, and to estimate the conditions for the genesis of the Fe-Ti oxide layers. The Big Mac intrusion appears to have crystallized from high-Fe parental magmas that were injected from a feeder conduit located in the northernmost part of the intrusion. Based on the presence of more primitive magnetite and ilmenite compositions in the northern part of the intrusion and more evolved signatures in the southern part, the rocks in the northern part likely represent more conduit-proximal facies that are more prospective for Fe-Ti-V mineralization, whereas the rocks in the southern part likely represent more distal facies that are more prospective for Fe-Ti-P mineralization. The trace element contents of magnetite also suggest that the crystallization of the Fe-Ti oxide layers in the Big Mac intrusion occurs under relatively oxidized conditions (fO_2 > FMQ + 1). The Big Mac

magnetite displays many characteristics (e.g., texture, chemical composition) in common with magnetite in other mafic-dominated intrusions of the Ekwan River subsuite (e.g., Thunderbird, Butler West, Butler East). This attests to the Fe-Ti-V-(P) potential of the large ferrogabbroic magmatic event that affected the MLGB at ca. 2735-2732 Ma [3] and formed the Ekwan River subsuite.

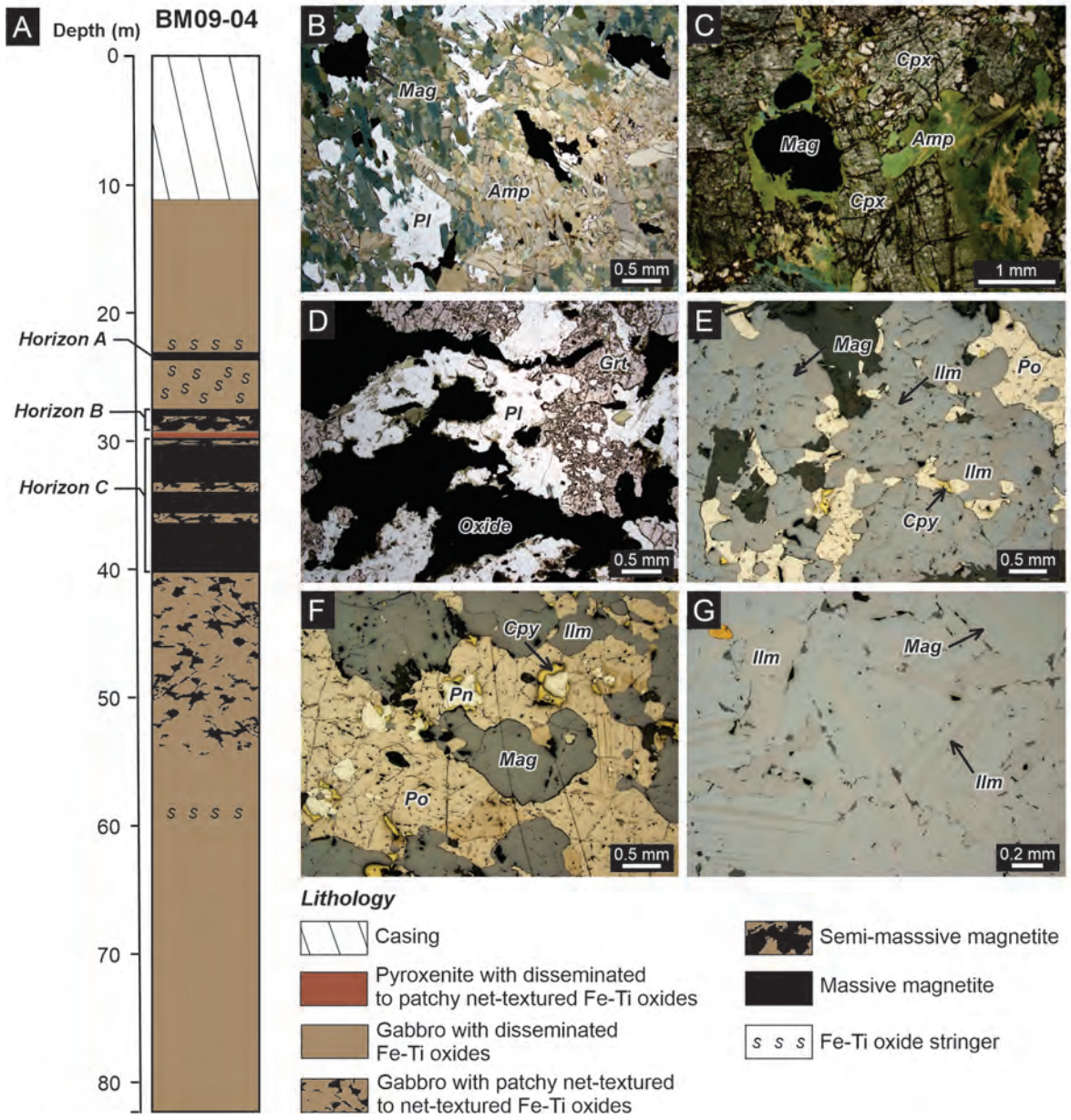


Figure 1: (A) Simplified and schematic graphic log of drill core BM09-04 located in the northern part of the Big Mac intrusion. (B-G) Photomicrographs of polished thin sections in plane-polarized transmitted (B-D) and reflected (E-G) light showing the different oxide textural facies in the Big Mac intrusion. (B) Disseminated, anhedral grain of magnetite in mesocratic gabbro. (C) Disseminated, rounded grain of magnetite in clinopyroxenite. (D) Net-textured magnetite in melanocratic gabbro. (E-F) Semi-massive magnetite with patchy net-textured pyrrhotite, pentlandite, and chalcopyrite. Anhedral magnetite contains ilmenite exsolutions as anhedral grains and lamellae. (G) Massive magnetite with ilmenite exsolutions as anhedral crystals and thick lamellae. Abbreviations: Amp = amphibole, Cpx = clinopyroxene, Cpy = chalcopyrite, Grt = garnet, Ilm = ilmenite, Mag = magnetite, Pl = plagioclase, Pn = pentlandite, Po = pyrrhotite.

References:

[1] Houlé M.G. et al. (2015) Geological Survey of Canada, Open File 7856, pp. 35–48.

[2] Houlé M.G. et al. (2019) Geological Survey of Canada, Open File 8549, pp. 441–448.

[3] Houlé M.G. et al. (2020) Geological Survey of Canada, Open File 8722, p. 141–163.

Complexly zoned pyroxenes at Kevitsa record magma mixing and survive alteration

Schoneveld, L.[1], Luolavirta, K.[2,3], Barnes, SJ[1] , Hu, S.[1] , Verrall, M.[1] and Le Vaillant, M.[1]

[1]CSIRO Mineral Resources, Perth, 6151, Australia
[2]Geopool Oy, Teknobulevardi 3−5, 01530 Vantaa, Finland. kirsi.luolavirta@geopool.fi
[3]Oulu Mining School, Faculty of Technology P.O. Box 3000, FI-90014 University of Oulu, Finland

---

Magmatic Ni-Cu-(Platinum Group Element—PGE) sulfide deposits are generally linked to dynamic systems and conduit-type emplacements of mafic-ultramafic magmas. Schoneveld et al. [1] demonstrated a common feature of variable titanium (Ti) and chromium (Cr) zoning patterns in cumulus pyroxenes in various mineralized intrusions (e.g. Noril'sk-Talnakh, Nova-Bollinger, Jinchuan) and attributed these features to reflect a high-flux magmatic environment with wall rock assimilation and related fluctuating cooling rates where pyroxenes crystallized. On the contrary, according to the authors, barren intrusions were characterized by simple normally zoned pyroxenes. Pyroxene zoning was therefore suggested to serve as a potential prospectivity indicator for magmatic Ni-Cu-PGE sulfide deposits. However, on many occasions, the primary mineralogy of the ore hosts has been subjected to variable degrees of hydrothermal alteration, potentially hindering the usability of the pyroxene zoning approach in exploration. This dilemma is being tackled by mapping pyroxene zoning patterns of samples recording variable degrees of amphibole alteration. Additionally, pyroxene has been shown to record magma histories in volcanic settings [2] and also has the potential to record important magmatic histories in these ore deposits.

In this research, microbeam X-ray fluorescence (XRF) mapping techniques were applied to the mineralized Kevitsa intrusion, in northern Finland to study pyroxene zoning patterns. Synchrotron-based μXRF chemical imaging using multidetector Maia arrays has proved especially effective [3], allowing entire thin sections to be imaged at micrometer-scale resolution in a matter of hours (Australian Synchrotron, operated by ANSTO). This allows many grains with varying crystal orientations to be analyzed and detailed visualization of chemical zoning.

The mafic-ultramafic Kevitsa intrusion (2.06 Ga) is hosted by a volcano-sedimentary sequence in the Central Lapland greenstone belt. A disseminated Ni-Cu-(PGE, Au, Co) sulfide ore deposit occurs within the central parts of ultramafic olivine-pyroxene cumulates. The deposit has been mined since late 2011 and is currently operated by Boliden. The sample set comprises 29 thin sections collected from various parts of the intrusion representing mineralized and non-mineralized domains within the intrusion. Most of the samples are clinopyroxene-olivine mesocumulates with variable modes of olivine, augite, and oikocrystic or transitional cumulus to poikilitic orthopyroxene (bronzite/enstatite). These textures are characteristic throughout the ultramafic part of the Kevitsa intrusion. The samples have also been exposed to variable degrees of hydrothermal alteration and many clinopyroxene grains have begun the transformation to amphibole.

Very complex pyroxene zoning patterns are observed throughout the Kevitsa intrusion (Figure 1). Hence, the Kevitsa intrusion provides yet another example of a sulfide ore-bearing variant of a mafic-ultramafic intrusive body with diagnostic complex zoning patterns of pyroxene minerals. The observed styles and magnitudes of clinopyroxene zonation in Kevitsa, however, are unusual when compared to other ore-bearing intrusive bodies [1]. A common feature for clinopyroxe grains is highly Cr-poor cores, followed by strong oscillatory patterns in the mantles, often ending in a rim of very low Cr and high Ti values. Similarly, the clinopyroxene in the most nickel-rich ore zones shows enriched nickel rims. These patterns are best explained by open magma chamber processes, consistent with Luolavirta et al. [4]. The nickel enrichment and chemical oscillations recorded in the pyroxene crystal structure suggest an influx of new, Ni-rich melt into the partially solidified crystal mush at Kevitsa. The clinopyroxene zoning patterns are not reflected in the oikocrystic

orthopyroxene that generally records smooth normal zoning. This indicates post-cumulus growth of orthopyroxene (cf. slow nucleation as cumulus mineral).

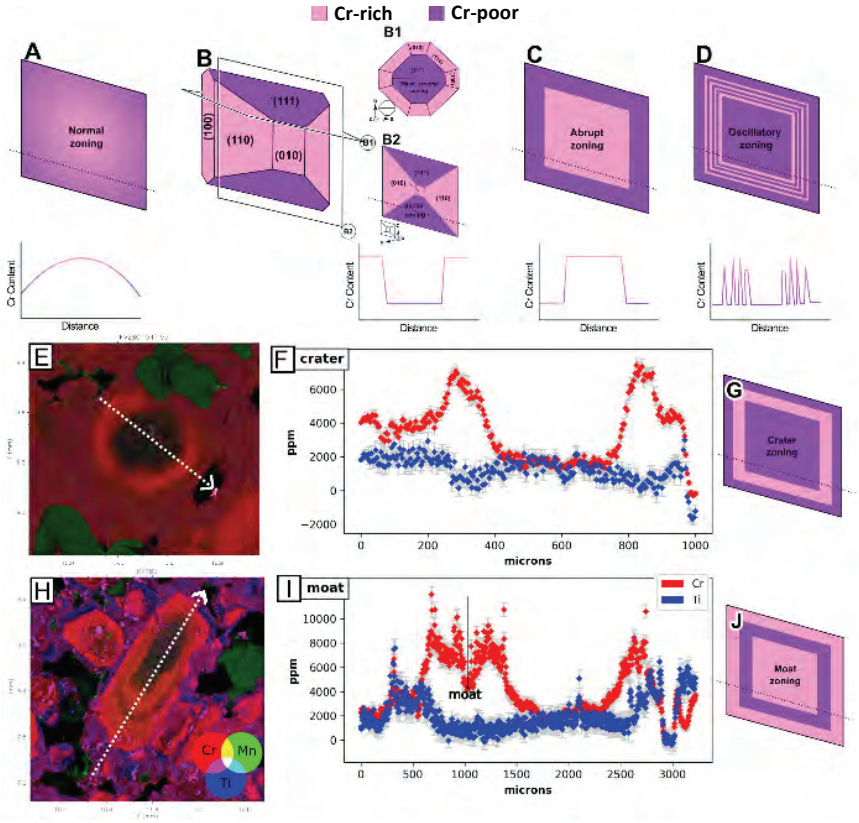


Figure 1. Examples of end-member zoning styles in the Kevitsa pyroxenes with traverses across the grains showing the Cr and Ti content that causes each distinct zoning type. A) normal zoning from trapped liquid reactions B) sector zoning with B1 and B2 showing different sectioning effects of this zoning type C) abrupt zoning D) oscillatory zoning E) crater-zoned clinopyroxene with the content of Cr and Ti of the traverse shown in F). G) crater zoning schematic H) Moat zoned clinopyroxene grain I) traverse of Cr and Ti content across the grain J) moat zoning schematic.

The examination of the preservation of the zoning patterns with alteration reveals that Cr zonation is visible through the early stages of amphibole alteration, with preservation being enabled by the presence of Cr-rich epitaxial amphibole. However, the remnant zoning is lost as the amphibole alteration progresses.

It is worth noting that the complex zoning patterns are observed in almost every sample, regardless of the location relative to the ore-bearing domain of the intrusion (some are located up to a few hundred meters away from the deposit). Hence, to enhance the methodology as an exploration tool, further research is needed to outline the distal extent of this fingerprint away from the ore within mineralized intrusions of reasonable size.

References:

[1] Schoneveld et al. (2020) Zoned Pyroxenes as Prospectivity Indicators for Magmatic Ni-Cu Sulfide Mineralization. Front. Earth Sci. 8:256.

[2] Ubide et al. (2019) Sector-zoned clinopyroxene as a recorder of magma history, eruption triggers, and ascent rates: Geochim. Cosmochim. Acta. 251:265-283.

[3] Barnes et al. (2020) Imaging trace-element zoning in pyroxenes using synchrotron XRF mapping with the Maia detector array: Benefit of low-incident energy. Am. Min. 105:136–140

[4] Luolavirta et al. (2018) In-situ strontium and sulfur isotope investigation of the Ni-Cu-(PGE) sulfide ore-bearing Kevitsa intrusion, northern Finland. Min. Dep. 53:1019–1038

New indicator mineral signatures for nickel sulfide exploration

Schoneveld, L.E.[1], Williams M.[1], Salama, W.[1], Spaggiari, C. V.[1], Barnes, S. J. [1], Le Vaillant, M. 1, Siegel, C. [1], Hu, S. [1], Birchall, R. [1], Baumgartner, R. [1], Shelton, T. [1], Verrall, M. [1], and Walmsley, J. [1]

[1]Mineral Resources, CSIRO, Western Australia
Corresponding Author: Louise.Schoneveld@csiro.au

Discovery of new ore deposits is becoming more difficult as we explore beneath deep cover. Commonly, exploration programs start from geophysical targeting and move straight into drilling, which is expensive and has a low sampling density. Nickel sulfide deposits specifically have little to no hydrothermal footprints and usually have small sulfide targets, therefore, this sampling practice risks missing potential key sulfide intercepts and abandoning fertile ground. Exploring using indicator minerals can give additional information before drilling has commenced to identified prospective areas and can continue to be used in early drilling programs to allow focus on more prospective intrusions. In this study, we develop key chemical signatures within minerals that indicate Ni prospectivity and prove the effectiveness of mineral indicators for use in exploration. Australia hosts one third of the world's nickel (Ni) deposits and most are located in Western Australia therefore this area was the focus of our study.

Comprising 11 detailed case studies from Western Australia and one from South Australia, paired with existing global mineral chemistry data from CSIRO databases, the aim of each case study was to understand the mineral deposit or exploration camp in detail, to provide context for the indicator mineral signatures that were measured. We analysed both komatiitic systems as well as intrusion-hosted systems, sampling from both known mineralised and apparently barren examples. Further, we sampled the regolith and cover above these deposits to determine as to whether indicator minerals can survive weathering and transport processes.

We analysed spinel minerals (chromite-magnetite), olivine, pyroxene, apatite, ilmenite, and plagioclase for their trace elements using laser ablation inductively coupled plasma mass spectrometry (LA-ICP-MS). This large and robust dataset is ideal for machine learning applications. We used random forest models to distinguish the key trace element contents of each mineral that signifies mineralisation and the confidence of each prediction.

Spinel was the largest dataset in this study, with over 7,000 LA-ICP-MS analyses. This large dataset allowed for confident (77%) predictions of mineralised vs non-mineralised occurrences using the machine learning models. The key elements underpinning these predictions were Co, Ga, V, Ni, and Cr. Using the trace element data, it may also be possible to predict the volume of sulfide associated with an individual spinel grain. This has implications for vectoring toward larger and more economic deposits. Analysis of the cover and regolith showed that chromite is not significantly affected by weathering. A study of the Black Swan nickel mine in Western Australia shows that the trace element contents in spinel are consistent across the talc-altered, serpentine-altered, and fresh examples of the komatiite. This suggests that the spinel family would be a robust resistate indicator mineral for Ni exploration.

Olivine is this database's next largest mineral collection, with over 1,400 LA-ICP-MS analyses. Using the machine learning models, the trace elements in olivine can be used to accurately (95%) predict

that the host intrusion was mineralised; however, the unmineralised category has poorer recall (60%), which suggests a greater likelihood of false positive predictions. Pyroxene can be examined for trace element (Cr-Ti) variation within grains to understand if the intrusion has the potential to be a conduit. Although not a direct indicator of sulfide presence, it can indicate the potential for high-R factors and, therefore, a metal-rich sulfide (if sulfide saturation has occurred). Minerals such as olivine, pyroxene, and plagioclase do not survive weathering and are not considered resistant indicator minerals. However, they can still be analysed in fresh rock to assess as to whether the subject intrusion has potential to host Ni-sulfide orebodies.

The other minerals (apatite, ilmenite, and plagioclase) have less than 1,000 LA-ICP-MS analyses for each phase in this database. Although they show promise in being robust indicator minerals, a larger training dataset should be accumulated before their use in exploration. Ilmenite specifically was found to be the most common mineral in heavy mineral concentrates and is easily separated with a magnet (figure 1). The trace elements in ilmenite show confident predictions for prospectivity, however, the database needs to be expanded to develop ilmenite as an additional resistant indicator mineral.

In this project, we have developed analysis and data-handling workflows, and machine-learning models for Ni-sulfide exploration. Although these models were primarily developed using Western Australian case studies, these exploration tools are applicable globally.

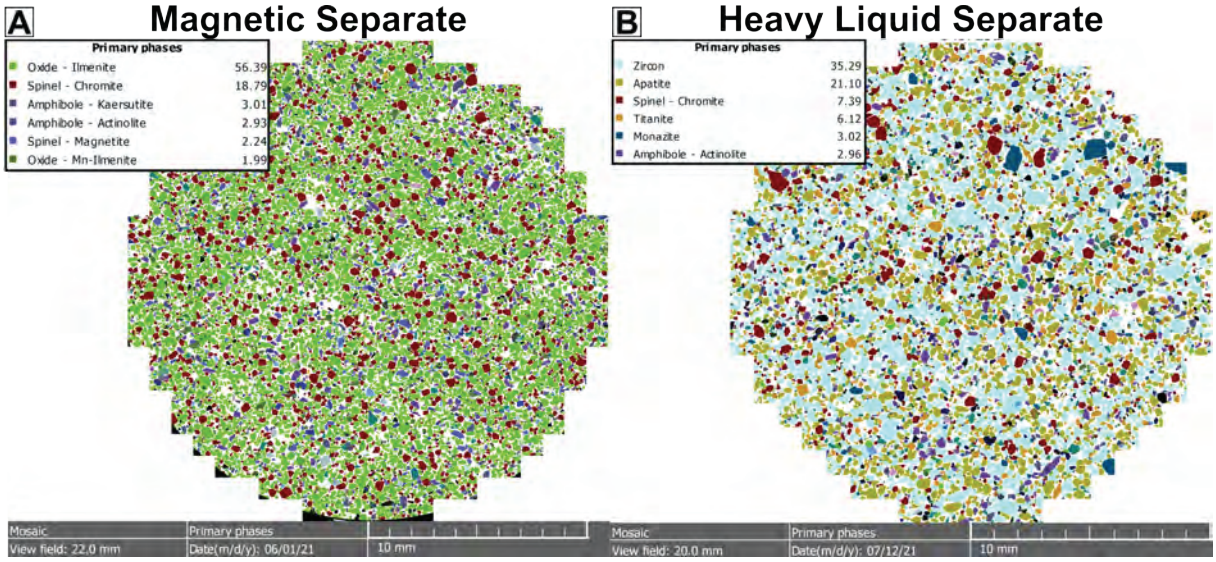


Figure 11: Magnetic and heavy liquid separation from the same stream sediment sample, A) magnetically separated; B) heavy liquid separation. The heavy liquid separation was carried out on the remaining fraction after magnetic separation.

Apatite as an indicator for volatile involvement in the genesis of the Marathon Cu-PGE deposit, northwestern Ontario

Shahabi Far, M.[1], Good, D.[2] and Samson, I[3]

[1]Department of Earth Sciences, Carleton University, Ottawa, ON (maryam.shahabifar@carleton.ca)
[2]Department of Earth Sciences, Western University, London, ON
[3]Department of Earth and Environmental Sciences, University of Windsor, ON

The Marathon Cu-PGE deposit of the Mesoproterozoic (1106 ± 1 Ma) Coldwell alkaline complex contains three types of mineralization with different textural, mineralogical, and geochemical characteristics: Footwall Zone, Main Zone, and W-Horizon. The relative roles of volatiles in metal enrichment in this deposit remain a point of debate. In this study, the significance of hydrothermal fluids in directly precipitating ore minerals or causing their later modification using the texture and composition of apatite is investigated.

The textural relationships of apatite with other minerals indicate two types of apatite generation: early apatite and late apatite. Early apatite crystals are homogeneous with no textural or chemical zoning. Late apatite crystals exhibit diverse zoning patterns including oscillatory zoning, patchy zoning, and replacement textures (Fig. 1). The zoning in apatite is associated with Si and rare earth elements (REE) changes. Late apatite grains reveal replacement zones along crystal rims as well as around cracks containing monazite and/or allanite inclusions; this feature will be referred to as replacement apatite in this study (Fig. 1). The earlier apatite grains that show replacement zones are referred to as late metasomatized apatite.

The overall decrease in Cl/F ratios of the late apatite from the Footwall to the W Horizon (Fig. 2) can be explained by magma degassing similar to the suggested model for the Bushveld and Stillwater complexes [1][2][3]. Primary fluid and monazite inclusions in the replacement rims of the metasomatized late apatite associated with hydrous minerals can be interpreted to have resulted from the interaction of volatiles with the late-stage gabbroic melts. Experimental studies indicate that monazite and other REE-minerals can be formed as a result of fluid-induced coupled dissolution-reprecipitation processes [4] via fluorapatite interaction with H2O, 40/60 CO2/H2O, and KCl brine [5][6]. Given that the metasomatized late apatite has an overall higher Cl/F ratio compared to the other apatite grains (Fig. 2), the fluid must have been Cl-rich. The metasomatized late apatite and their replacement rims with monazite inclusions are usually associated with residual hydrous melt aggregates and are more abundant in W Horizon. This indicates that late-stage hydrous melts and associated exsolved fluids are more abundant in the W Horizon than in the other two zones. The ubiquitous presence of hydrothermal alteration around the residual hydrous melt aggregates certainly indicates that a hydrous fluid exsolved from the late-stage melts. The presence of hydrothermal carbonate and epidote in the late assemblages as well as the presence of carbonate as an alteration of apatite in the replacement rims indicates that fluid also must have contained CO2 or other carbonic species. Given that sulfide minerals in the W Horizon mostly occur in association with biotite and hornblende as either interstitial coarse crystals or interstitial phase in the residual hydrous melt aggregates, the Cl- carbonic-enriched volatiles exsolved from late-stage magma must have been played a critical role for PGE-enrichment in the W Horizon.

Allanite as either inclusions, filling voids or cracks, or along the rims of late metasomatized apatite or independent grains are much coarser grains compared to monazite (Fig. 1) suggesting that the early nucleated monazite must have interacted with later possibly more NaCl or CaCl2-rich fluid reacted with the surrounding silicate rocks to form allanite [5][6][7][8]. This is consistent with elevated Cl contents of alteration products (amphibole with up to 3.9 wt% Cl) associated with metasomatized

late apatite with higher Cl content and suggests that the late-stage hydrothermal fluid was Cl-enriched. The occurrence of allanite in the Footwall Zone and Main Zone but rare occurrence in the W Horizon indicates that the late-stage fluid infiltration must have been less dominant in the W Horizon. This is consistent with relatively fewer secondary hydrous minerals in the W Horizon. High metal contents of the replacement rims of apatite in the Footwall Zone and their association with chalcopyrite indicate that metals and S were mobilized by these volatiles. Much of the chalcopyrite in the Main Zone has replaced pyrrhotite and is intergrown with hydrous silicate minerals, which also suggests that Cu was introduced into the system, presumably by volatiles. This observation can be explained by a process in which volatiles fluxed through the Footwall Zone and transported Cu to the Main Zone. Replacement of pyrrhotite by chalcopyrite in the Main Zone and associated Cu metasomatism must have occurred after pyrrhotite crystallization in the Main Zone suggesting Cu remobilized with later-stage hydrothermal fluid. Chalcopyrite inclusions occurrence within voids in the replacement zones of apatite as well as along the cracks within apatite where allanite occurs, could suggests that this fluid could be the Cl-rich hydrothermal fluid that is responsible for the allanite formation. The sources of these late-stage volatiles are not constrained yet, although one possibility could be the devolatilization of the Archean country rocks.

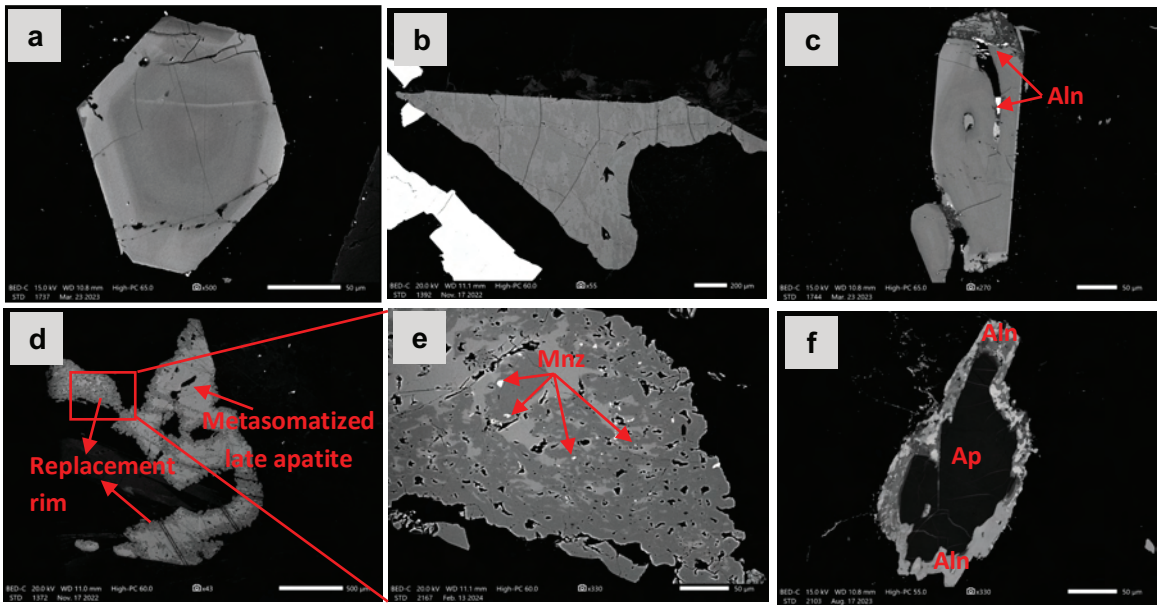


Fig. 1: Back-scattered electron images (BSE) showing diverse zoning and textures in the late apatite: a) oscillatory zoning with Si and REE changes between zones, b) patchy zoning of late apatite from W Horizon showing difference is carbon concentration between the zones, c) allanite filling the cracks and voids within apatite, d) metasomatized late apatite showing replacement zones around the rims and along cracks, e) zoomed-in image from red box on image c showing monazite inclusions within the replacement zone, f) allanite as overgrowth rim of apatite. Aln: alanite, Ap: apatite, Mnz: monazite.

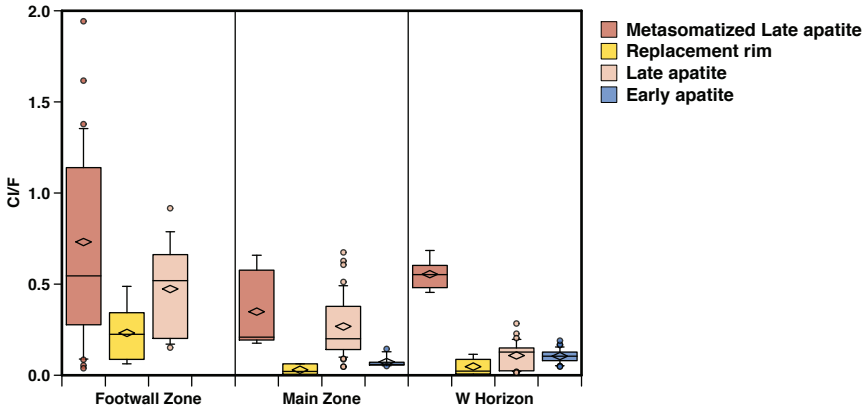


Fig. 2: Box-whisker plot comparing Cl/F values of different apatite generations and textures from different part of the Marathon deposit. The lower, middle, and upper lines in each box represent 25%, median and, and 75% of the data, respectively. The lower whisker represents the 10th percentile and the upper whisker represents the 90th percentile. Circles show outliers.

References:

[1] Boudreau A and McCallum I (1989) Contrib Mineral Petrol 102:138-153

[2] Boudreau A et al. (1995) Contrib Mineal Petrol 122:289-300

[3] Willmore C et al. (2000) J Petrol 41:1517-1539

[4] Pan Y and Fleet M (2002) Rev in Mineral Geochem 48:13-49

[5] Harlov D and Förster (2003) Amer Miner 88:1209-1229

[6] Spear F (2010) Chem Geol 279:55-62

[7] Budzyń B et al. (2011) Amer Miner 96:1547-1567

[8] Jonsson E et al. (2016) Amer Miner 101:1769-1782

Geochemical and Petrologic Investigation of the Eagle's Nest Intrusion, McFaulds Lake Greenstone Belt, Ontario, Canada

Sheshnev, V.[1], Hollings, P.[1], Phillips N.J.[1], Weston, R.J.[2], Deller, M.[2] and Campbell, D.[2]

[1]Department of Geology, Lakehead University, 955 Oliver Road, Thunder Bay, Ontario, P7B 5E1.
vsheshne@lakeheadu.ca
[2]Wyloo Metals, 1-1127 Premier Way, Thunder Bay, Ontario, P7B 0A3.

The Eagle's Nest orthomagmatic Ni-Cu-(PGE) deposit is situated in the northern portion of the Superior Province within the McFaulds Lake greenstone belt, approximately 500km northeast of Thunder Bay, Ontario. The deposit contains 11.1 million tonnes of proven and probable reserves grading 1.68% Ni, 0.87% Cu, 0.89g/t Pt, 3.09g/t Pd and 0.18g/t Au [1]. The Eagle's Nest intrusion is associated with the mafic-ultramafic magmatism of the Ring of Fire intrusive suite between 2736 and 2732 Ma and is part of the ultramafic-dominated Koper Lake subsuite [2,3]. The Eagle's Nest intrusion was emplaced along a sub-horizontal conduit, forming a blade-shaped dike [4]. Mineralization is consistent with gravitational sulfide segregation at the basal, northwestern contact of the intrusion. A post emplacement, regional deformation event, rotated the intrusion into its present day, subvertical orientation, with a width of ~500m, thickness of ~150m and vertical extent >1600m. The mineralized ore body of the Eagle's Nest intrusion consists of a zoned pyrrhotite – pentlandite – chalcopyrite assemblage with massive sulfide mineralization at the northwestern contact gradationally becoming, net-textured and disseminated to the southeast [5].

Mungall et al. [6] estimated the parental magma to be a low-Mg komatiitic magma with ~22% MgO and ~12% FeO^T. More recently, Zuccarelli et al. [5] reported the most magnesian olivine within the mineralized portion of the intrusion is Fo_{86}, which is consistent with a picritic parental magma composition. Contradictions among the estimated parental magma composition and the most magnesian olivine found within the intrusion, require further constraints on the composition of the melt that formed the mineralized system. Geochemical, petrographic, mineral chemistry, and radiogenic isotope techniques, are being used to characterize the unmineralized portions of the Eagle's Nest intrusion, to characterize the associated chilled dikes in the vicinity of the intrusion, and to constrain the parental magma characteristics that formed the Eagle's Nest deposit. This will allow for a more holistic approach to determining the primary melt composition.

One-hundred and thirty-six samples were collected from drill core. Samples comprise five tonalitic wall-rock samples, 44 mafic-ultramafic chilled dike samples, and 87 intrusion samples. Intrusion samples comprise of mafic-ultramafic lithologies that include peridotite (Fig. 1), gabbro, and units identified as chilled margins of the main intrusion. One-hundred and twenty-one samples were analysed using Inductively Coupled Plasma Atomic Emission Spectroscopy and Inductively Coupled Mass Spectroscopy for major oxides and trace elements. A total of 30 polished thin section were prepared comprising seven peridotite, eight contact, and 15 offshoot dike samples. A total of 20 samples were selected for analysis of Sm-Nd isotopes.

Three different approaches are used to evaluate the parental magma composition that formed the Eagle's Nest intrusion. The first two approaches will examine chilled margins preserved along the length of the intrusion and within the magmatic breccia matrix situated within the hanging-wall of the chonolith. The third approach will examine the chemical composition of olivine grains preserved within the ultramafic lithologies of the intrusion. To further constrain the contamination history and identify primitive melt compositions, Sm-Nd isotope data will also be examined.

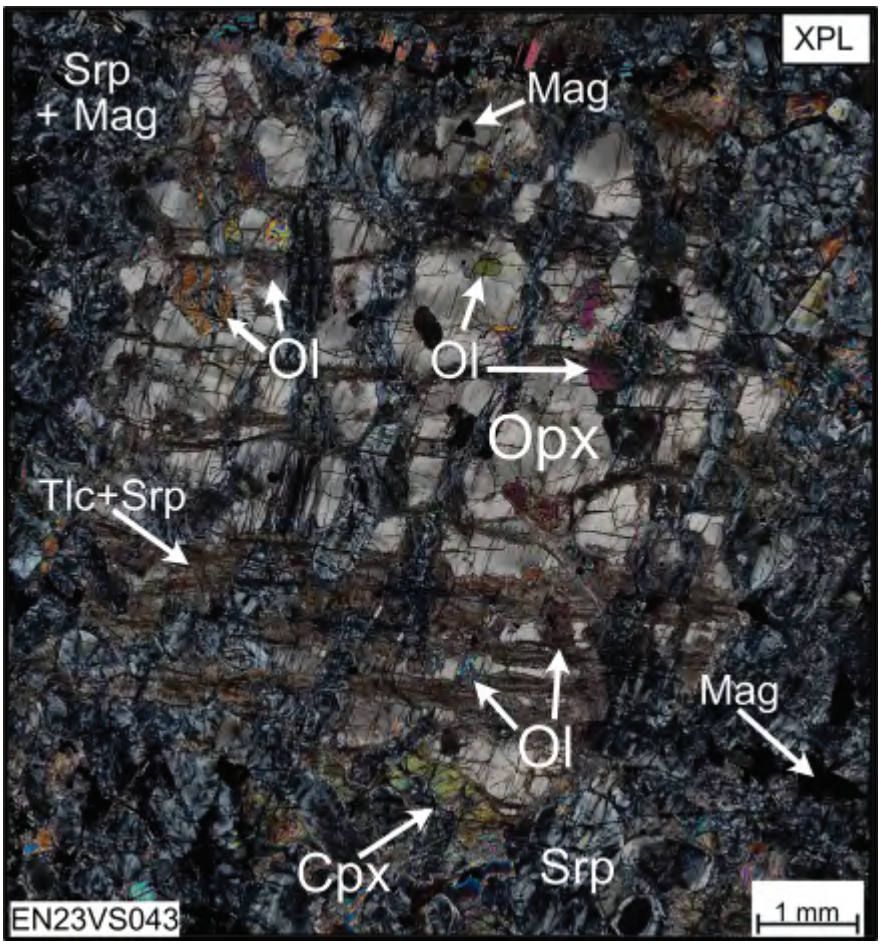


Figure 1. Photomicrograph of a peridotite sample depicting poikilitic textured orthopyroxene with preserved fresh olivine within the oikocryst surrounded by cumulus serpentinized olivine (XPL: cross-polarized light).

References:

[1] Burgess et al. (2012) Micon Int Ltd: 197
[2] Metsaranta et al. (2015) Geol Surv of Can Opn File Rep 7856: 61-73
[3] Houlé et al. (2020) Geol Surv of Can Opn File Rep 8722: 141-163
[4] Barnes S.J. and Mungall J.E. (2018) Econ Geol 113: 789-798
[5] Zuccarelli et al. (2022) Econ Geol 117(8): 1731-1759
[6] Mungall et al. (2010) Soc of Econ Geol Sp Pub 15: 539-557

Reconstitution of the Merensky Reef footwall during chamber replenishment

Smith, W.D.[1,2], Henry, H.[3], Maier, W.D.[4], Muir, D.D.[4], Heinonen, J.S.[5,6], Andersen, J.Ø[7]

[1]Department of Earth Sciences, Carleton University, 1125 Colonel By Drive, Ottawa, ON K1S 5B6, Canada
[2]CSIRO Mineral Resources, 26 Dick Perry Avenue, Kensington, Perth, WA 6151, Australia
[3]Géosciences Environment Toulouse, Université de Toulouse III Paul Sabatier, 14 Avenue E. Belin, 31400 Toulouse, France
[4]School of Earth & Environmental Sciences, Cardiff University, United Kingdom, CF10 3AT
[5]Department of Geosciences and Geography, University of Helsinki, P.O. Box 64, 00014, Helsinki, Finland
[6]Geology and Mineralogy, Åbo Akademi University, Akademigatan 1, 20500 Åbo, Finland
[7]Camborne School of Mines, University of Exeter, Penryn, United Kingdom, TR10 9EZ

The Merensky Reef of the Bushveld Complex was discovered in 1924 by Hans Merensky, whilst following up on platinum-group mineral concentrates that Andries Lombaard had panned from a stream in the eastern Bushveld Complex [1]. This discovery was to be significant, and the aptly named Merensky Reef was the focus of intense scientific research for the ensuing 100 years, providing insight into the formation of reef-style platinum-group element occurrences in layered mafic-ultramafic intrusions. However, many aspects of the petrogenesis of such reef-style occurrences remain debated despite a century of investigations.

The layered mafic-ultramafic rocks of the 2.056 Ga Bushveld Complex are together known as the Rustenburg Layered Suite, which itself has been divided into five stratigraphic units, including the Marginal, Lower, Critical, Main, and Upper Zones [2]. The Merensky Reef occurs in the Upper Critical Zone, which predominantly consists of interlayered norite, anorthosite, chromitite, and orthopyroxenite [3]. Several researchers have proposed that the Merensky Reef marks a regional unconformity that formed when preexisting semicrystalline cumulates (*i.e.,* resident cumulates) interacted with relatively primitive melt that replenished the overlying melt column [4,5]. This replenishment event is believed to have thermally- and (or) chemically-eroded the resident cumulates, leading to the development of the Merensky Reef stratigraphy and its world-class platinum-group element mineralization.

This study represents a detailed investigation of the Merensky Reef footwall at the Rustenburg Platinum Mine in the western lobe of the Bushveld Complex. At this location, the Merensky Reef is a single layer of coarse-grained orthopyroxenite that is bracketed by mm-scale chromitite seams. These units are underlain by a cm-scale anorthosite that in-turn is underlain by leuconorite. We have employed electron probe microanalysis and electron back-scatter diffraction to characterize changes in the footwall rocks with proximity to the reef and thermodynamic simulations using Magma Chamber Simulator to constrain the effect chamber replenishment may have on different resident cumulates.

The leuconorite hosts normally zoned orthopyroxene crystals with poikilitic overgrowths and cumulus plagioclase crystals that define a non-random fabric consistent with gravitational settling in a quiescent melt. The anorthosite consists of variably zoned cumulus plagioclase crystals that are traversed by sub-vertical domains of sulfides, pyroxenes, and accessory phases. These plagioclase crystals record a non-random fabric that strengthens with proximity to the reef, and it is proposed to have formed by gravitational settling followed by the removal of phases in the plagioclase interstices. The contact between the leuconorite and anorthosite is marked by features that are consistent with trapped liquid shift, such as a relatively increased abundance of intercumulus phases and relatively low orthopyroxene molar Mg/(Mg+Fe)] values. Very fine-grained chromite crystals are concentrated at the margins of orthopyroxene crystals in the leuconorite, but practically vanish in the overlying anorthosite where they occur only sparsely in the sub-vertical domains. The lower chromitite shares a knife-sharp contact with the underlying anorthosite. The lower chromitite comprises both amoeboidal and blocky chromite crystals [6], that display no spatial preference (*i.e.,* host grain, stratigraphic location) nor any statistically significant chemical differences. The key difference

between the two chromite forms is that amoeboidal crystals host greater degrees of internal misorientation as well as abundant polymineralic inclusions.

Thermodynamic simulations show that anorthosite residues, amongst other lithologies, may form as replenishing melts react with noritic cumulates. The initial modelled footwall melts assimilated by the replenishing melt are relatively volatile-rich and become Cr-bearing once resident cumulus orthopyroxene is consumed [7]. It is proposed that chamber replenishment triggered the reconstitution of resident noritic cumulates to anorthosite residues (Fig. 1A-B). The replenishing melt was likely saturated in chromite and sulfide melt, whereby skeletal chromite precipitated close to the melt-cumulate interface. The porosity generated in the footwall facilitated the downward percolation of sulfide melt that in turn helped to displace trapped silicate melts upward to the level of the proto-reef (Fig. 1C-D). The initially relatively volatile-rich footwall melts triggered dissolution-reprecipitation of skeletal to amoeboidal chromite, and the chromitite grew as auxiliary Cr^{3+} and Al^{3+} was liberated from the footwall.

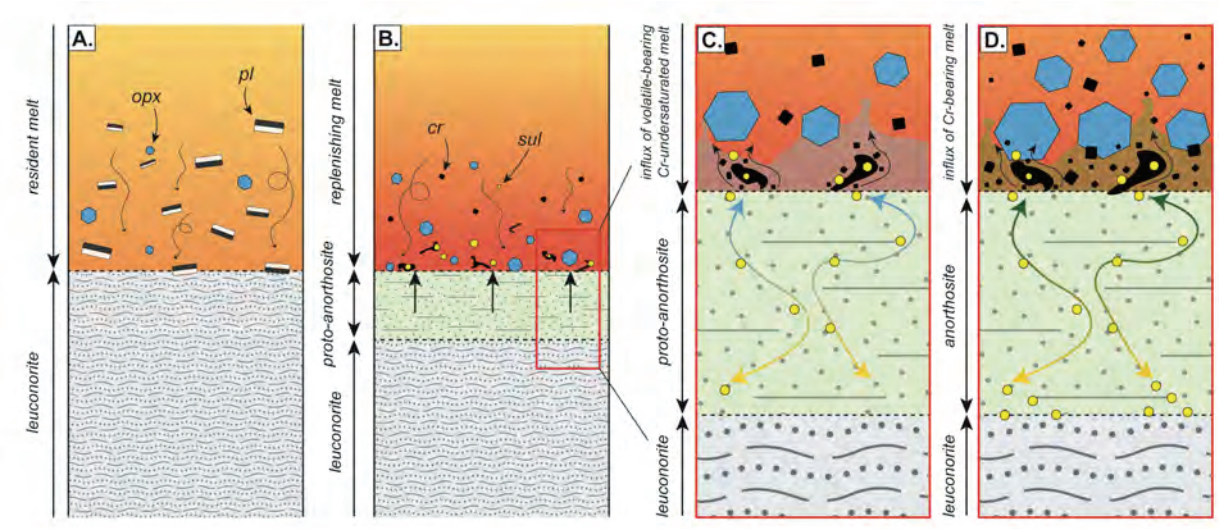


Figure 1. Petrogenetic model for replenishment-driven footwall reconstitution at the Rustenburg Platinum Mine. **A.** Deposition of leuconoritic (orthopyroxene = opx + plagioclase = pl) cumulates by gravitational settling of silicates in a quiescent melt. **B.** Basal influx of relatively primitive melt that entrains blocky chromite (cr) and sulfide (sul) melt. Skeletal chromite crystals form by supercooling close to the base of the replenishing melt and reconstitution of resident leuconoritic cumulates begins. **C.** Footwall melts are initially volatile-bearing and Cr-undersaturated (light blue arrows), triggering dissolution-reprecipitation of skeletal chromitites to form amoeboidal chromites. **D.** The footwall melts become Cr-saturated (green arrows) as orthopyroxene and accessory chromite are consumed. This leads to further chromite precipitation and the formation of the lower chromitite. These footwall melts are displaced upwards by down-going sulfide melts, which may also instigate coarsening of plagioclase and orthopyroxene oikocrysts. Black arrows to the side of diagrams denote the lithology.

References:

[1] Cawthorn RG (1999) S. Afr. J. Geol. 102(3):178-183
[2] Cawthorn RG (2015) In:Layered Intrusions pp. 517-587
[3] Cameron EN (1982) Econ Geol 77:1307-1327
[4] Viring RG and Cowell MW (1999) S. Afr. J. Geol. 102:192-208
[5] Roberts MD et al. (2007) Min Dep 79:169-186
[6] Vukmanovic Z et al. (2013) Contrib Min Pet 165:1031-1050
[7] Scoon RN and Costin G (2018) J. Pet. 59(8):1551-1578

Future research areas to aid in exploration for Ni sulfides

Sproule, R.A.[1]

[1]Rio Tinto Exploration, Salt Lake City, UT, USA

Discovery rates for magmatic nickel sulphide deposits have declined over the last thirty years and particularly over the last ten years. We are not discovering a sufficient number of high-quality low carbon footprint nickel sulphide deposits in a timely manner to meet society's needs.

Exploration is moderately successful at the deposit scale in a fertile intrusion and after initial discovery of sulfides. This is largely determined by the effectiveness of detection of conductive sulphides by EM technologies in massive-dominated NiS deposits, or the generally large footprint (e.g., magnetics, gravity, surface geochemistry) of large disseminated NiS deposits amenable to open pit mining. However, exploration struggles to identify new fertile lithospheric regions, new favourable terranes and potential camps.

We also lack fundamental detailed understandings on the relationship and timing of nickel sulfide deposits to tectonic cycles, and the processes that form, enrich and accumulate sulfides. This is particularly true when we consider the full range of prospective parental magma compositions and host rock lithologies over the complete range of crustal levels. Moreover, both research and exploration activity have also largely focussed on magmatic Ni systems to the relative detriment of other types of important NiS deposits including sediment-hosted (e.g., Enterprise, Zambia) and hydrothermal types (e.g., Jaguar, Brazil).

At present, our knowledge can be improved by developing: (1) an improved understanding of fertile lithospheric regions; (2) other geological environments conducive to forming Tier 1 NiS deposits; (3) detailed 3D nickel sulphide ore deposit models and footprints (geology, geophysics, geochemistry and mineralogy) for mineralized systems from a range of parental magma compositions, crustal depths and a range of tectonic settings.

Exploring the footwall: Sulfide Mineralization in the footwall Granite of the Maturi Deposit, Minnesota.

Steiner, R. A.[1]

[1]Big Rock Exploration, 2505 W Superior Street, Duluth MN 55806. alex@bigrockexploration.com

---

The 1.1 Ga Keweenawan large igneous province generated voluminous magmatism resulting in the eruption of extensive flood basalts and the emplacement of sub-volcanic intrusions now exposed along the flanks of Lake Superior [1]. In northeastern Minnesota, two intrusive sequences of the Layered Series, the Partridge River Intrusion (PRI) and South Kawishiwi Intrusion (SKI), are known to host significant Cu-Ni-PGE sulfide mineralization [1].

The Maturi Cu-Ni-PGE deposit is located in the northern part of the SKI where the footwall is composed of granitic rocks of the Giants Range Batholith (GRB). The majority of Cu-Ni-PGE-enriched sulfides are disseminated throughout a 50-150m-thick basal mineralized zone (BMZ), though locally occur as massive to semi-massive sulfide occurrences along the basal contact (Figure 1). The mineralized rocks of the BMZ were emplaced in a series of three crystal-laden troctolitic pulses or stages that are divided on the basis of sulfide metal tenor, whole rock composition, and textural variations detailed in Peterson [2] (Figure 1). The first pulse, Stage 1, is sulfide poor and begins to delaminate the overlying anorthosite rocks from the footwall. Stage 2 contains abundant country rock xenoliths and more sulfide droplets that are carried within the crystal slurry and those sulfides are higher Cu, Ni, and PGE tenors than the prior Stage 1. Stage 3 is yet more enriched in metals, with the highest metal tenors found there and is also the most mafic pulse, often containing mela-troctolite or sub-dunite horizons. Stages 2 and 3 are broadly emplaced above prior pulses, but locally erode down into the previous pulse in areas of channelized magma flow and may erode down to the granite below.

Enigmatically, the underlying granite commonly hosts magmatic sulfide mineralization. That mineralization may occur as massive Ni-rich sulfide at the intrusion contact or extend as deep as 100 meters below the basal contact as Cu-rich sulfides (Figure 1). Sulfur isotope data show that the sulfide in the mineralized granite originated from the same source as that in the overlying troctolite [3, 4]. Here we present a mechanism by which melting and density-driven displacement drives magmatic Cu-Ni-PGE sulfide mineralization into the footwall granite of the Maturi deposit.

Three of the drill cores were selected from the Maturi deposit that represent all three stages in contact with the underlying footwall granite [2]. Core logging and subsequent petrographic observations show that the granite reached pyroxene hornfels grade metamorphism and underwent partial melting due to thermal input from the overlying intrusion (Figure 2). Abundant leucosomes and sieve textured feldspars with trapped silicate melt record pervasive melting in the GRB. Leucosome patches and feldspar sieves have been observed to contain massive to semi-massive sulfide suggesting a relationship between location of partial melts and sulfide liquid, perhaps physical displacement of the former by the latter (Figure 3).

Mass-balance equations using the isocon method of Grant [5] were used to explore the geochemical parameters to provide insight into the relationship of partial melts and sulfide liquid. When elements that partition into pyroxene (Cr, Mg, Mn) are treated as restite (not removed or added to the original

lithology) it becomes clear that an exchange of sulfide for partial melt is occurring (Figure 4). Elements that would partition into the silicate liquid during melting (REE, LIL, K, Ba) become depleted relative to the restite while components of the sulfide (S, Ni, Cu) become enriched. Samples of the footwall with the strongest sulfide mineralization show the strongest depletion of partial melt elements and the strongest enrichment of sulfide liquid components. The face that sulfide liquid and partial melts occupy the same textural space within the rock (e.g., leucosome patches between restite phases and sieve texture in plagioclase) and the geochemical signature showing the removal of partial melt components and addition of sulfide liquid components leads to the conclusion that mineralization in the footwall of the Maturi deposit is caused by the displacement of partial melt for a denser sulfide liquid. Such a process should not only result in mineralization of the footwall but also contamination of the overlying intrusion by partial melts. White [6] identified geochemical markers for contamination of the overlying BMZ by the footwall rocks, which became more intense in proximity to the footwall contact.

This study finds abundant as networks and pods of partial melts throughout the GRB. Therefore, it is reasonable to assume that the amount of liquid displacement that can occur is limited by the amount of sulfide liquid available to penetrate the footwall. While there is large reservoir of sulfide present as the disseminated sulfides in the intrusions, that amount of that sulfide that may interact with the footwall interface is unclear. However, contamination of the silicate magma in the vicinity of the footwall rocks would reduce the sulfur carrying capacity in a magma that is already sulfur saturated thus providing an additional sulfide liquid reservoir to displace partial melts in the GRB. The formation of such a reservoir is evidenced by Ni-rich massive sulfide occurrences at the footwall contact intercepted during drilling. It is notable that the majority of the massive sulfide occurrences are found where the footwall is in contact with Stage 3; this being the latest mineralizing pulse would therefore introduce the greatest heat budget to the footwall rocks (Figure 1). It is below these locations that partial melting and footwall mineralization is most intense.

By understanding both the emplacement sequence and mechanism of mineralized intrusions it is possible to constrain the focusing of heat into the country rock. Such constraints provide insight into targeting basal accumulations of sulfide within intrusions as well as unconventional mineralization hosted within the country rocks.

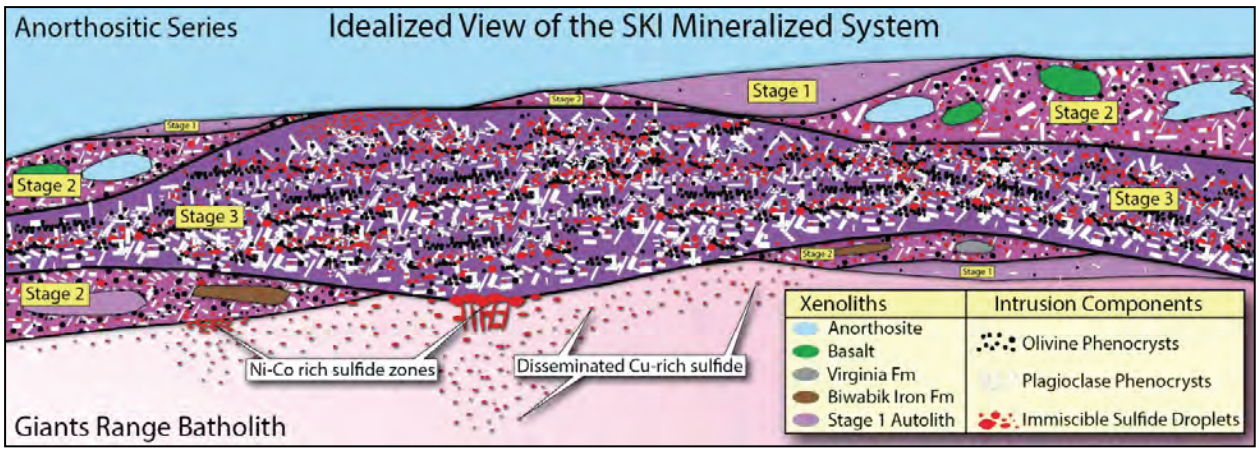


Figure 1 – cartoon cross-section of the basal mineralized zone at Maturi highlighting areas on footwall mineralization below stages 2 and 3.

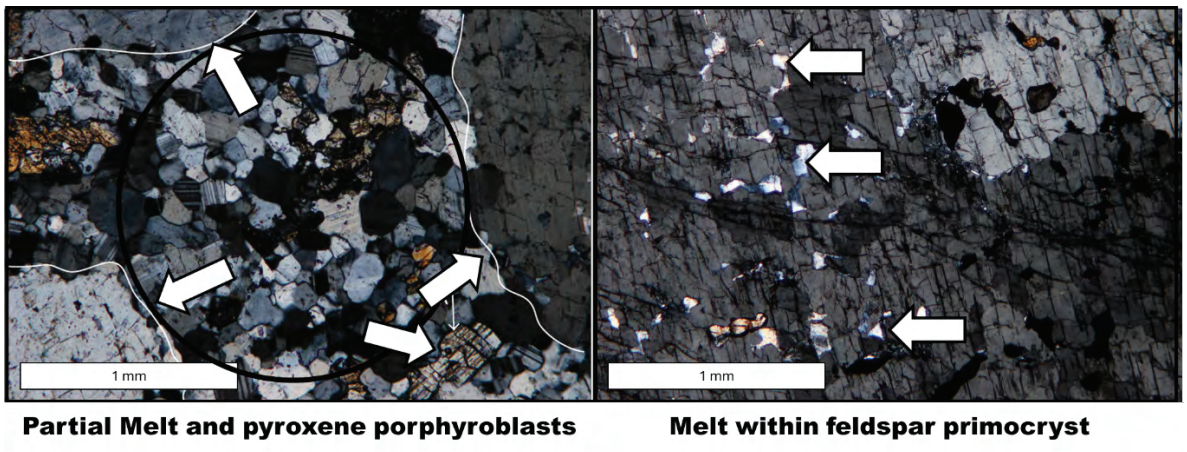


Figure 2 – partial melt pocket or leucosome surrounding remnant feldspar grains with orthopyroxene found in the melt (left). Melt pockets inside of feldspar grain resulting in sieve texture.

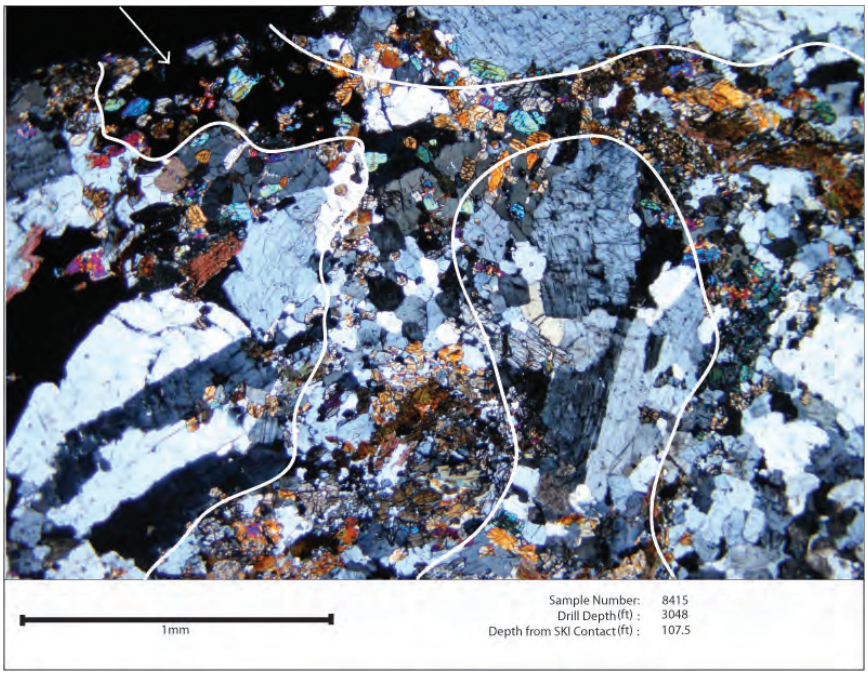


Figure 3 – net-textured partial melt + pyroxene surrounding remnant feldspar and pyroxene. Arrow indicates sulfide that surrounds pyroxene in the same manner as partial melts elsewhere in the section.

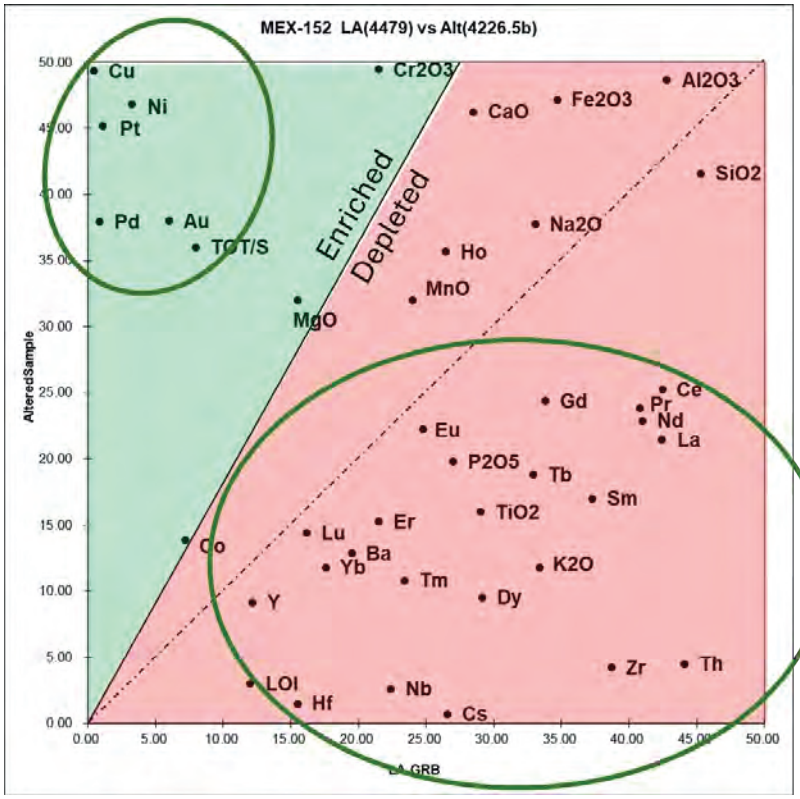


Figure 4 – example isocon plot where the isocon is a best-fit line for MgO, MnO, and Cr_2O_3. The green field indicates components that are enriched relative to the isocon while the red field indicates depletion.

References:

[1] Miller, J.D. Jr. et al (2002) Minnesota Geological Survey Report of Investigations 58
[2] Peterson D.M. (2012), Duluth Metals ltd Presentation to Twin Metals Minnesota LLC
[3] Ripley, E. M. and Alawi, J. A. (1986) Canadian Mineralogist 24:347-368
[4] Molnar, F. et al., (2009) Geological Society of America Abstract
[5] Grant, J. A. (1986) Economic Geology 81:1976-1982
[6] White, C. R. (2010) MS Thesis University of Minnesota Duluth

The Anatomy of a Cu-Ni-Co-PGE Mineralized Mafic Magmatic System: The South Kawishiwi Intrusion of the Duluth Complex, Northeastern Minnesota

Sweet, G.S.[1] and Peterson, D.M.[2]

[1,2] Big Rock Exploration, 2505 West Superior Street, Duluth MN, 55806, gabe@bigrockexploration.com

---

In 1977, the Minnesota Department of Natural Resources published the first district-scale grade-tonnage estimate [1] of Cu-Ni and TiO_2 along the western margin of the Duluth Complex. These estimates, which utilized 324 of the 903 holes drilled through 1976 (285,902 meters), included 4.4 billion tons at 0.66% Cu and 0.2% Ni as well as 220 million tons at >10% TiO_2 and brought to light the potential world-class scale of the Duluth Complex mafic magmatic system. Since the 1977 grade-tonnage estimate, approximately 1,993 new exploration holes totaling over 802,360 meters have been drilled in the Duluth Complex area by a number of companies and the State of Minnesota.

The physical formation processes of sulfide-bearing mafic intrusions remains one of the most important concepts for geologists engaged in exploring mafic magmatic systems for ore deposits. It is critically important to understand that the delivery of sulfide-bearing and potentially crystal-laden magmas into a growing intrusion is an iterative process confined to the spatial geometry of the system. The delivered magma will change with time (intrusion rate, crystallinity, xenolith content, sulfide content & tenor) and early batches of crystallizing magma are commonly cut and eroded by subsequent magmas (with their own unique intrusion rate, crystallinity, sulfide content & tenor). This work describes a new synthesis of decades of detailed mapping (>30,000 outcrops mapped), exploration and definition drilling (787,908 meters of core in 1899 holes), geochemistry (101,882 drill core and 8,267 surface sample analyses), geophysical surveying, and modeling by the authors and others in the South Kawishiwi Intrusion (SKI) and its Nickel Lake Macrodike (NLM) feeder dike. The outcomes of this new synthesis can perhaps be used as a proxy from which geologists can explore other mafic magmatic systems across the globe.

The SKI is a shallow dipping (~24º east-southeast) sill-like troctolitic intrusion exposed in a 10- x 32-kilometer arcuate band along the northwestern margin of the Duluth Complex. It extends from the edge of the Mesaba deposit (which is within the adjacent Partridge River and Bathtub intrusions) on the southwest, to the Spruce Road deposit on the northeast (Fig. 1). The SKI initially intruded between a hangingwall of the Duluth Complex Anorthositic Series rocks and a footwall composed of Paleoproterozoic sedimentary rocks, i.e., the Virginia Formation (VF) and Biwabik Iron Formation (BIF) in the southwest, and exclusively granitoid rocks of the Archean Giants Range Batholith in the northeast. The local presence of xenoliths of the BIF and VF as inclusions within the northern SKI and the NLM are interpreted as far-traveled country-rock blocks and not, as Severson et al. [2] interpreted, Paleoproterozoic sedimentary units assimilated in-situ from the immediate footwall during emplacement of the SKI.

The basal stratigraphic section of the SKI was first described in great detail by Severson [3] and culminated with the SKI igneous stratigraphy being subdivided into 17 different units. In 2008, geologists from Duluth Metals Limited came to the realization that the contact-type mineralization at the Maturi deposit formed from initial basaltic composition SKI magmas that intruded as sulfide-bearing, crystal-laden (plagioclase & olivine), magmatic slurries. Based on this interpretation, the company reinterpreted the sulfide-bearing basal zone of the SKI at the Maturi deposit into the Basal Mineralized Zone, or BMZ. This new interpretation was based on the geometry of the system (sill-like sub-horizontal intrusion) and the inherent crystallinity of the SKI magmas. The channelized flow of these phenocryst-rich magmas led to crystal sorting and melting of the footwall granitic rocks to create the heterogeneous lithologies and textures of the BMZ. Years of detailed geological mapping, integrated with geological logging of all available drill holes, and a comprehensive assembly and interpretation of all geochemical data has led to a simplified overall igneous stratigraphy of the

intrusion. This stratigraphy has been subdivided into five basic units, including the Upper SKI, the SKI Break, the Middle SKI, the Main AGT, and the BMZ (Figure 2).

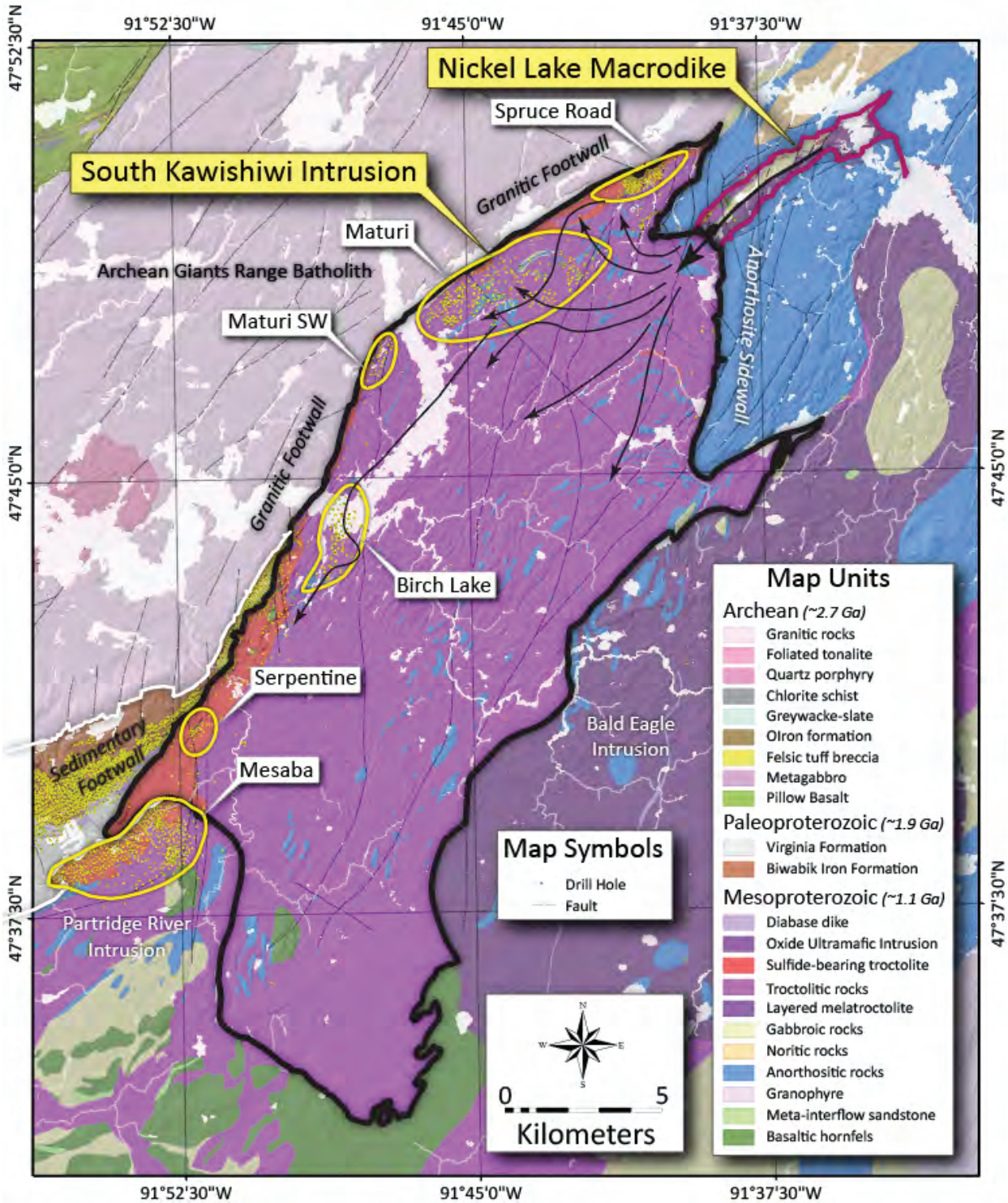


Figure 1. Bedrock geologic map of the South Kawishiwi Intrusion and surrounding terranes. Yellow outlines define the approximate boundaries of compliant NI 43-101 resource estimates of the labeled Cu-Ni-Co-PGE deposits.

In 2012, and after much additional drilling, the geology of the Maturi deposit BMZ was reevaluated once again by the geologic staff of Duluth Metals Limited, Twin Metals Minnesota, and geologists from the consulting firm AMEC. The reanalysis utilized a significant volume of new, high-quality geochemical and geological data to complete an updated mineral resource classification by AMEC. Mineralization in both the BMZ and footwall at the Maturi deposit area were reclassified based on patterns in the physical distribution of mineralization as projected on down-hole plots. Sulfide mineralization at Maturi is characterized by several distinct patterns, including A) very low grade,

fine-grained intervals showing low variability (Stage 1) that probably represent initial chilled magmas, B) moderate Cu-Ni and low PGE grade, xenolith-bearing (BIF, VF, basalt & anorthosite), mineralized zones showing low variability (Stage 2), and C) clean, higher grade, (Cu-Ni and PGE), xenolith-poor mineralized troctolite zones with higher variability and commonly bounded by low grade selvages (Stage 3).

Significantly, most of the contacts between different mineralized intervals are typically quite abrupt. A single hole might contain one or several distinct mineralized intervals within the BMZ, including higher grade intervals with the highest-grade intervals occurring at the top, middle, or bottom of the section. Based on these criteria, four intrusive subunits, characterized by common grade profiles, were defined in the BMZ. In addition, two distinct suites of mineralization were identified in the footwall rocks, including Ni-Co enriched semi-massive to massive sulfide zones and disseminated Cu-PGE enriched zones deep in the footwall granitoids. All the newly classified zones of the BMZ at the Maturi Deposit are shown stratigraphically in Figure 3 and diagrammatically in Figure 4.

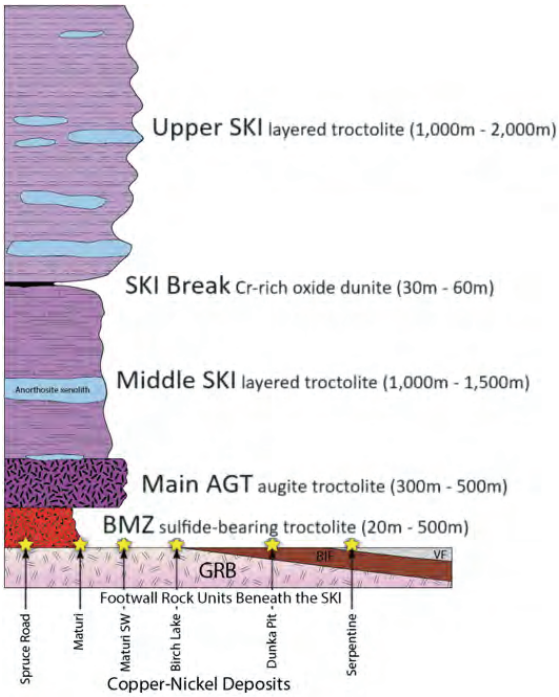


Figure 2. Simplified igneous stratigraphy of

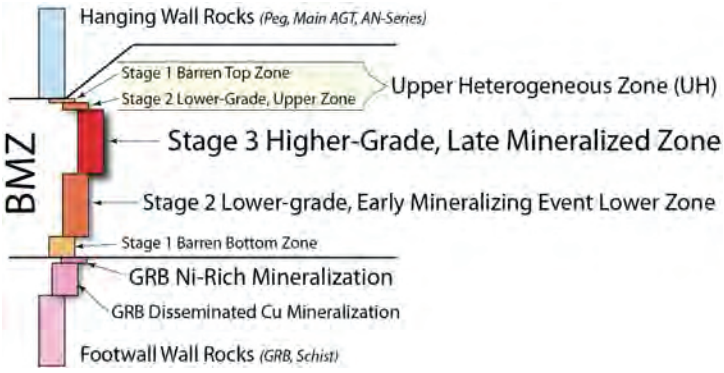


Figure 3. Revised igneous stratigraphy of the BMZ and adjacent rocks within the Maturi deposit.

The classifications derived from this exercise were validated by multivariate statistical analysis of geochemical data, including principal component analysis and factor analysis. This investigation revealed distinct geochemical fingerprints of mineralization within the BMZ as well as several possible subdivisions of the BMZ based on both the physical distribution patterns of mineralization and the geochemistry of the host rocks. The Maturi subunits defined and validated were determined to occur in a consistent stratigraphic order and are correlative across the deposit.

The current lithostratigraphic model for Maturi effectively discriminates between higher- and lower-grade SKI mineralization and provides a realistic geological model for mineralization throughout the intrusion. The new data allowed correlation of units from hole-to-hole and section-to-section

resulting in a very robust geologic model upon which Twin Metals Minnesota is building preliminary mine plans.

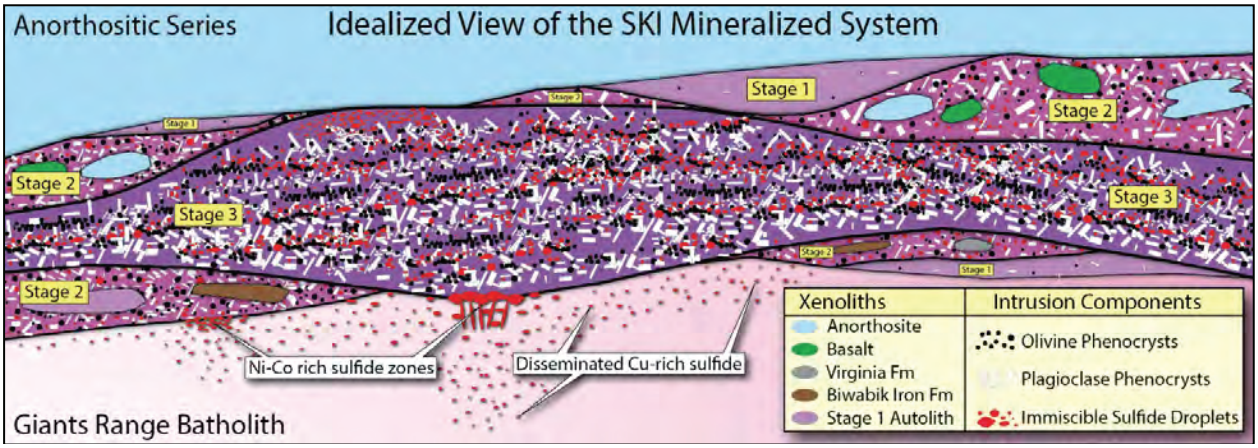


Figure 4. Detailed idealized view of the BMZ intrusive stages at the Maturi Cu-Ni-PGE deposit.

A fundamental aspect of the ever-developing ore deposit model of the SKI is an understanding of the initial conditions of the magmatic system – its crystallinity, sulfur capacity, geochemistry, and geometry – and how the sulfur saturated SKI magma lived, worked, and died. Such understanding includes the realization that the magma was a crystal-liquid (silicate and sulfide liquids) slurry and the identification of magma channel ways and sub-channels and their associated thermal anomalies. In addition, the SKI magmas locally melted the footwall granitoid rocks, and the addition of SiO_2 into the sulfide-bearing troctolitic melts of the SKI induced additional sulfide immiscibility, stripping the melts of dissolved Ni and Co and forming high-grade massive sulfide ores locally at the basal contact and within the highly metamorphosed footwall Archean granitoids. In the end, hard work and intellectual geologic thought has been used to identify and understand one of the world's largest resources of Cu-Ni-PGEs (Table 1).

Table 1. Grade-Tonnage tabulation for deposits of the SKI.

DEPOSIT	INTRUSION	YEAR	CATEGORY	TONNES	CU %	NI %	CO %	PT ppm	PD ppm	AU ppm	SKI STAGE	TBM %	CU/NI	TPM ppm	PD/PT
Spruce Road	SKI	2013	Inferred	434,448,676	0.430	0.160	0.010	0.100	0.200	0.050	2	0.600	2.688	0.350	2.000
Maturi	SKI	2013	Measured	267,891,654	0.630	0.200	0.010	0.148	0.345	0.084	2 << 3	0.840	3.150	0.577	2.331
Maturi	SKI	2013	Indicated	702,342,426	0.580	0.190	0.010	0.160	0.360	0.071	2 < 3	0.780	3.053	0.591	2.250
Maturi	SKI	2013	Inferred	509,837,824	0.510	0.170	0.010	0.138	0.317	0.047	2 & 3	0.690	3.000	0.502	2.297
Maturi	SKI	2013	North Target	394,625,362	0.510	0.175	0.010	0.120	0.290	0.070	2 & 3	0.695	2.914	0.480	2.417
Maturi	SKI	2013	South Target	453,592,370	0.520	0.160	0.010	0.180	0.380	0.090	2 & 3	0.690	3.250	0.650	2.111
Maturi	SKI	2013	West Target	889,041,046	0.465	0.165	0.010	0.120	0.290	0.070	2 > 3	0.640	2.818	0.480	2.417
Maturi SW	SKI	2013	Indicated	93,440,028	0.480	0.170	0.012	0.080	0.185	0.048	2 >> 3	0.662	2.824	0.313	2.313
Maturi SW	SKI	2013	Inferred	29,029,912	0.430	0.150	0.012	0.065	0.157	0.041	2 >> 3	0.592	2.867	0.263	2.415
Birch Lake	SKI	2013	Indicated	90,446,319	0.520	0.160	0.010	0.233	0.511	0.114	1 < < 3	0.690	3.250	0.858	2.193
Birch Lake	SKI	2013	Inferred	216,998,590	0.460	0.150	0.010	0.180	0.370	0.087	1 < < 3	0.620	3.067	0.637	2.056
Birch Lake	SKI	2013	Target	302,999,703	0.410	0.135	0.010	0.135	0.275	0.065	1 < 3	0.555	3.037	0.475	2.037
Serpentine	SKI	2010	Inferred	445,524,000	0.260	0.090	0.017	0.026	0.064	0.024	1 & 2	0.367	2.889	0.114	2.462
TBM = Cu+Ni+Co; TPM = Pt+Pd+AU			Total Wt. Ave.	4,830,217,911	0.480	0.161	0.011	0.129	0.290	0.065		0.652	2.972	0.484	2.243

References

[1] Listerud W and Meineke D (1977) MNDNR Report 93: 1-74
[2] Severson M et al. (2002) MGS RI 58: 164-200
[3] Severson, M (1994) NRRI TR 93/94: 1-210

Multi-thermochronological records of cooling, denudation and preservation of ancient ultrabasic magmatic ore deposits: An example from the Neoproterozoic Jinchuan giant magmatic Cu-Ni sulfide deposit

Ni Tao[1,2]*, Jiangang Jiao[1], Jun Duan[1], Haiqing Yan[1], Ruohong Jiao[3], Hanjie Wen[1]

[1]Department of Geology, Northwest University, Xi'an, China, ni.tao@chd.edu.cn
[2]School of Earth Science and Resources, Chang'an University, Xi'an, China
[3]School of Earth and Ocean Sciences, University of Victoria, Victoria, Canada

---

The post-mineralization denudation history and preservation of ore deposits have significant scientific and practical implications for ore deposit preservation condition, ore-forming potential evaluation, and deep ore prospecting. Ancient Cu-Ni sulfide ore deposits are characterized by complex magmatic evolution and a long-term geological history. How to quantify their denudation degree and emplacement depth is currently the focus and challenge of ore deposit preservation research. This study strategically chooses the Jinchuan giant magmatic Cu-Ni sulfide deposit as an example, with the Neoproterozoic ore-bearing plagioclase lherzolite as the main target, combined with its Paleoproterozoic metamorphic country rocks and early Paleozoic diorite veins for comparison. Multi-thermochronological analyses applied include apatite and zircon (U-Th)/He dating, apatite fission-track analysis, plagioclase and hornblende 40Ar/39Ar dating. The aims are to trace the thermal history of the ore-bearing intrusion, calculate its denudation thickness by integrating regional geological records, set up inversion models for verifying the calculated denudation thickness as well as determining emplacement depth of the ore-bearing intrusion. On this basis, by judging the relationship between the denudation thickness and the emplacement depth of the ore-bearing intrusion, this study clarifies the preservation degree of Jinchuan Cu-Ni sulfide deposit. The results may provide a new thermochronological paradigm for studying the preservation conditions and evaluating deep ore exploration potential of (ancient) ultrabasic Cu-Ni sulfide magmatic ore deposits.

Compositional variability in olivine: New data on the occurrences of Ni and Co as guides to mineral prospectivity

Thakurta, J.[1], Wagner, Z.[1], Nagurney, A.[2], and Schaef, H.T. [2]

[1]Natural Resources Research Institute, University of Minnesota, 5013 Miller Trunk Highway, Hermantown, MN 55811, USA
[2]Pacific Northwest National Laboratory, 902 Battelle Boulevard, P.O. Box 999, Richland, WA 99352 USA

Concentrations of trace constituents in olivine have been measured from a wide variety of mafic-ultramafic intrusive and volcanic igneous rocks in different tectonic settings in North America. Samples include rocks from different locations of the 1.1 Ga old Midcontinent Rift System (MRS), such as the layered Duluth gabbroic Complex in Minnesota, and the peridotitic intrusions at Eagle in Michigan and Tamarack in Minnesota. The Cretaceous to Jurassic Dunite-peridotite rocks from Red Mountain Ultramafic Complex at the Kenai Chrome mine, the Eklutna ultramafic rocks, and the Alaskan-type ultramafic complex at Duke Island in Alaska represent small intrusive bodies in convergent tectonic settings. Alkali basalts with olivine phenocrysts from the Springville volcanic suite in Arizona constitute Pleistocene volcanic rocks. While the content of Ni is inversely correlated with the presence of sulfide minerals in the assemblages, a larger and more significant variation has been observed with respect to the origin, modes of occurrence and tectonic settings of the rocks in this study.

Considerable variations are observed in different intrusions of the Duluth Complex in terms of the nature of the host rock: whether olivine gabbro or troctolite. Ni in the olivine gabbro ranges between 1800 and 2000 ppm while in the representative troctolite units it ranges between 700 to 900 ppm. Very high contents of Ni in olivine, ranging from 2000 to 2700 ppm are seen in small peridotitic intrusive bodies at the MRS such as feldspathic peridotite in Eagle, the Bowl and Fine Grained Olivine (FGO) intrusions of Tamarack. The dunite-peridotite at Kenai and Eklutna show comparable high values but values in the olivine clinopyroxenite unit of the Alaskan-type Complex at Duke Island are less than 800 ppm. A substantial range in Ni-content of olivine from 500 to almost 2500 ppm is observed in the olivine basalt at the Springville Volcanic Suite where individual phenocrysts of olivine show growth rims of changing Ni-content from core to rim (Figure 1). The Co-content of olivine in the olivine gabbro and troctolite units of the Duluth complex range from 300 to 400 ppm and 400 to 600 ppm respectively. Samples from Eagle, Tamarack as well as Duke Island cluster between 300 and 400 ppm. However, the dunite-peridotite at Kenai and Eklutna show values less than 250 ppm.

From the new dataset and data available from previous studies [1, 2 and 3] it is evident, that with other factors being similar, Ni shows a positive correlation with the MgO-content while a negative correlation with Co is evident from the new data. Starting with the composition of magma from source rocks, changing fO_2 conditions and H_2O-content, leading to factors such as liquid evolution by fractional crystallization, assimilation, and re-equilibration of magma with preexisting Ni- and Co-rich rocks, a continuous spectrum of changing concentrations of trace metals in olivine can be envisioned from the available dataset.

Such trace metal concentrations in olivine are important not only as indicators of Ni-rich sulfide mineralized zones in the associated rocks, but also as tools to evaluate the possibility of extraction of such critical metals from the ongoing development of new methods of metal-extraction from non-conventional sources such as olivine.

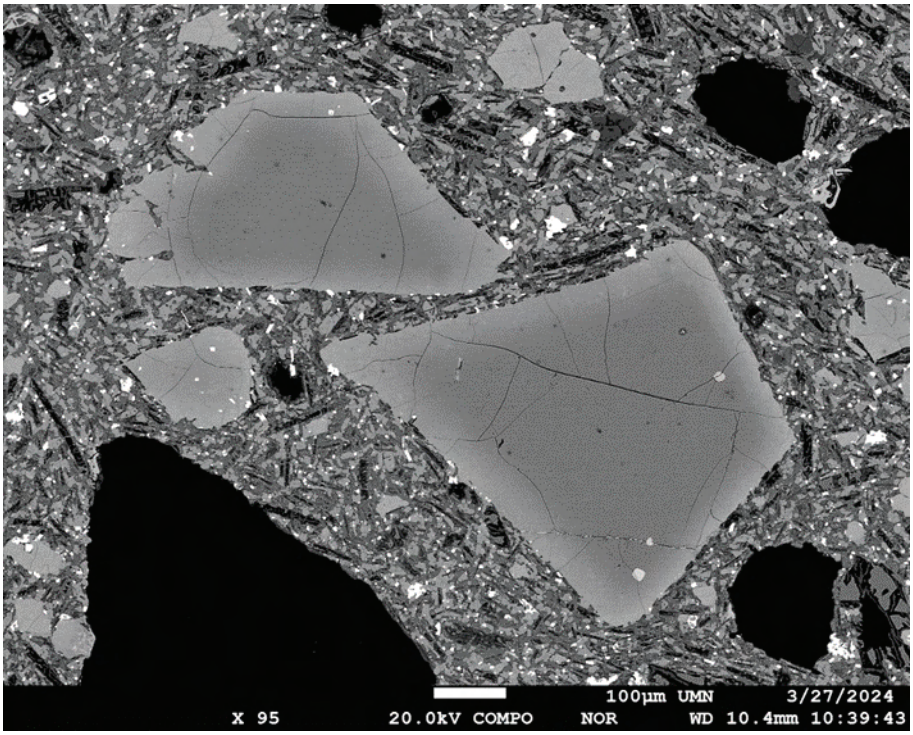


Figure 1: Concentrically zoned olivine phenocrysts in an olivine basalt from the Springville Volcanic Field in Arizona. Ni-Co concentrations change along the zones.

References:

[1] Barnes, J.B. (2023) Am Min 108:1-17

[2] Li, C. and Ripley, E.M. (2010) Chem Geo 275: 99-104

[3] Marek, L., Arevalo, R.D., Puchtel, I.S., Fiorentini, M.L. and Nisbet, E.G. (2019) Am Min 104: 1143-1155

The effects of diagenetic and metamorphic processes on the sulphur liberation from the Virginia Formation black shale during magmatic assimilation by the Duluth Complex, Minnesota, USA

Virtanen V.J.[1,2], Heinonen J.S.[2,3], Märki L. [4], Galvez M.E. [5] and Molnár F.[6]

[1]Institute des Sciences de la Terre d'Orléans (ISTO), CNRS-Université d'Orléans-BRGM, France
[2]Department of Geosciences and Geography, University of Helsinki, Helsinki, Finland
[3]Geology and Mineralogy, Faculty of Science and Engineering, Åbo Akademi University, Turku, Finland
[4]METAS, Federal Institute of Metrology, Bern, Switzerland
[5]Department of Earth Sciences, ETH Zürich, Zürich, Switzerland
[6]Department of Mineralogy, Institute of Geography and Earth Sciences, Eötvös Loránd University, Budapest, Hungary

---

The Duluth Complex, Minnesota, USA, contains large low-grade disseminated Cu-Ni(-PGE) sulphide resources hosted in troctolites and smaller massive sulphide lenses hosted in norites [1]. Several lines of evidence, including sulphur isotopes, suggest that both deposit types formed by assimilation of sulphur from the Virginia Formation black shale. In the Virginia Formation, sulphur is mainly hosted in micron-scale disseminated pyrite with the exception of the peculiar carbon and sulphur-rich Bedded Pyrrhotite Unit that is characterized by pyrrhotite laminae with mm-scale thickness [1,2]. The Bedded Pyrrhotite Unit has been identified as an important source of sulphur especially to the norite-hosted massive sulphide occurrences [1,2]. However, the processes that caused the carbon and sulphur enrichment in the Bedded Pyrrhotite Unit have not been studied in detail.

We used optical and scanning electron microscopy as well as Raman spectroscopy to characterize the normal Virginia Formation black shale and the Bedded Pyrrhotite Unit with emphasis on the carbonaceous materials (CM) and sulphides. Regionally metamorphosed and contact-metamorphosed samples were studied from both units. Whole-rock chemical data was acquired to measure H_2O, C_{org}, and S in the samples. In the normal Virginia Formation, CM is present as uniformly dispersed submicron-scale flakes as typical for buried organic material (Fig. 1a). Raman spectroscopy revealed several defect bands (D1 to D4, see Fig. 1) meaning that the CM is structurally aromatic but turbostratic (i.e., aromatic sheets as in graphite but not in highly organized stacked-sheet structure). Structural ordering of residual CM is a suitable geothermometer as it changes systematically with temperature and it is not subject to retrograde resetting [3,4]. The CM geothermometer of Lahfid et al. [4] indicates that the Virginia Formation reached peak temperature of 300–340 ± 50 °C during regional metamorphism prior to the formation of the Duluth Complex.

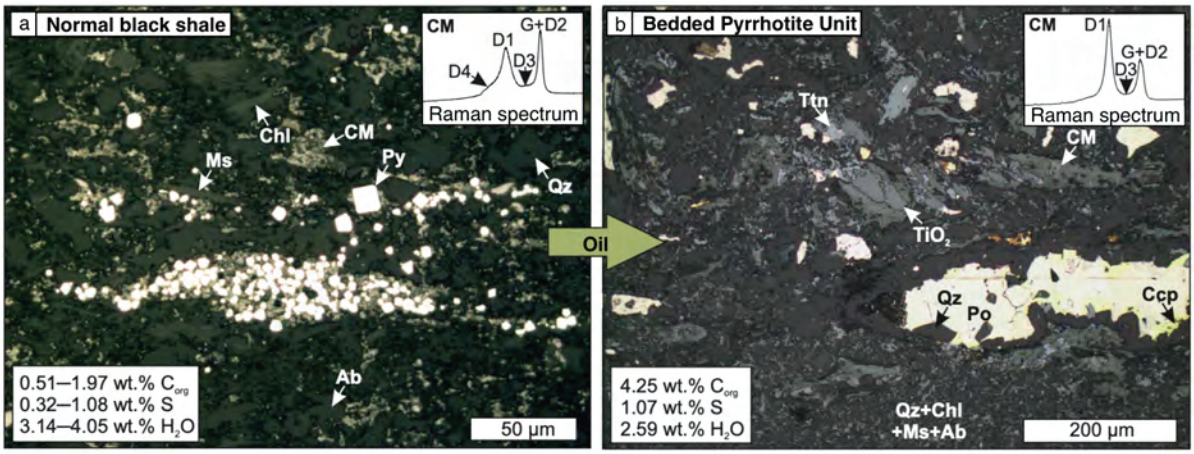


Figure 12. Reflected-light microphotographs of a) the normal black shale and b) the Bedded Pyrrhotite Unit in the regionally metamorphosed Virginia Formation. Typical Raman spectra of the carbonaceous materials (CM) with structure-related bands (G, D1 to D4) indicated as well as the whole-rock C_{org}, sulphur (S), and H_2O

contents are shown. The arrow indicates that CM in b) represents remnants of accumulated oil. Abbreviations: Ab = albite, Ccp = chalcopyrite, Chl = chlorite, Ms = muscovite, Po = pyrrhotite, Py = pyrite, Qz = Quartz.

The regionally metamorphosed Bedded Pyrrhotite Unit contains microscale fracture zones enriched in CM and sulphur (Fig. 1b). These zones are characterized by irregularly shaped quartz and sulphide grains that are rotated relative to the bedding (Fig. 1b). Carbonaceous material is found as pore space fillings (Fig. 1b) and as grain coatings suggesting that it represents oil residuals. Raman spectroscopy confirms that the CM in the Bedded Pyrrhotite Unit is structurally different from the CM in the normal black shale (Fig. 1b). Due to the migratory origin of the CM, we cannot reliably apply the geothermometer to the Bedded Pyrrhotite Unit. We suggest that the pore space, which facilitated oil infiltration, formed in the microfracture zones due to dissolution of soluble precursor sedimentary clasts, which are now replaced by quartz and sulphides (Fig. 1b). Pyrrhotite precipitation in diagenetic conditions is kinetically limited, hence the original sulphide in the Bedded Pyrrhotite Unit was probably pyrite (or some typical metastable diagenetic sulphide like greigite). We suggest that the original sulphide was converted to pyrrhotite during low-temperature hydropyrolysis of the CM during regional metamorphism.

Whole-rock chemical data shows that the pyrite-bearing normal black shale experienced loss of H_2O, C_{org}, and sulphur due to muscovite and chlorite breakdown as well as pyrite conversion to pyrrhotite caused by the Duluth Complex. The contact-metamorphosed Bedded Pyrrhotite Unit experienced the same metamorphic conditions but shows no systematic depletion of volatiles. In fact, the contact-metamorphosed Bedded Pyrrhotite Unit is the most C_{org} and sulphur rich part of the Virginia Formation. We suggest that sulphur was conserved through contact metamorphism because of the stability of pyrrhotite during devolatilization as shown in previous experiments [5]. This means that extensive partial melting of the Bedded Pyrrhotite Unit was required to liberate sulphur to the Duluth Complex magma. Consequently, the sulphide occurrences in association with Bedded Pyrrhotite Unit xenoliths are generally in the norites, which show more signs of assimilation Unit compared to the troctolites [1,2]. We also observed that prograde cordierite in the contact-metamorphosed Bedded Pyrrhotite Unit (Fig. 2a) is consistently replaced by biotite and muscovite at the vicinity of the pyrrhotite laminae (Fig. 2b). This indicates retrograde hydration event introduced H_2O and possibly C_{org} and sulphur to the contact-metamorphosed normal black shale. Our findings highlight some key diagenetic and regional metamorphic processes that are important for magmatic ore genesis as they affect the CM and sulphur budget in black shales as well as the reactions that liberate sulphur upon magmatic assimilation.

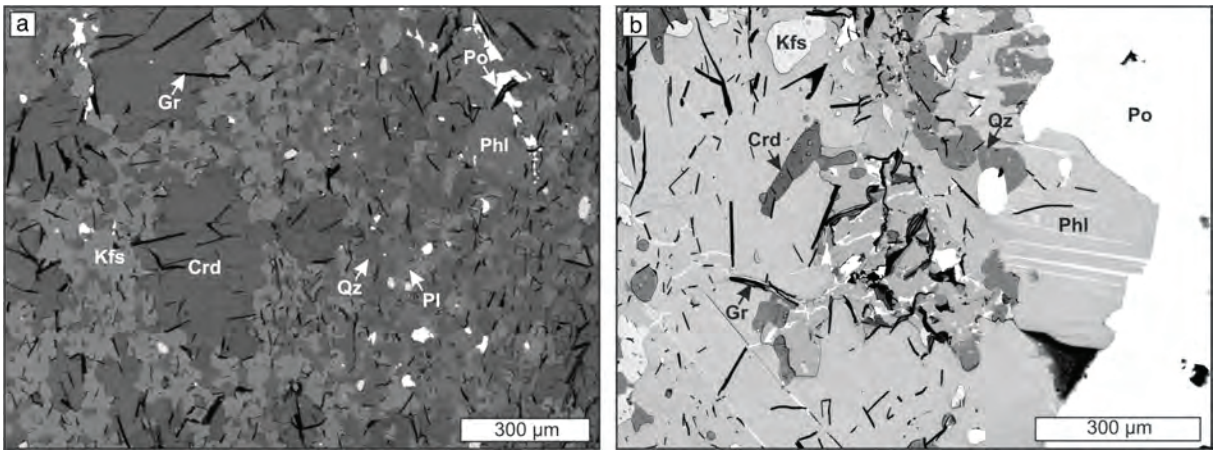


Figure 13. Back-scattered electron images showing a) the prograde mineral assemblage and b) the retrograde mineral assemblage of the contact-metamorphosed Bedded Pyrrhotite Unit. In a) prograde cordierite (crd) is surrounded by K-feldspar (Kfs), whereas in b) small anhedral cordierite is surrounded by retrograde phlogopite (Phl). Abbreviations: Gr = graphite, Pl = plagioclase, Po = pyrrhotite, Qz = quartz.

References:

[1] Thériault R and Barnes S-J (1998) Can Min 36:869-886

[2] Samalens N et al. (2017) Ore Geol Rev 81:173-187

[3] Beyssac O et al. (2002) J Metamorphic Geol 20:859-871

[4] Lahfid A et al. (2010) Terra Nova 22:354-360

[5] Virtanen V et al. (2021) Nat Commun 12:1-12

Mantle-to-crust scale chemical fractionation and sulphide saturation of the Paleoproterozoic komatiites of the Central Lapland Greenstone Belt, Finland – implications for geochemical exploration

Virtanen V.J.1,[2], Höytiä H.M.A.[2], Iacono-Marziano G.[1], Yang S.[3], Moilanen M.[3] and Törmänen T.[4]

[1]Institut des Sciences de la Terre d'Orléans, UMR 7327, CNRS/Université d'Orléans/BRGM, Orléans, France
[2]Department of Geosciences and Geography, University of Helsinki, Helsinki, Finland
[3]Oulu Mining School, University of Oulu, Oulu, Finland
[4]Geological Survey of Finland, Rovaniemi, Finland

In the Central Lapland Greenstone Belt (CLGB) komatiites are present along a >250 km long SE-NW zone across the northern Finland (Fig. 1). The CLGB komatiites formed at ca. 2.05 Ga mostly as underwater eruptions on a sedimentary basin, which is known to have contained abundant sulphurous black shales and evaporites [1]. This association with sulphurous sedimentary rocks makes the CLGB komatiites promising targets for Cu-Ni-PGE sulphide deposits. Indeed, these sedimentary rocks supplied sulphur to the Kevitsa and Sakatti Cu-Ni(-PGE) sulphide deposits (Fig. 1), which formed during the same magmatic event as the CLGB komatiites [1,2]. To understand the petrogenesis of the CLGB komatiites from their mantle source to their crustal sink, we conducted computational thermodynamic simulations to constrain the chemical fractionation and sulphide saturation state without the effects of assimilation. These simulations guide identification of chemical anomalies related to assimilation and sulphide saturation in the CLGB komatiites and related intrusive rocks.

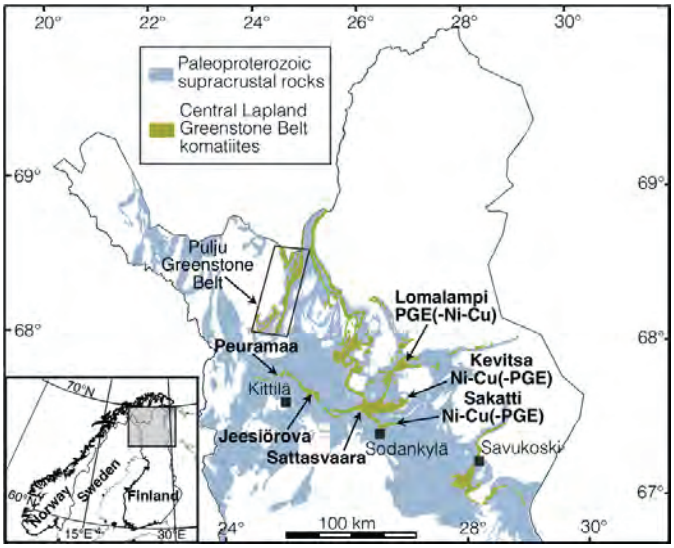


Figure 14. Geological map showing the distribution of the Central Lapland Greenstone Belt komatiites.

We defined the parental melt of the CLGB komatiites using a chilled margin of a komatiitic dyke from Kevitsa, which represents quenched olivine-saturated melt [3]. We added olivine to the chilled margin composition to reversely fractionate it to be in equilibrium with the most primitive olivine (Fo_{92}) in Sakatti [1]. Using this method, we constrained major element oxides, Ni, Cu, and rare earth elements (REE) for the komatiitic (MgO = 20.6 wt.%) parental melt. Assuming adiabatic propagation through the lithosphere, the parental melt should be compositionally identical to the primary mantle melt and allows constraining the mantle melting conditions. We used REEBOX PRO [4] to define Ti and REE contents as well as temperature of the adiabatically melting mantle source. Several mantle sources and mantle potential temperatures were tested. Consistent with the previous studies related to the mantle source of the CLGB komatiites [3,5,6], we found that pyrolite mantle-source with depleted MORB -type REE contents is suitable. The best fit of Ti, REE, and temperature was reached with the mantle potential temperature of 1575 °C and with degree of melting at 15–20 %. The

mantle potential temperature determines that melting starts at ca. 5 GPa and the required degree of melting is reached at ca. 3 GPa (equivalent to ca. 100 km depth). Major element oxide composition of the parental melt (assumed here as identical to the primary mantle melt as noted above) is well compatible with literature data from mantle melting experiments with pyrolite mantle source [7]. We calculated the sulphur content at sulphide saturation (SCSS) for the primary mantle melt using the parental melt composition (major element oxides, Ni, and Cu) and the final pressure-temperature conditions in the mantle using the parameterization of Smythe et al. [8]. This constrains the maximum sulphur content of the primary mantle melt to 1172 ppm. With the typical range of sulphur content for a depleted mantle source of 150–200 ppm [9] and with the degree of mantle melting at 15–20%, the initial sulphur content of the CLGB komatiites is estimated to be 750–1172 ppm.

To examine chemical fractionation of the CLGB komatiites in crustal conditions (25 MPa), we conducted closed-system fractional crystallization simulations using Magma Chamber Simulator [10]. For SCSS, we used the same parameterization [7] as with the mantle melting simulations. Using new and literature data [1,2,3,5,6,11,12,13,14], we compiled a comprehensive whole-rock (n = 299–403 depending on the element) and olivine (n = 917) chemistry database for the CLGB komatiites and spatiotemporally related rocks (from Kevitsa and Sakatti) to evaluate the simulation results. We find that closed-system fractional crystallization produces a good fit to the reference data for major element oxides and Ni (Fig. 2a). Importantly, simulated Ni contents in olivine are in good agreement with natural data (Fig. 2a) and could be used to identify Ni-depleted olivine to indicate those CLGB komatiites that experienced early sulphide saturation. Sulphur and Cu show highly incoherent behaviour in the reference data set and were likely affected by sulphide accumulation, degassing, and post-magmatic alteration. However, the simulation results are compatible with literature data for S (Fig. 2b) and Cu from chromite-hosted melt inclusions from the CLGB komatiites [6], which show relatively coherent behaviour compared to the whole-rock data. Depending on the initial S content (750–1172 ppm, see above), our SCSS simulations show that both Ni-rich (Ni/Cu = 1.9) and Cu-rich (Ni/Cu = 0.4) sulphide melt could have formed from the CLGB komatiite melt upon closed-system fractional crystallization (Fig. 2b). Moreover, the simulations indicate that the S content of CLGB komatiite melt was constantly close to SCSS starting from the liquidus (Fig. 2b). Accordingly, assimilation of sulphur-bearing country rocks has the potential to form relatively large sulphide accumulations within this region.

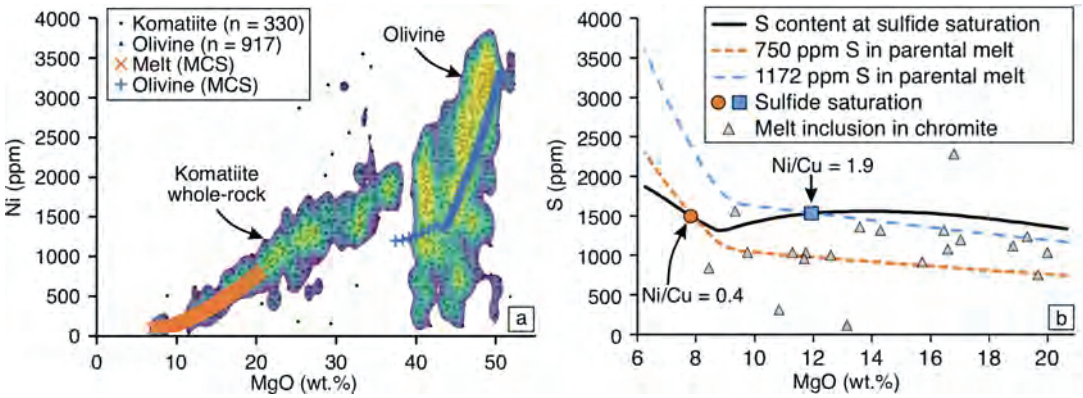


Figure 15. Closed-system fractional crystallization simulation results shown on a) MgO (wt.%) vs Ni (ppm) and b) MgO (wt.%) vs. S (ppm) diagrams. The data clouds in a) represent whole-rock and olivine data from the Central Lapland Greenstone Belt (CLGB) komatiites and related rocks (Kevitsa and Sakatti). Sulphur contents in b) are shown only for chromite-hosted melt inclusions from the CLGB komatiites.

References:

[1] Brownscombe W et al. (2015) Min Dep of Finland 211-252
[2] Luolavirta K et al. (2018) Lithos 296-299:37-53
[3] Puchtel I et al. (2020) Chem Geol 554:1-23
[4] Brown E and Lesher C (2016) Geochem Geophys Geosystems 17:3929-3968
[5] Hanski E et al. (2001) J Pet 42:855-876
[6] Hanski E and Kamenetsky V (2013) Chem Geol 343:25-37
[7] Walter M (1998) J Pet 39:29-60
[8] Smythe D et al. (2017) Am Min 102:795-803
[9] Lorand J-P and Luquet A (2016) Rev Mineral Geochem 81:441-488
[10] Bohrson W et al. (2014) J Pet 55:1685-1717
[11] Luolavirta K et al. (2018) Bull Geol Soc Finland 90:5-32
[12] Patten C et al. (2023) Min Dep 58:461-488
[13] Saverikko M (1985) Bull Geol Soc Finland 57:55-87
[14] Törmänen T et al. (2016) Min Dep 51:411-430

Ni-Cu-PGE prospectivity of the Mackenzie Large Igneous Province

Williamson, M.-C.[1], Rainbird, R.H.[1], O'Driscoll, B.[2] and Scoates, J.S.[3]

[1]Geological Survey of Canada, 601 Booth St, Ottawa, ON, K1A 0E8 Canada
Email: marie-claude.williamson@nrcan-rncan.gc.ca
[2]University of Ottawa, Marion Hall, Ottawa, ON, K1N 6N5 Canada
[3]PCIGR, University of British Columbia, 2020-2207 Main Mall, Vancouver, BC, V6T 1Z4 Canada

---

Large igneous provinces (LIPs) are high volume, intraplate magmatic events that consist of flood basalts, gabbro sills and dykes +/- layered intrusions. Most LIPs are emplaced over a time span of ~50 My or less [1], and there is strong evidence that the flood basalt volcanism occurs over even shorter time intervals (<1-2 My). The 1.27 Ga Mackenzie LIP includes flood basalts and feeder dykes of the Coppermine River Group (CRG), the Muskox intrusion and the Mackenzie dyke swarm. Previous studies of the Mackenzie LIP have focused on each of these three elements of the magmatic architecture, which resulted in many geological maps, datasets and samples archived at the GSC's Earth Materials Facility [2, 3, 4]. We propose to revisit previous work [5] and fill knowledge gaps [6] to produce a regional synthesis of the Mackenzie LIP that specifically highlights Ni-Cu-PGE prospectivity.

Knowledge about the Ni-Cu-PGE prospectivity of the Mackenzie LIP is largely based on previous mapping and laboratory studies of the Muskox intrusion and its putative feeder dyke [7, 8]. In contrast, the prospectivity of CRG flood basalts and feeder dykes is unknown. In this presentation, we summarize the methodology and anticipated results of a new GSC project on the Ni-Cu-PGE prospectivity of the Mackenzie LIP. We will adopt a multidisciplinary approach and a different research lens, one that specifically investigates the contact zone(s) and structures between the CRG and the Muskox intrusion. Our objectives are to: (1) fill knowledge gaps on the CRG feeder dykes and marginal rocks of the Muskox intrusion and evaluate the prospectivity of contact zones between intrusions and country rocks; (2) identify channelized lava flows, sills and dykes using remote predictive mapping; and (3) publish a synthesis that will focus specifically on Ni-Cu-PGE prospectivity.

Detailed remote predictive mapping of feeder dykes will further our understanding of ore genesis in channelized lava flows, sills, and dykes [9]. Additionally, mineralogical and geochemical studies of picritic lava flows will establish mantle melting temperatures, thus providing constraints on the timing and composition of magma fluxes during the lifetime of the LIP. Another important aspect of studying the picrites is to establish genetic links with the Muskox feeder dyke. Finally, our aim is to reconstruct the timing and duration of magmatism in the Mackenzie LIP and establish links to potential mineralization using high-precision geochronology of the Mackenzie dykes and of the CRG lava flows. The results will increase our knowledge base of Mackenzie LIP architecture, and of the Ni-Cu-PGE prospectivity of the CRG flood basalts and feeder dykes, and of the marginal rocks of the Muskox intrusion.

References:

[1] Ernst R E and Bleeker W (2010) Can J Earth Sci 47, 695-739
[2] Mackie R A et al. (2009) Precambrian Res 172: 46-66
[3] Skulski T et al. (2018) GSC Open File 8522, 37 p.
[4] Williamson M-C et al. (2023) 14th Int Pt Symp: 160-163
[5] Ernst R E et al. (2010) GSC Open File 6016, 14 p.
[6] Scoates J S and Scoates R F J (2024) Lithos 474-475: 107560
[7] Hulbert L (2005) GSC Open File 4881 (CD-ROM)
[8] Day J M D et al. (2013) Lithos 182-183: 242-258
[9] Lesher M (2019) Can J Earth Sci 56: 756-773

Siluro-Devonian Mafic-Ultramafic Intrusions in New Brunswick, Northern Appalachians, and their Associated Nickel-Copper-Cobalt Sulphide Deposits: A preliminary review

Yousefi, F.[1], Lentz D.R.[1], Walker J.A.[2] ,Thorne K.G.[3], and Karbalaeiramezanali A.[3]

[1]1: Department of Earth Sciences, University of New Brunswick, Fredericton, NB E3B5A3 Canada
fazilat.yousefi@unb.ca
[2] Geological Surveys Branch, Department of Natural Resources and Energy Development, Bathurst, New Brunswick, E2A 7B8 Canada
[3] Geological Surveys Branch, Department of Natural Resources and Energy Development, Fredericton, New Brunswick, E3B 5H1Canada

---

In the Appalachian-Caledonian region, several mafic-ultramafic intrusions host notable Ni-Cu-Co sulphide mineralization, as well as platinum-group elements. Notable examples in New Brunswick (NB) [1] include St. Stephen, Goodwin Lake, Mechanic Settlement, and Portage Brook intrusions. With the exception of Mechanic Settlement (Proterozoic), these occurrences are Silurian-Early Devonian, and formed during the terminal stages of the Acadian Orogeny [2]. Powderhorn Lake and Portage Ni-Cu occurrences represent examples associated with mafic and ultramafic intrusions in Newfoundland (NF). The Moxie, Katahdin, Union, Alexander, Moosehorn Plutonic Suite, and Pocomoonshine Gabbro-Diorite in Maine (USA) are examples of hosting Ni-Cu sulphide mineralization [3, 4]. The location of Devonian mafic-ultramafic intrusions linked to Ni-Cu, Co, and PGE sulphide mineralization in Maine, NB, and NF are shown below on a map, showing the tectonic zones of the Canadian Appalachians (Fig. 1). This preliminary study explores occurrences of Ni-Cu sulphide mineralization, cobalt, platinum-group elements, and their mafic-ultramafic intrusions in NB. The compositions of these mafic-ultramafic intrusions include gabbro, gabbronorite, olivine gabbro, olivine gabbronorite, anorthosite, peridotite, and troctolite. The sulphide mineral assemblages in these mafic-ultramafic rocks are dominated by pyrrhotite, pentlandite, and chalcopyrite. The assimilation of sulphide-bearing Cambro-Ordovician metasedimentary rocks typical of the Gander zone, and the local attainment of sulphide-silicate equilibrium are key factors in the formation of immiscible sulphide melts. For instance, in southern NB, the Siluro-Devonian St. Stephen Intrusion has an extremely low mass ratio of silicate magma to sulphide melt indicating a preferential assimilation of sulphide-rich portions of the Cambro-Ordovician Cookson Formation within the host St. Croix terrane. The scattered coarse sulphide blebs within the host intrusion indicates either solidification of the rock shortly after the formation of immiscible sulphide droplets or a high yield strength of the magma that prevented sulphide blebs from efficiently settling – differentially segregating [1]. The mafic-ultramafic intrusions in New Brunswick have low silica contents (38.2 to 51.28 wt.%) and FeOt/MgO ratios (<5), displaying calc-alkaline to tholeiitic features. Variations in Al_2O_3, $Fe_2O_3^t$, MgO, and CaO in most samples can be explained by the fractional crystallization - accumulation of olivine, both pyroxenes, and plagioclase. Preliminary lithogeochemistry indicates a wide variation in Cr (up to 1300), with Ni (up to 1100 ppm), Cu (up to 635 ppm), and Co (up to 150 ppm) content outside of the mineralized zones. Earlier separation of sulphides seems to be the reason for the typically low concentrations of chalcophile and platinum-group elements in these basic intrusive rocks. There is an enrichment of light rare earth elements relative to heavy rare earth elements in these mafic-ultramafic intrusions. The host intrusions are characterized by enrichment of large-ion lithophile elements (e.g., Rb, Ba, Sr) and are depleted in high-field strength elements (e.g., Nb, Ta, Zr, Hf, Ti), with much lower Ta/La (0.04) than primitive mantle (0.06; [5]). These unique characteristics may be attributed to the involvement of continental crust, which generally lacks Ta and Nb. The elevated Th/Nb(averaging 0.25) and La/Hf (averaging 8.6) support an island arc basalt affinity for these intrusions. Referring to an example (Moxie Pluton) in Maine Appalachian Orogeny [6], the emplacement of mafic-ultramafic intrusions occurred due to crustal fracturing in the late stages of the Acadian Orogeny, leading to a local tensional regime that generated a bimodal (mafic & felsic) igneous suite. According to the high positive εNd values

presented [7], it is inferred that the magmas responsible for forming these mafic-ultramafic intrusions originated by decompression of a modified mantle.

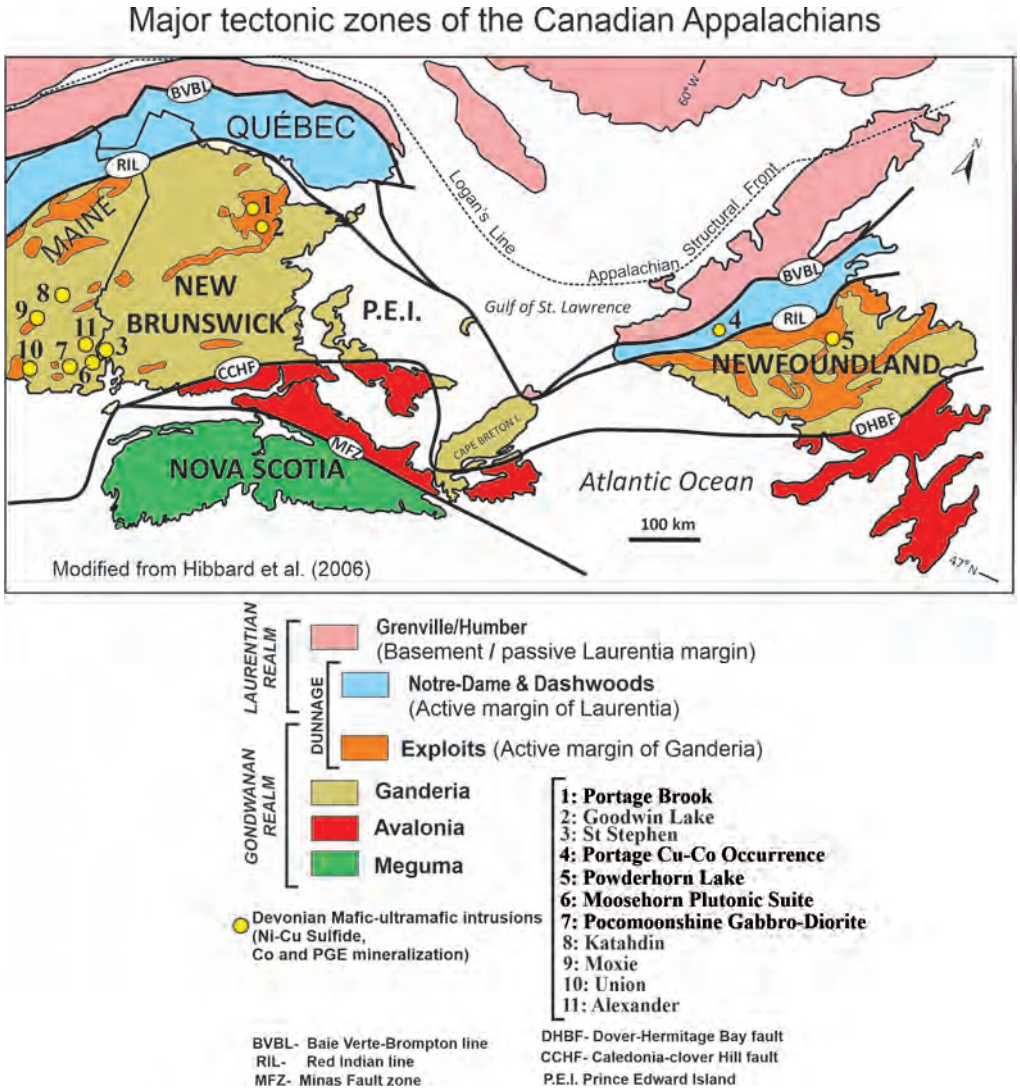


Fig. 1: Distribution of Devonian mafic-ultramafic intrusions associated with Ni-Cu sulphide, cobalt, and platinum group element (PGE) mineralization in Maine (USA), New Brunswick, and Newfoundland, situated within the Canadian Appalachians (modified from [8]).

References:

[1] Paktunc A.D (1989) Econ Geol 84: 817-840

[2] Ruitenberg A (1968) NB Dept. Nat. Resources Rept. Inv 7: 47 p

[3] McLaughlin K.J et al. (2003) Atl. Geol 39: 123-146

[4] Slack J.F et al. (2022) Atl. Geol 58: 155-191

[5] Ye X.T (2015) J Asian Earth Sci 113: 75-89

[6] Thompson J.F.H (1984) Am J Sci 284: 462-483

[7] Whalen et al. (1996) Can J Earth Sci 33: 140-155

[8] Hibbard J and Karabinos P (2013) Geosci. Canada 40: 303-317

Geochemistry of Archean komatiitic greenstone terranes of the Wyoming Province: implications for geodynamic setting and mineralization

Zieman, L.J.[1*], Poletti, J.E.[1], and Jenkins, M.C.[1]

[1]U.S. Geological Survey, Geology, Minerals, Energy, and Geophysics Science Center, Spokane, Washington, USA
*lzieman@usgs.gov

Archean komatiites are important host rocks of some Ni-Cu sulfide deposits [1] and are hypothesized to be the parental melt of several Archean layered mafic intrusions that host world-class platinum-group element (PGE) deposits [*e.g*., 2, 3]. The Archean Wyoming Province in the western United States contains two greenstone terranes that include komatiitic metavolcanic rocks: South Pass in the southern Wind River Range and Bradley Peak in the Seminoe Mountains, Wyoming. These Archean greenstone terranes have primarily been explored for Au, Cu, Fe, and Zn [4, 5]. However, the age, geodynamic setting, and sulfide mineralization potential of the spatially associated mafic-ultramafic metavolcanic rocks are poorly understood. Here, new major and trace element geochemistry as well as detrital zircon geochronology constrain the volcanic environment and the emplacement ages of these komatiitic metavolcanic units.

Metavolcanic units from the Bradley Peak region preserve primary igneous textures, including parallel and random spinifex (Fig. 1A), whereas igneous textures are overprinted by schistose textures in the South Pass metavolcanic rocks. Like most global komatiites, mafic-ultramafic rocks from both terranes have been metamorphosed up to amphibolite facies and contain tremolite, actinolite, serpentinite, chlorite, talc, and/or epidote. This work focuses on elements that are resistant to alteration [*e.g.,* Mg, Al, Ti, and rare earth elements (REE); 6].

The metavolcanic rocks in both Bradley Peak and South Pass greenstone belts contain basaltic to ultramafic komatiites, as well as high-Mg and high-Fe tholeiitic basalts based on the Al-Mg-(Fe+Ti) classification scheme of [7] (Fig. 1B). The subset of komatiitic samples (n = 20) have MgO contents predominantly ranging from 10 to 23 wt. %. These low MgO contents (< 30 wt. %) suggest low degrees of partial melting or high degrees of crustal contamination relative to komatiites associated with major Ni deposits [*e.g.,* 8]. Like most Archean komatiites [*e.g.,* 6], komatiites from both greenstone terranes are predominately Al-undepleted (*i.e.,* Munro-type) based on their chondritic Gd/Yb and Al_2O_3/TiO_2 ratios (Fig. 1C). The absence of heavy REE enrichments indicates the komatiitic magmas were generated at mantle depths shallower than the garnet stability field (< 300 km). The South Pass komatiites are highly enriched in light REE relative to a primitive komatiite melt, whereas the Bradley Peak komatiites are not enriched in light REE. These trends suggest that the South Pass komatiites have experienced higher percentages of crustal assimilation than the Bradley Peak komatiites. This interpretation supports previous studies that proposed the South Pass ultramafic rocks intruded continental shelf sedimentary rocks at the southern margin of the Wyoming craton, whereas the Bradley Peak ultramafic rocks were deposited in a sediment-starved ocean basin within a rift [9, 10].

Because komatiites lack minerals suitable for geochronology, emplacement ages of the ultramafic units were better constrained using detrital zircon U-Pb geochronology for metasedimentary rocks interbedded with the metavolcanic rocks in each greenstone terrane (Fig. 1D). Significant age populations were determined to identify the youngest age peak, which corresponds with the maximum depositional age (MDA), in addition to the weighted mean age for each sample [11]. In the Bradley Peak region, the weighted mean age for a metagraywacke from the Seminoe Formation, which overlies the ultramafic rocks, constrains the Bradley Peak ultramafic rocks to be older than 2721 ± 15 Ma. In the South Pass region, a metagraywacke from the unit overlying the komatiites (Miners Delight Formation) has a weighted mean age of 2673 ± 16 Ma, which agrees with published data and the previously accepted age for this greenstone terrane of 2.67 Ga [12]. Two pelitic schist samples interbedded with the komatiite units record MDA ranges ca. 3007-3049 Ma. This MDA range constrains komatiite units to younger than 3.01 Ga, but permits the komatiite units to be older than the previously assumed age of 2.67 Ga.

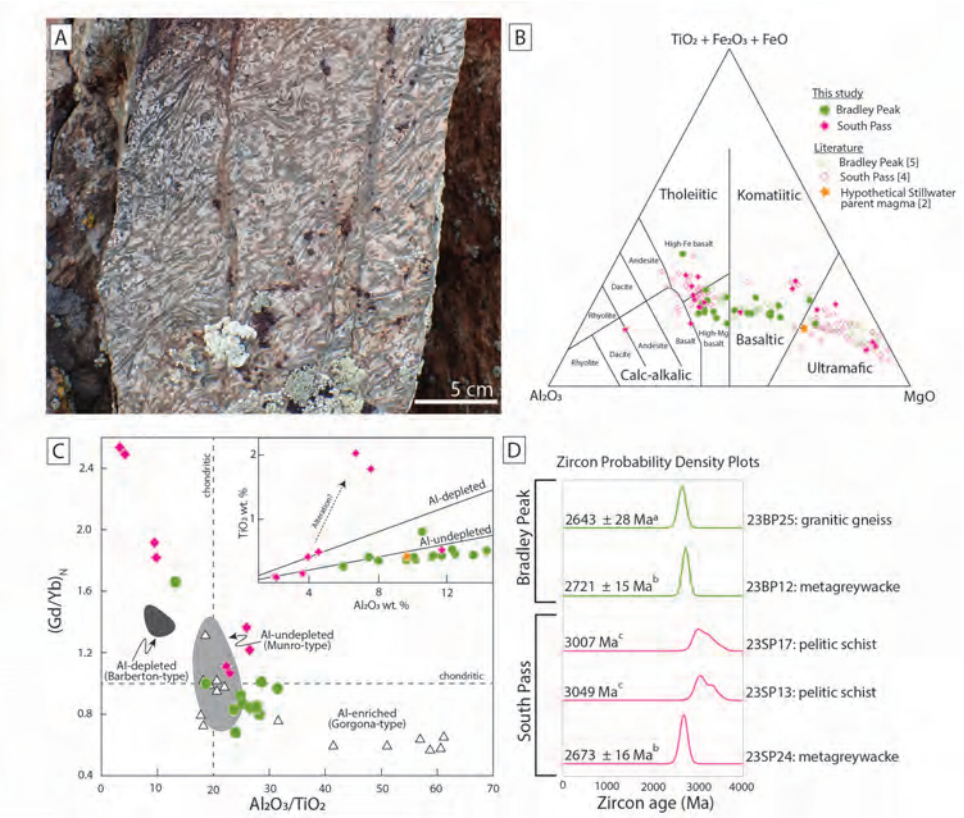


Figure 1. A) Sub-parallel spinifex texture preserved in the Bradley Peak metavolcanic rocks. B) Al-Mg-(Fe+Ti) cation classification plot after [7]. Hypothetical Stillwater parental melt (orange star) is from [2]. C) Gd/Yb vs. Al_2O_3/TiO_2 for the subset of komatiitic rocks from (B) in comparison to global komatiites after [12]. Inset: TiO_2 vs. Al_2O_3 illustrating Al-depleted ($Al_2O_3/TiO_2 \approx 20$) and Al-undepleted ($Al_2O_3/TiO_2 \approx 10$) trends. D) Detrital zircon age data. Vertical scales in probability density plots, calculated after [12], are reduced to 25%. A crystallization age is given for igneous sample 23BP25 (a). Weighted mean age (b) is given for samples with one significant age peak. The MDA (c) is given for samples with more than one significant age population.

These komatiites do not satisfy several criteria typically thought to be important for Ni-Cu ore genesis [*e.g.,* 1]— they were generated from relatively low degree partial melting and, in the case of the Bradley Peak greenstone, lack geochemical signatures of significant crustal assimilation, which is widely accepted to be a source of sulfur for ore genesis [1]. Contrarily, they are Al-undepleted and erupted at cratonic margins, characteristic of komatiites that have been associated with major Ni deposits [8]. Furthermore, the geochronological data do not rule out that either greenstone terrane was erupted synchronously with the emplacement of the 2.7 Ga Stillwater Complex in the Archean Wyoming Province, which is thought to have an Al-undepleted komatiitic parental melt (see Fig. 1B and 1C). Future work is needed to test if eruption of the komatiites is related to the emplacement of this layered intrusion or other magmatic systems in the Wyoming Province.

References:

[1] Barnes S J et al. (2016) Ore Geol Rev 76:296-316
[2] Jenkins M C et al. (2021) Precambr Res 367:106457
[3] Eales H and Costin G (2012) Econ Geol 107:445-465
[4] Hausel D (1991) WY State Geo Survey 44:1-129
[5] Hausel D (1994) WY State Geo Survey 50:1-24
[6] Barnes S J et al. (2004) Mineral Petrol 82:259-293
[7] Jensen (1976) Ontario Geo Survey 66
[8] Mole D et al. (2014) Proc Natl Acad Sci 111:10083-10088
[9] Grace et al. (2006) Can J Earth Sci 43:1445-1466
[10] Frost C et al. (2006) Can J Earth Sci 43:1533-1555
[11] Gehrels G (2009) Excel Age Pick Program
[12] Arndt N and Lesher C (2004) Cambridge U Press
[13] Saylor J and Sundell K (2016) Geosphere 12:203-22

Note: Any use of trade, firm, or product names is for descriptive purposes only and does not imply endorsement by the U.S. Government.